学位論文

I-ball formation and its evolution for an oscillating scalar field during reheating

(再加熱中の振動スカラー場が形成する I-ball とその発展)

平成26年12月博士(理学)申請

東京大学大学院理学系研究科

物理学専攻

武田　直幸

Ph.D Thesis

I-ball formation and its evolution for an oscillating scalar field during reheating

Department of Physics, Graduate School of Science
University of Tokyo

Naoyuki Takeda

Abstract

Scalar fields such as inflaton could play crucial roles in the early Universe. To estimate the effects of the scalar fields on the cosmological scenario, the dynamics of them is usually calculated in perturbative ways. However, it is known that through non-perturbative effects, scalar fields form localized objects, and by the formation of those objects, dynamics of the scalar fields such as decay processes would be changed. In this thesis, we study a class of such localized objects, namely I-balls.

I-balls are spatially localized objects. By numerical simulations, it is known that they are formed for a flatter potential than the quadratic one. The flatter potentials appear in various situations in cosmology. In this thesis, we study whether I-balls are formed for the R^2 inflation, and then find that the formation does not occur. Thus, our results validate the estimation of the decay rate of the inflaton of the R^2 inflation, which is calculated by the perturbative way. We also study the formation of I-balls for the logarithmic potential $M^2 \Lambda^2 \ln\left[1 + \phi^2/\Lambda^2\right]$ motivated by the quantum or thermal correction during reheating. Then, it is found that for this potential, I-balls are formed. We show that the I-balls are formed when the potential is dominated by the quadratic term, which is consistent with an idea that the stability of I-balls is due to conservation of an conserved quantity called adiabatic charge.

The analytical understandings of I-balls are not yet obtained well. In this thesis, we try to verify the stability of I-balls analytically based on the adiabatic charge. We give a rigorous proof of conservation of the adiabatic charge for a potential that allows a periodic motion of a scalar field even in the presence of the non-negligible spatial gradient energy. We show that such potential is uniquely determined to the quadratic one with a logarithmic correction $(m^2/2)\phi^2 \left[1 - K \ln\left(\phi^2/M^2\right)\right]$, and that for this potential, the adiabatic charge is conserved. We numerically check the conservation of the adiabatic charge of I-balls by slowly varying the coefficient of the logarithmic term. The result supports the idea that the stability of I-balls is due to the adiabatic charge.

Contents

Chapter 1

Introduction

1.1 Overview

By the discovery of the Higgs boson in the Large Hadron Collider [1, 2], it has been established that a scalar field exists in nature. Furthermore, cosmological observations suggest that other scalar fields exist and would have played various crucial roles in the early Universe. A scalar field called inflaton can induce inflation in the early Universe [3–7]. In other cases, an oscillating scalar field can be a candidate of the dark matter [8, 9]. A light scalar field can obtain large fluctuations during inflation, and it might be the origin of cosmological perturbations instead of the inflaton [10–12]. Decays of scalar fields which have baryon charge can be a source of the present baryon asymmetry [13–16]. In some cases, decays of scalar fields would spoil the hot big bang nucleosynthesis (BBN) [17–19].

It has been known that in some class of potentials scalar fields form solitons. The solitons are spatially localized and long-lived classical objects formed through non-linear processes. These solitons are classified into the topological solitons [20, 21] and non-topological solitons by the topological structure of the scalar potentials. As examples of the non-topological solitons, there exist Q-balls [22] and I-balls (oscillons) [23–26] which are formed from coherently oscillating scalar fields. By the formation of these solitons, the dynamics of the scalar fields such as the decay rates [22, 27] would be affected. Thus, to predict the effect of the scalar fields on the cosmology, we have to pay attention to the formation of those solitons.

Properties of the topological solitons or Q-balls are understood based on conserved quantities. In the case of topological solitons, topological numbers account for their stabilities, and in the case of Q-balls, $U(1)$ global charge does. However, in the case of I-balls, their properties are not yet analytically understood well since it is difficult to define a conserved quantity for them. Thus, to study the I-balls, non-linear numerical simulations such as lattice simulations are required. In this thesis, we focus on these non-topological solitons, I-balls.

The I-balls are spatially localized objects, which consist of a real scalar field. Inside the I-balls, the scalar field is periodically oscillating, and the period is approximately given by the inverse of the mass of the field. By numerical simulations, it is known that the formation of I-balls takes place for a specific shape of potentials that are flatter than

the quadratic one. When the scalar field is oscillating with small fluctuations, I-balls are formed through rapid growth of fluctuations of the scalar field by parametric resonance or other non-perturbative effects [28, 29]. Numerical simulations also have revealed that in some potentials I-balls emit scalar waves from their surface, but the lifetime of I-balls is significantly larger than the period of oscillations. Thus, if I-balls are formed in the early Universe, they might survive for cosmological time scales, and then affect cosmological scenarios.

Scalar fields with the flatter potentials would appear in various situations in the early Universe. From observations of cosmic microwave background (CMB) such as Planck [30], it is suggested that the shape of the inflaton potential would be flatter. The flatter potentials also appear in the theories of scalar fields whose potentials have logarithmic forms by the thermal or quantum corrections (e.g. thermal log potential [31]). In this thesis, we investigate the formation of I-balls for two cases, one is a specific model of inflation, R^2 inflation [5, 32], and the other is the logarithmic potential motivated by the thermal or quantum corrections.

A distinctive feature of the R^2 inflation is that the dynamics of the inflaton is determined by only one mass parameter. This mass parameter determines the amplitude of fluctuations of the inflaton during inflation, and the decay rate of the inflaton into other particles. Thus, by evaluating the decay rate precisely, we can give predictions for CMB uniquely. In [33–35], the decay rate is evaluated in perturbative ways, and the predictions of the spectral index and tensor-to-scalar ratio are given by $n_s \simeq 0.963$ and $r \simeq 0.004$, which can be tested by future observations of CMB. However, the formation of I-balls might change this predictions since their formation would change the decay process of the inflaton and hence the decay rate. The potential of the R^2 inflation is flatter than the quadratic one for the field value larger than the Planck mass, and inflation takes place in that region. Thus, to validate the decay rate of the inflaton and test the R^2 inflation by the future observations of CMB, we study whether the inflaton of the R^2 inflation forms I-balls.

After inflation, the inflaton decays into other particles, and through subsequent decays and scatterings they make a thermal bath in the Universe. Then as the temperature of the Universe drops to a few MeV, BBN [36] begins. During this epoch, scalar fields interacting with the thermal bath would receive corrections for their potentials. Quantum corrections would also alter their potentials. If these corrections for a scalar potential is significant, the field would oscillate along the corrected potential whose form is often logarithmic. Since this logarithmic potential is flatter than the quadratic one, the field might be form I-balls, and their decay dynamics would be changed. Thus, motivated by the thermal or logarithmic corrections, in this thesis we study the formation of I-balls for the logarithmic potential. To study the formation, we use a non-linear numerical simulation, lattice simulation.

The logarithmic potential is also important to understand the properties of I-balls. In previously known cases, the formation of I-balls are confirmed for polynomial potentials, and it takes place when the quadratic terms dominate the potential. Since the logarithmic potential is not written with finite polynomial series, the formation of I-balls for the potential is nontrivial.

As mentioned, properties of I-balls are not yet analytically understood well. Thus,

numerical simulations are required to verify the properties such as the formation process or lifetime of them. If we can clarify what makes I-balls stable analytically, we could understand the dynamics better. In the case of other solitons such as the topological defects or Q-balls, their stabilities are accounted for by conserved quantities, topological number or $U(1)$ global charge. As for I-balls, we also expect a conserved quantity accounting for the stability of I-balls. In this thesis, we consider adiabatic charge as a conserved quantity.

In [26], it was conjectured that the stability of I-balls is due to conservation of the adiabatic charge. The adiabatic charge comes from the adiabatic invariant which is known in a classical mechanical system [37, 38] and can be extended to a scalar field theory. If the adiabatic charge is conserved for an oscillating field, we can consider the lowest energy state of the field for a fixed value of the charge. The authors of [26] showed that the configuration of the scalar field for the lowest energy state is a localized one if the potential is flatter than the quadratic one. Thus, by the adiabatic charge, we can understand the heuristic condition for the potentials to allow the formation of I-balls. In this thesis, we proved that the adiabatic charge is really conserved for a scalar field theory with specific potential. Further we showed that the potential is uniquely determined to the quadratic one with a logarithmic term $V = (m^2/2)\phi^2 \left[1 - K \ln\left(\phi^2/2M^2\right)\right]$. For this potential, the radius of the I-ball is determined by the dimension less parameter K and mass of the field m. If we vary K slowly, the I-ball deforms, while the adiabatic charge is conserved. In this thesis, we have investigated whether the deformation follows the profile estimated from the adiabatic charge performing lattice simulations.

This thesis is organized as follows. In chapter 2, we briefly review inflation. Next, in chapter 3, we briefly review I-balls. There we give the proof of the conservation of the adiabatic charge. In chapter 4, we investigate the formation of I-balls in the R^2 inflation. Next, in chapter 5, we move to the investigation of the formation of I-balls for the logarithmic potential. To confirm its formation, we perform lattice simulations. In chapter 6, we study the relation between I-balls and the adiabatic charge. To verify the relation, we perform lattice simulations. Finally in chapter 7, we conclude this thesis.

In this thesis, we work with the metric signature $(+, -, -, -)$, $R^{\alpha}{}_{\mu\beta\nu} = \partial_{\beta}\Gamma^{\alpha}{}_{\mu\nu} + \cdots$ and $R_{\mu\nu} = R^{\alpha}{}_{\mu\alpha\nu}$ for convention. We adopt the natural units in which $\hbar = c = k_B = 1$, and we use the reduced Planck mass, $M_p \equiv 1/\sqrt{8\pi G} \simeq 2.4 \times 10^{18} \text{GeV}$

Chapter 2

Review of Inflation

The standard cosmology is based on the Big Bang model. In the model, the Universe stars out from a hot and dense initial state, and subsequently it expands and cools [36]. In the early high energy state, elementary particles are produced, and the abundances of light elements such as ^{4}He are explained. At the same time, this model predicts that the Universe is filled with black body radiation, which is confirmed by the discovery of CMB by Penzias and Wilson [39]. Thus, the Big Bang model explains our Universe in many ways. However, there remains several problems to be solved such as the horizon and flatness problems, and, if we assume the GUT theory, the monopole problem. To solve these problems, we need some theory beyond the standard Big Bang model.

To solve the cosmological problems in the standard cosmology, the theory of inflation was invented [3–7]. This theory is based on assumptions that the potential energy (vacuum energy) of some scalar field dominates the Universe. The scalar field is called inflaton. If the domination is established, an accelerated expansion of the Universe, which is called inflation, starts, and then by the expansion, the cosmological problems are solved.

As inflation is achieved with a high energy density, which could be as high as GUT scale, quantum fluctuations of the inflaton are excited copiously. Then, by the accelerated expansion of the Universe, the momenta of excited fluctuations are stretched to cosmological scales. After sufficient expansion of the Universe, inflation ends, and then the inflaton decays into elementary particles. By the decay of the inflaton, the fluctuations of the inflaton are transferred to relativistic particles, which consist of elementary particles such as photons and baryons. As the energy density of the fluids is so high, the photons interact with the baryons strongly, but as the Universe cools, the interaction becomes inefficient, and the photons decouple from the fluids. After the decoupling, the photons propagate freely through the Universe. These freely propagating photons become CMB. Thus, by measuring CMB, we can test inflation. COBE [40] for the first time observed the temperature anisotropies of CMB with $\Delta T/T \simeq 10^{-5}$ whose spectrum is almost scale invariant. This nearly scale invariant spectrum is consistent with the predictions of inflation. In fact, the theory predicts a slight scale dependence. The scale dependence is measured by more precise observations such as WMAP [41] and Planck [30], which strongly suggests that inflation really occurs in the early Universe. As the scale dependence of the spectrum depends on the shape of the inflaton potential, by the measurements, we can obtain constraints on the inflaton potential. Indeed it is revealed that the shape of the potential

would be a flatter one than the quadratic potential.

In addition to fluctuations of the inflaton, there could also occur the excitation of gravitational waves, which is imprinted on CMB as tensor fluctuations. A distinctive feature of the gravitational waves is that their amplitude mainly depends on the energy scale of inflation, i.e., absolute value of the vacuum energy. Thus, if we can detect the gravitational waves or measure the tensor fluctuations of CMB caused by the gravitational waves, we can determine the absolute value of the potential, which will strongly support inflation.

As mentioned, the inflaton decays into other elementary particles after inflation [32, 42, 43]. When the decay rate of the inflaton becomes comparable with the Hubble expansion rate, the decay of the inflaton becomes efficient, and then the decay products dominate the Universe. Further decays and scatterings of the decay products produce a thermal bath. We call this epoch reheating. After the completion of reheating, the temperature of the thermal bath drops by the cosmic expansion. As the temperature drops to a few MeV, BBN proceeds.

In this chapter, we first briefly describe the standard cosmology, and then next review inflation. After reviewing the reheating process, we review a specific inflation model; R^2 inflation [5, 32]. This part is following the reviews and book [44–47].

2.1 Standard cosmology

First, we briefly describe the standard cosmology. In the standard Big Bang cosmology, the cosmological principle is assumed that the Universe is homogeneous and isotropic on averaging over large volumes. Based on this assumption, the metric of space-time is given by Friedmann-Robertson-Walker (FRW) form,

$$ds^2 = g_{\mu\nu}dx^\mu dx^\nu = dt^2 - a^2 \left[\frac{dr^2}{1 - K_c r^2} + r^2(d\theta^2 + \sin^2\theta d\phi^2) \right]. \qquad (2.1.1)$$

Here, t is the cosmic time, a is the scale factor and K_c is the spatial curvature. In this section, we neglect fluctuations of the metric. Furthermore, we assume that the action of the gravity and matter contents are given by the Einstein-Hilbert action,

$$S = \int d^4x \sqrt{-g} \left[\frac{M_p^2}{2}(\mathcal{R} + 2\Lambda_c) + \mathcal{L}_{\text{matter}} \right]. \qquad (2.1.2)$$

Here, g is the determinant of the metric, Λ_c is the cosmological constant, $\mathcal{L}_{\text{matter}}$ is the Lagrangian of matter contents and $\mathcal{R}$ is the Ricci scalar. By taking variation of the action with respect to the metric, we obtain the equation of motion for space-time, which is called Einstein equation,

$$\mathcal{R}_{\mu\nu} - \frac{1}{2}g_{\mu\nu}\mathcal{R} - \Lambda_c g_{\mu\nu} = \frac{1}{M_p^2}T_{\mu\nu}. \qquad (2.1.3)$$

Here M_p is the reduced Planck mass $M_p^2 \equiv 1/(8\pi G)$, and $T_{\mu\nu}$ is the energy momentum tensor given by

$$T_{\mu\nu} = \frac{2}{\sqrt{-9}} \left[\frac{\delta(\sqrt{-g}\mathcal{L}_{\text{matter}})}{\delta g^{\mu\nu}} - \frac{\partial}{\partial x^\alpha} \frac{\delta(\sqrt{-g}\mathcal{L}_{\text{matter}})}{\delta g^{\mu\nu}_{,\alpha}} \right]. \qquad (2.1.4)$$

5

From the Einstein equation, we can see that the geometry of the Universe is determined by the particle contents.

As we have assumed that the Universe is homogeneous and isotropic, the energy moment tensor is given by the form of a perfect fluid,

$$T_{\mu\nu} = (\rho + P) u_\mu u_\nu + P g_{\mu\nu}, \tag{2.1.5}$$

where u_ν is the 4-velocity normalized as $u_\mu u^\mu = 1$, ρ is the energy density and P is the pressure. Substituting this form and FRW metric into the Einstein equation, we obtain the Friedmann equation,

$$H^2 = \frac{\rho}{3M_p^2} - \frac{K_c}{a^2}, \tag{2.1.6}$$

and Raychaudhuri equation,

$$\frac{\ddot{a}}{a} = -\frac{\rho + 3P}{6M_p^2}, \tag{2.1.7}$$

where the over dot means the derivative with respect to t. We have defined the Hubble parameter by $H \equiv \dot{a}/a$, which gives the expansion rate of the Universe. Combining the above two equations, we obtain the continuity equation of the fluid,

$$\dot{\rho} + 3H(\rho + P) = 0. \tag{2.1.8}$$

From the Friedmann equation, we can see that the expansion rate of the Universe is determined by the energy density of the fluid. From the Raychaudhuri equation, we can see that the expansion is accelerated or decelerated depending on the equation of state $\omega_s = P/\rho$. In the case of $\omega_s < -1/3$, the expansion is accelerated: $\ddot{a} > 0$. If ω_s is time independent, we can solve the continuity equation and obtain

$$\rho \propto a^{-3(1+\omega_s)}. \tag{2.1.9}$$

Thus, we can see that the dilution rate of the energy density by the Hubble expansion is determined by the equation of state of the fluid.

Here let us consider some particles whose distribution function is given by the Bose-Einstein one or the Fermi-Dirac one,

$$f(\vec{k}) = \frac{1}{\exp\left[(\omega_k - \mu_c)/T\right] \mp 1}, \tag{2.1.10}$$

where $\vec{k}$ is the momentum of particles, μ_c is the chemical potential and ω_k is the energy of the particle given by $\omega_k = \sqrt{|\vec{k}|^2 + m^2}$ with m being the mass of the particle. For this distribution, the number density of the particle n, energy density ρ and pressure P are given by

$$\begin{cases} n = g_* \int \frac{d^3k}{(2\pi)^3} f(\vec{k}), \\ \rho = g_* \int \frac{d^3k}{(2\pi)^3} \omega_k f(\vec{k}), \\ P = g_* \int \frac{d^3k}{(2\pi)^3} \frac{\vec{k}^2}{3\omega_k} f(\vec{k}), \end{cases} \tag{2.1.11}$$

where g_* is the degree of freedom of the particle. We calculate the above equations in two limits of the temperature: relativistic limit $T \gg m$ and non-relativistic limit $T \ll m$. In the case of the relativistic limit, the equations are reduced to

$$
\begin{cases}
n_{\mathrm{r}} = g_* \dfrac{\zeta(3)}{\pi^2} T^3 \times \begin{cases} 1 & \text{boson} \\ 3/4 & \text{fermion} \end{cases}, \\[2mm]
\rho_{\mathrm{r}} = g_* \dfrac{\pi^2}{30} T^4 \times \begin{cases} 1 & \text{boson} \\ 7/8 & \text{fermion} \end{cases}, \\[2mm]
P_{\mathrm{r}} = \dfrac{1}{3}\rho.
\end{cases}
\tag{2.1.12}
$$

On the other hand, in case of the non-relativistic limit, they are reduced to

$$
\begin{cases}
n_{\mathrm{nr}} = g_* \left(\dfrac{mT}{2\pi} \right)^{3/2} \exp\left(-\dfrac{m - \mu_c}{T} \right), \\[2mm]
\rho_{\mathrm{nr}} = mn + \dfrac{3}{2} nT, \\[2mm]
P_{\mathrm{nr}} = nT.
\end{cases}
\tag{2.1.13}
$$

From eqs. (2.1.12) and (2.1.13), we can see that, for relativistic particles, the equation of state becomes $\omega_s = 1/3$ and for non-relativistic particles it becomes $\omega_s \simeq 0$. Hence, the energy density of relativistic particles dilutes as $\rho_{\mathrm{r}} \propto a^{-4}$ and that of non-relativistic particles as $\rho_{\mathrm{nr}} \propto a^{-3}$. From the Raychaudhuri equation, we can see that under the domination of relativistic or non-relativistic particles, the expansion of the Universe is decelerated.

Here we briefly explain the problems in the standard Big Bang model. Let us first define the critical energy density by the Hubble parameter as

$$
\rho_c \equiv 3M_p^2 H^2,
\tag{2.1.14}
$$

and we define a density parameter Ω by the ratio of the energy density to ρ_c,

$$
\Omega \equiv \frac{\rho}{3M_p^2 H^2} = \frac{\rho}{\rho_c}.
\tag{2.1.15}
$$

Using Ω and H, the Friedmann equation is written as

$$
\Omega - 1 = \frac{K}{a^2 H^2}.
\tag{2.1.16}
$$

Since the energy density consists of relativistic particles, non-relativistic particles, and dark energy, Ω is written as $\Omega = \Omega_{\mathrm{r}} + \Omega_{\mathrm{nr}} + \Omega_{DE}$ where $\Omega_{\mathrm{r}} = \rho_{\mathrm{r}}/\rho_c$, $\Omega_{\mathrm{nr}} = \rho_{\mathrm{nr}}/\rho_c$ and $\Omega_{\mathrm{DE}} = \rho_{\mathrm{DE}}/\rho_c$. Then, we rewrite the Friedmann equation as

$$
\Omega_r + \Omega_{\mathrm{nr}} + \Omega_{DE} + \Omega_{K_c} = 1,
\tag{2.1.17}
$$

where we have defined Ω_{K_c} by

$$
\Omega_{K_c} \equiv -\frac{K_c}{a^2 H^2}.
\tag{2.1.18}
$$

7

By the observation of CMB, it is confirmed that the present value of $|\Omega_{K_c}|$ is smaller than unity. From eq. (2.1.18), when the cosmic expansion is decelerated, $|\Omega_{K_c}|$ in the early Universe is much smaller than the present value. Thus, the density parameter Ω should be extremely close to unity in the past such as $|\Omega - 1| < \mathcal{O}(10^{-16})$ at BBN [47]. This is called flatness problem.

There exists other problems for the decelerated expansion of the Universe. Due to the deceleration, causally connected regions at the last scattering surface of CMB are smaller than today's Hubble radius, which corresponds to an angle of order $1°$. However the observations of CMB show that temperature fluctuations are order $\Delta T/T \simeq 10^{-5}$ in all directions. This is called horizon problem. Furthermore, if we assume the GUT, symmetry breaking of a gauge group in the early Universe leads to production of monopoles. In that case, about one monopole would be produced within a causally related region at the symmetry breaking. The number density of monopoles produced at that time would be estimated as $n_{\mathrm{mon}} \simeq 1/[(1/H_{\mathrm{GUT}})^3] \simeq T_{\mathrm{GUT}}^6/M_p^3$. Since the monopoles are diluted as like non-relativistic particles, its ratio to the entropy is conserved up to now as $n_{\mathrm{mon}}/s \simeq (T_{\mathrm{GUT}}/M_p)^3 \simeq 10^{-6}(10^{16}\mathrm{GeV}/M_p)^3$. This ratio is much larger than the baryon to entropy ratio, resulting in $\Omega_{\mathrm{now}} \gg 1$. This is called monopole problem.

In the standard cosmology, it is difficult to solve the above cosmological problems, however, if there occurs an accelerated expansion in the very early Universe (inflation), such problems can be solved. By inflation, Ω_{K_c} and monopoles are diluted away, and then the flatness and monopole problems are solved. By inflation, causally un-connected regions at present are connected in the early Universe, and then the horizon problem is solved. From the Raychaudhuri equation, we can see that inflation is achieved when an energy component with a negative equation of state: $\omega_s < -1/3$ dominates the Universe. This negative ω_s could be achieved by some scalar filed, in other words, inflaton. We explain this inflation theory in the next section.

2.2 Inflation

Let us consider a scalar field ϕ with a Lagrangian:

$$\mathcal{L} = \frac{1}{2}\partial_\mu\phi\partial^\mu\phi - V(\phi), \tag{2.2.1}$$

where $V(\phi)$ is the potential of ϕ. Inflation is achieved if the potential energy dominates the Universe for a sufficiently long time, which is explained as following.

The energy momentum tensor of ϕ is given by

$$T^{\mu\nu} = \partial^\mu\phi\partial^\nu\phi - g^{\mu\nu}\mathcal{L}. \tag{2.2.2}$$

In this section, we assume the FRW metric and neglect fluctuations of the field and metric. For the homogeneous field, the energy density and pressure are given by

$$\begin{cases} \rho = \dfrac{1}{2}\dot{\phi}^2 + V(\phi), \\ P = \dfrac{1}{2}\dot{\phi}^2 - V(\phi). \end{cases} \tag{2.2.3}$$

Thus, the equation of sate is given by

$$\omega_s = \frac{\frac{1}{2}\dot{\phi}^2 - V(\phi)}{\frac{1}{2}\dot{\phi}^2 + V(\phi)}. \tag{2.2.4}$$

From the above equation, we can see that, if the potential energy dominates over the kinetic energy, the equation of state is approximately given by $\omega_s \simeq -1$. As we can see from the Raychaudhuri equation (2.1.7), the accelerated expansion is achieved for $\omega_s \lesssim -1/3$. Thus, by the domination of the potential energy with $\omega_s \simeq -1$, inflation is achieved.

Let us define e-folding number as

$$N_{\rm e} \equiv \ln \frac{a_e}{a} = \int_{t_p}^{t_f} H dt, \tag{2.2.5}$$

where t_e and a_e are the cosmic time and the scale factor when inflation ends. Here t_p is the time when the length scale corresponding to the present Hubble radius leaves he horizon $\sim H^{-1}$ during inflation. By using $N_{\rm e}$, we can discuss how much the Universe expands during the inflation from $t = t_p$ to t_e. The exact value of N_e depends on the energy scale of inflation and cosmological scenario after inflation. Conversely, predictions of inflation for observations depend on $N_{\rm e}$ as explained later. In this section, we assume typically $N_{\rm e} \simeq 55$.

Next we briefly explain the dynamics of inflaton during inflation, and define several parameters, which are useful for the discussion of inflation. The equation of motion for ϕ is given by

$$\ddot{\phi} + 3H\dot{\phi} + \frac{\partial V}{\partial \phi} = 0. \tag{2.2.6}$$

During inflation, the Universe is dominated by the inflaton. Thus, the Hubble parameter is determined by the energy density of the inflaton:

$$H^2 = \frac{1}{3M_p^2} \left(\frac{1}{2}\dot{\phi}^2 + V(\phi) \right). \tag{2.2.7}$$

The domination of the potential energy over the kinetic energy $V \gg \dot{\phi}^2$ should continue over cosmological times $\gtrsim N_{\rm e}/H$. This long domination of the potential is achieved when the inflaton slowly rolls down along the potential. In the slow-roll regime, the friction term in the equation of motion dominates over the acceleration term:

$$|\ddot{\phi}| \ll 3H|\dot{\phi}|. \tag{2.2.8}$$

Thus, by neglecting $\ddot{\phi}$, we can approximate the equation of motion as

$$3H\dot{\phi} \simeq -\frac{\partial V}{\partial \phi}. \tag{2.2.9}$$

The dynamics of the inflaton during inflation is approximately given by the above equation. We have mentioned two conditions for inflation: $\dot{\phi}^2/V \ll 1$ and $|\ddot{\phi}|/(3H\dot{\phi}) \ll 1$, which we call as slow-roll conditions.

For later discussions, we introduce several parameters. Using eq. (2.2.9), $\dot{\phi}^2/V \ll 1$ is reduced to

$$\epsilon_V \equiv \frac{M_p^2}{2}\left(\frac{V'}{V}\right)^2 \ll 1, \tag{2.2.10}$$

where the prime means the derivative with respect to ϕ. We call this parameter ϵ_V as slow-roll parameter. We can define the other slow-roll parameter:

$$\eta_V \equiv M_p^2 \frac{V''}{V}, \tag{2.2.11}$$

which should be much smaller than unity ($\eta_v \ll 1$) from eq. (2.2.8). For later use, we define another parameter:

$$\xi_V^2 \equiv M_p^2 \frac{V'V'''}{V}, \tag{2.2.12}$$

which is also required to be much smaller than unity for inflation. The accelerated expansion $\ddot{a} > 0$ is identical to the condition that the evolution rate of the Hubble parameter during one Hubble time is smaller than unity,

$$\ddot{a} > 0 \Longleftrightarrow \epsilon_H \equiv \frac{|\dot{H}|}{H^2} < 1. \tag{2.2.13}$$

With the time derivative of eq. (2.2.7) and the equation of motion for ϕ, $\dot{H}$ is written as $\dot{H} = -\dot{\phi}^2/(2M_p^2)$. From this relation and eq. (2.2.9), ϵ_H is reduced to ϵ_V as

$$\begin{aligned}
\epsilon_H &= \frac{\dot{\phi}^2/(2M_p^2)}{H^2} \simeq \frac{1}{2M_p^2}\frac{V'^2}{9H^4} \\
&\simeq \frac{M_p^2}{2}\left(\frac{V'}{V}\right)^2 \\
&= \epsilon_V, \tag{2.2.14}
\end{aligned}$$

where we have approximated the Hubble parameter as $H^2 \simeq V/(3M_p^2)$ in the third equality.

As we have mentioned, for the achievement of inflation, the slow-roll parameters are required to be smaller than unity. From the definition of the parameters (2.2.10) and (2.2.11), the condition implies that the slope and curvature of the potential should be sufficiently small for the enough duration of inflation. Thus, we expect that the inflaton potential would be flat.

2.3 Cosmological perturbation

Next, we consider fluctuations of the inflaton and metric. The inflaton acquires quantum fluctuations during inflation and, as the inflaton is coupled with the metric by the Einstein equation, they are related to the fluctuations of the metric. After inflation, the fluctuations give seeds of the large scale structures [48, 49]. The fluctuations are also imprinted on the temperature anisotropies of CMB. Measuring the anisotropies, we can constrain inflationary models [30].

Here we treat fluctuations of the inflaton as well as the metric perturbations at linear level. Let us divide ϕ into its background ϕ_0 and fluctuations $\delta\phi$ as

$$\phi(t, \vec{x}) = \phi_0(t) + \delta\phi(t, \vec{x}). \tag{2.3.1}$$

We also consider perturbations for the FRW metric,

$$\begin{aligned} ds^2 &= (1 + 2A_g)dt^2 - 2a(\partial_i B_g - S_{gi})dx^i dt \\ &\quad + a^2\left[(1 - 2\psi_g)\delta_{ij} + 2\partial_{ij}E_g + \partial_i F_{gj} + \partial_j F_{gi} + h_{ij}\right]. \end{aligned} \tag{2.3.2}$$

Here, A_g, B_g, ψ_g and E_g are scalar modes, S_{gi} and F_{gi} are vector modes, which are transverse as $\partial_i S_{gi} = \partial_i F_{gi} = 0$, and h_{ij} is a tensor mode, which is traceless and transverse as $\partial_i h_{ij} = h_{ii} = 0$. The perturbations of ϕ and metric are related through the Einstein equation. If we consider a single field inflation model, the vector modes S_{gi} and F_{gi} damp significantly compared with other modes. So, in this section, we mainly focus on the scalar and tensor modes.

Gauge invariant variable

The perturbations are not invariant variables under coordinate transformations: $x^\mu \to x^\mu + \xi^\mu$ where

$$\xi^\mu = (\delta t, \delta^{ij}\partial_i \delta x + \delta x^i). \tag{2.3.3}$$

Here, δt and δx are scalar transformations and δx^i is a vector one. (Explicit transformation law is given in Appendix A.) Thus, in order to remove the gauge freedoms, we have to fix the gauge or construct gauge invariant variables. In the following, we show some gauge invariant variables.

First, we show two gauge invariant variables constructed only by the perturbations of the metric. In the shear zero gauge frame $B_g = 0$ and $E_g = 0$, A_g and ψ_g become gauge invariant variables:

$$\Phi_g \equiv A_g|_{E_g=B_g=0} = A_g - \frac{d}{dt}\left[a^2(\dot{E}_g - B_g/a)\right], \tag{2.3.4}$$

$$\Psi_g \equiv \psi_g|_{E_g=B_g=0} = \psi_g + a^2 H\left(\dot{E}_g - B_g/a\right). \tag{2.3.5}$$

These invariant variables Φ_g and Ψ_g are called Bardeen potentials. As the energy momentum tensor is defined by the variation of the Einstein-Hilbert action with respect to the metric, perturbations for matter contents are also gauge dependent variables. Under the gauge transformation, the perturbations for the energy density and pressure transform as $\delta\rho \to \delta\rho - \dot{\bar{\rho}}\delta t$ and $\delta P \to \delta P - \dot{\bar{P}}\delta t$. From these transformations, the pressure perturbation at the uniform density gauge ($\delta\rho = 0$) is gauge invariant:

$$\delta P_{\text{nad}} \equiv \delta P - \frac{\dot{\bar{P}}}{\dot{\bar{\rho}}}\delta\rho. \tag{2.3.6}$$

If a single inflaton achieves inflation, the perturbation for the pressure is proportional to that for the energy density ($\delta P = (\dot{\bar{P}}/\dot{\bar{\rho}})\delta\rho$), and the perturbation is adiabatic. We show

another gauge invariant variable. The $(0, i)$ component of the energy momentum tensor $\delta T_{0i} = \partial_i \delta q$ transforms as

$$\delta q \to \delta q + (\bar{\rho} + \bar{P})\delta t. \tag{2.3.7}$$

Thus, the perturbation for the energy density at the comoving gauge ($\delta q = 0$) is gauge invariant:

$$\delta \rho_c \equiv \delta \rho - 3H\delta q. \tag{2.3.8}$$

Combinations of the metric perturbations and matter perturbations can be also gauge invariant variables. The curvature perturbation on the uniform density gauge is gauge invariant:

$$-\zeta \equiv \psi_g + \frac{H}{\dot{\bar{\rho}}}\delta \rho. \tag{2.3.9}$$

The curvature perturbation on the comoving gauge is also gauge invariant:

$$\mathcal{R}_c \equiv \psi_g - \frac{H}{\bar{\rho} + \bar{P}}\delta q. \tag{2.3.10}$$

These two curvature perturbations are related by $\delta \rho_c$ as

$$-\zeta = \mathcal{R}_c + \frac{H}{\dot{\bar{\rho}}}\delta \rho_c. \tag{2.3.11}$$

We note that the tensor perturbation $h_{\mu\nu}$ is also gauge invariant.

Here let us construct a useful variable with the perturbations of ϕ. The perturbation of the scalar field (2.3.1) transforms as $\delta\phi \to \delta\phi - \dot{\phi}\delta t$. Combining with the metric perturbations, we can construct a gauge invariant variable. The perturbation of the field in the flat gauge $\psi_g = 0$ is a gauge invariant variable:

$$\delta\phi_{\psi_g} \equiv \delta\phi + \frac{\dot{\phi}}{H}\psi_g. \tag{2.3.12}$$

This gauge invariant variable is called Sasaki-Mukanov variable [50–52]. This Sasaki-Mukanov variable is related to the comoving curvature perturbation as

$$\mathcal{R}_c \equiv \frac{H}{\dot{\phi}}\delta\phi_{\psi_g}. \tag{2.3.13}$$

Evolution of perturbations

We have shown some gauge invariant variables. Next, we consider their evolutions. The evolutions of the perturbations are given by the Einstein equation,

$$\delta G_{\mu\nu} = \frac{1}{M_p^2}\delta T_{\mu\nu}. \tag{2.3.14}$$

Calculating the $(0,0)$ and $(0,i)$ components, we obtain the following constraint equations:

$$\begin{cases} 3H\left(\dot{\psi}_g + HA_g\right) + \dfrac{k^2}{a^2}\left[\psi_g + H(a^2\dot{E}_g - aB_g)\right] = -\dfrac{\delta\rho}{2M_p^2} & (0,0), \\[4mm] \dot{\psi}_g + HA_g = -\dfrac{\delta q}{2M_p^2} & (i,0). \end{cases} \tag{2.3.15}$$

Combining these two equations, we obtain the Poisson equation,

$$\frac{k^2}{a^2}\Psi_g = -\frac{1}{2}\frac{\delta\rho_c}{M_p^2}, \tag{2.3.16}$$

which is gauge invariant. Calculating the (i, j) components, we obtain two independent equations as

$$\begin{cases} \ddot{\psi}_g + 3H\dot{\psi}_g + H\dot{A}_g + (3H^2 + 2\dot{H})A_g = \frac{1}{2M_p^2}\left[\delta P - \frac{2}{3}k^2\delta\Pi\right], \\ \frac{d}{dt}\left(\dot{E}_g - B_g/a\right) + 3H\left(\dot{E}_g - B_g/a\right) + \frac{\psi_g - A_g}{a^2} = \frac{\delta\Pi}{2M_p^2}, \end{cases} \tag{2.3.17}$$

where $\delta\Pi$ is the scalar mode of the anisotropic stress. The second equation can be rewritten with the Bardeen potentials as

$$\Psi_g - \Phi_g = \frac{1}{M_p^2}a^2\delta\Pi. \tag{2.3.18}$$

From this relation, we can see that, in the absence of the anisotropic stress, the two Bardeen potentials are identical, $\Psi_g = \Phi_g$.

From the conservation of the energy-momentum tensor, we obtain the equations of motion for $\delta\rho$ and δq as

$$\begin{cases} \dot{\delta\rho} + 3H(\delta\rho + \delta P) = \frac{k^2}{a^2}\delta q + (\bar{\rho} + \bar{P})\left[3\dot{\psi}_g + k^2\left(\dot{E}_g - B_g/a\right)\right], \\ \dot{\delta q} + 3H\delta q = -\delta P + \frac{2}{3}k^2\delta\Pi - (\bar{\rho} + \bar{P})A_g. \end{cases} \tag{2.3.19}$$

We can rewrite the equation for $\delta\rho$ using gauge invariant variables, and then obtain the equation of motion for the uniform density curvature perturbation,

$$\dot{\zeta} = -H\frac{\delta P_{\text{nad}}}{\bar{\rho} + \bar{P}} - \Sigma. \tag{2.3.20}$$

Here Σ is defined by

$$\frac{\Sigma}{H} \equiv -\frac{1}{3}\left(\frac{k}{aH^2}\right)\zeta - \frac{1}{3}\left(\frac{k}{aH}\right)^2\Psi_g\left[1 - \frac{2}{9}\frac{\bar{\rho}}{\bar{\rho} + \bar{P}}\left(\frac{k}{aH}\right)^2\right]. \tag{2.3.21}$$

For the single field inflation, the non-adiabatic perturbation δP_{and} vanishes. In that case, the time derivative of the curvature perturbation on the super horizon scale $k/(aH) \ll 1$ becomes zero $\dot{\zeta} \simeq 0$ until the scale reenters in the horizon $k/(aH) \gtrsim 1$.

The comoving curvature perturbation is related to the uniform density curvature perturbation as eq. (2.3.11). Thus, using the Poisson equation (2.3.16), we can rewrite the curvature perturbation as

$$\mathcal{R}_c = -\zeta - \frac{2}{9}\frac{\bar{\rho}}{\bar{P}}\left(\frac{k}{aH}\right)^2\Psi_g. \tag{2.3.22}$$

13

We can see that on the super horizon scale, the two curvature perturbations are identical except for the sign: $\mathcal{R}_c \simeq -\zeta$ for $k/aH \ll 1$.

As for the tensor mode, the equation of motion is given by

$$\ddot{h}_{ij} + 3H\dot{h}_{ij} + \frac{k^2}{a^2}h_{ij} = 2\frac{\delta\Pi_{ij}^T}{M_p^2}, \tag{2.3.23}$$

where $\delta\Pi_{ij}^T$ is the tensor mode of perturbations of the fluid. Thus, in the absence of $\delta\Pi_{ij}^T$, the evolution of h_{ij} is identical to that of a massless scalar field in the unperturbed FRW.

Here we again make a remark on vector perturbations. In absence of the anisotropic stress, the vector modes of the metric damp out quickly. If inflation is achieved by a single scalar field, the anisotropic stress is not produced. Thus, we neglect the vector modes.

Perturbations from inflaton

We calculate perturbations from a single field inflation model. For the single inflaton, the perturbations of the energy density, pressure and momentum are given by

$$\begin{cases} \delta\rho = \dot{\phi}_0\left(\delta\dot{\phi} - \dot{\phi}_0 A_g\right) + V'\delta\phi, \\ \delta P = \dot{\phi}_0\left(\delta\dot{\phi} - \dot{\phi}_0 A_g\right) - V'\delta\phi, \\ \delta q = -\dot{\phi}_0\delta\phi. \end{cases} \tag{2.3.24}$$

From these perturbations, the comoving density perturbation is written as

$$\delta\rho_c = \dot{\phi}_0(\delta\dot{\phi} - \dot{\phi}_0 A_g - \ddot{\phi}_0\delta\phi). \tag{2.3.25}$$

Substituting these forms into the equation of motion for $\delta\rho$ (2.3.19), we obtain the equation of motion for $\delta\phi$ as

$$\delta\ddot{\phi} + 3H\delta\dot{\phi} + \frac{k^2}{a^2}\delta\phi + V''\delta\phi = -2V'A_g + \dot{\phi}_0\left[\dot{A}_g + 3\dot{\psi}_g + \frac{k^2}{a^2}\left(a^2\dot{E}_g - aB_g\right)\right], \tag{2.3.26}$$

where we have used the equation of motion for ϕ_0 and continuity equation.

Let us take the flat gauge and calculate the evolution of perturbations. In the flat gauge $\psi_g = 0$, A_g and $(\dot{E}_g - B_g/a)$ become

$$A_g|_{\psi_g=0} = -\left.\frac{\delta q}{2M_p^2 H}\right|_{\psi_g=0} = \frac{\dot{\phi}_0}{2M_p^2 H}\delta\phi_{\psi_g}, \tag{2.3.27}$$

and

$$\begin{aligned}
\left.\frac{k^2}{a^2}a^2\left(\dot{E}_g - \frac{B_g}{a}\right)\right|_{\psi_g=0} &= \frac{k^2}{a^2}\frac{\Psi_g}{H} = -\frac{\delta\rho_c}{2M_p^2 H} \\
&= -\frac{\dot{\phi}_0\delta\dot{\phi}_{\psi_g} - \ddot{\phi}_0\delta\phi_{\psi_g} - \dot{\phi}_0^2\,A_g|_{\psi_g=0}}{2M_p^2 H},
\end{aligned} \tag{2.3.28}$$

where we have used the momentum constraint of the Einstein equation and the poisson equation. Substituting these relations into the equation of motion for $\delta\phi$, we can reduce the equation to

$$\delta\ddot{\phi}_{\psi_g} + 3H\delta\dot{\phi}_{\psi_g} + \left[\frac{k^2}{a^2} + V'' - \frac{1}{M_p^2}a^{-3}\frac{d}{dt}\left(\frac{a^3\dot{\phi}_0^2}{H}\right)\right]\delta\phi_{\psi_g} = 0. \tag{2.3.29}$$

This equation is simplified by using of variables $v_k = a\delta\phi_{\psi_g}$, $z = a\dot{\phi}_0/H$ and $d\tau = a^{-1}dt$ to

$$\frac{d^2}{d\tau^2}v_k + \left(k^2 - \frac{\partial_\tau^2 z}{z}\right)v_k = 0. \tag{2.3.30}$$

This equation is called Sasaki-Mukanov equation. Here $\partial_\tau^2 z/z$ is written using slow-roll parameters [53, 54] as

$$\frac{\partial_\tau^2 z}{z} = (aH)^2\left[2 + 5\epsilon_H - 3\eta_H + 9\epsilon_H^2 - 7\epsilon_H\eta_H + \eta_H^2 + \xi_H^2\right], \tag{2.3.31}$$

where

$$\eta_H \equiv 2\epsilon_H - \frac{\dot{\epsilon}_H}{2H\epsilon_H}, \quad \xi_H^2 \equiv \left(2\epsilon_H - \frac{\dot{\eta}_H}{H\eta_H}\right)\eta_H. \tag{2.3.32}$$

If the slow-roll approximation is satisfied, these parameters are approximately identical to η_V and ξ_V^2 respectively at leading order. During the slow-roll regime, we can treat ϵ_H, η_H and ξ_H^2 as time independent variables. Thus, the conformal time and the effective mass $\partial_\tau^2 z/z$ are given by

$$\tau \simeq -\frac{1}{(1 - \epsilon_H)aH}, \tag{2.3.33}$$

and

$$\frac{\partial_\tau^2 z}{z} = \frac{\nu_R^2 - 1/4}{\tau^2}, \tag{2.3.34}$$

where

$$\nu_R \simeq \frac{3}{2} + 3\epsilon_H - \eta_H. \tag{2.3.35}$$

With these approximations, the solution of the Sasaki-Mukanov equation is given by Hankel functions as

$$v_k \simeq \frac{\sqrt{\pi|\tau|}}{2}e^{i(1+2\nu_R)\pi/4}\left[c_1 H_{\nu_R}^{(1)}(k|\tau|) + c_2 H_{\nu_R}^{(2)}(k|\tau|)\right]. \tag{2.3.36}$$

Here c_1 and c_2 are arbitrary constants. We assume that the fluctuations within the horizon are in the vacuum state and normalize the mode function as

$$v_k(\tau) = \frac{1}{\sqrt{2k}}e^{-ik\tau} \tag{2.3.37}$$

for $-k\tau \gg 1$. This assumption is identical to the choice of parameters as $c_1 = 1$ and $c_2 = 0$. Thus, for the normalized mode function, the power spectrum on the super horizon

scale is given by

$$\mathcal{P}_{\delta\phi_{\psi_g}} \equiv \frac{k^3}{2\pi^2} |\delta\phi_{\psi_g}|^2$$
$$= \left(\frac{H}{2\pi}\right)^2 \left(\frac{k}{aH}\right)^{3-2\nu_R} (1 - \epsilon_H)^{2\nu_R - 1} 2^{2\nu_R - 3} \left[\frac{\Gamma(\nu_R)}{\Gamma(3/2)}\right]^2, \qquad (2.3.38)$$

where we have used the asymptotic form of the Hankel function:

$$H_\nu^{(1)}(k|\tau|) \to -(i/\pi)\Gamma(\nu)(k|\tau|/2)^{-\nu} \qquad (2.3.39)$$

for $k/(aH) \to 0$. Using the relation between the comoving curvature perturbation $\mathcal{R}_c$ and the Sasaki-Mukanov variable (2.3.13), we obtain the power spectrum of the curvature perturbation as

$$\mathcal{P}_{\mathcal{R}_c} \equiv \frac{k^3}{2\pi^2} |\mathcal{R}_c|^2 = \left(\frac{H}{\dot{\phi}_0}\right)^2 \mathcal{P}_{\delta\phi_{\psi_g}}$$
$$= \left(\frac{H^2}{2\pi\dot{\phi}_0}\right)^2 \left(\frac{k}{aH}\right)^{3-2\nu_R}, \qquad (2.3.40)$$

where we have assumed that the slow-roll parameters are small, $\epsilon_H \ll 1$ and $\eta_H \ll 1$.

In the super horizon scales, the amplitude of the curvature perturbations does not change. Thus, the initial conditions of temperature anisotropies are determined by the value of the curvature perturbations at the exit of the horizon. Therefore, the measurement of temperature anisotropies gives constraints on the curvature perturbations at $k = aH$,

$$\mathcal{P}_{\mathcal{R}_c}|_{k=aH} = \left(\frac{H^2}{2\pi}\dot{\phi}_0\right)^2$$
$$\simeq \frac{1}{12\pi^2} \frac{V^3}{M_p^6 V'^2} \simeq \frac{1}{24\pi^2} \frac{V}{M_p^4 \epsilon}. \qquad (2.3.41)$$

By the observation of CMB, we obtain $\mathcal{P}_{\mathcal{R}_c} \simeq 2 \times 10^{-9}$ at the pivot scale ($k^{-1} = 0.002\,\text{Mpc}^{-1}$) [30]. The scale dependence of the curvature perturbations is characterized by the spectrum index and running as

$$n_s - 1 \equiv \left.\frac{d \ln \mathcal{P}_{\mathcal{R}_c}}{d \ln k}\right|_{k=aH} \simeq 1 - 6\epsilon_H + 2\eta_H \simeq 1 - 6\epsilon_V + 2\eta_V, \qquad (2.3.42)$$

$$\alpha_{\mathcal{R}_c} \equiv \left.\frac{dn_s}{d \ln k}\right|_{k=aH} \simeq 16\epsilon_H - 24\epsilon_H^2 - 2\xi_H^2 \simeq 16\epsilon_V - 24\epsilon_V^2 - 2\xi_V^2. \quad (2.3.43)$$

We can also calculate the power spectrum of the tensor mode which is given by

$$\mathcal{P}_T \simeq \frac{8}{M_p^2} \left(\frac{H}{2\pi}\right)^2 \left(\frac{k}{aH}\right)^{-2\epsilon_H} 2^{2\epsilon_H} \left[(1 - \epsilon_H)\frac{\Gamma(\nu_T)}{\Gamma(3/2)}\right]^2, \qquad (2.3.44)$$

where

$$\nu_T = \frac{3}{2} + \epsilon_H. \qquad (2.3.45)$$

At the horizon exit, $k \simeq aH$, the power spectrum of the tensor mode is determined as

$$\mathcal{P}_T|_{k=aH} \simeq \frac{8}{M_p^2} \left(\frac{H}{2\pi}\right)^2.$$ (2.3.46)

The spectral index and running of the tensor mode are given by

$$n_T \simeq -\epsilon_T,$$ (2.3.47)

$$\alpha_T \simeq -4\epsilon_H^2 + 8\epsilon_H\eta_H.$$ (2.3.48)

The ratio of the power spectrum of the curvature perturbations to that of the tensor mode is given by

$$r \equiv \frac{\mathcal{P}_T}{\mathcal{P}_{\mathcal{R}_c}} \simeq 16\epsilon.$$ (2.3.49)

Substituting the value of the curvature perturbation $\mathcal{P}_{\mathcal{R}_c} \simeq 2\times10^{-9}$, we obtain the relation between the energy scale of inflation V and tensor to scalar ratio r as

$$\frac{V^{1/4}}{10^{16}\text{GeV}} \simeq 3 \left(\frac{r}{0.1}\right)^{1/4} \left(\frac{\mathcal{P}_{R_c}}{2\times10^{-9}}\right)^{1/4}.$$ (2.3.50)

Thus, the measurement of r determines the energy scale of inflation.

Constraints from observations

As we have explained, the quantum fluctuations of the inflaton field induce the curvature perturbations, which are conserved in the super horizon scales. After the perturbations re-enter the horizon, they give the seeds of temperature anisotropies. In photon-baryon relativistic fluids, the anisotropies evolve following the Boltzmann equation and after the recombination, photons start to freely propagate in the Universe. Thus, by measuring these photons, we can constrain inflation models.

Here we show the constraints on the spectral index n_s and tensor to scalar ratio r given by Planck satellite in fig. 2.1 [30]. On the same panel, predictions of n_s and r for each inflation model are plotted. For example, the simple quadratic inflation model ($V \propto \phi^2$) is on the edge of the 2σ excluded region, whose width on the (n_s, r) plane is due to the ambiguity of the e-folding number N_e. As like the simple model, other inflation models also have some ambiguities for the predictions on the (n_s, r) plane. In the near future, by more precise managements of the tensor mode of CMB, the constraint on r would be improved. Thus, in order to test inflation models, we have to give predictions with low ambiguities.

2.4 Reheating

The vacuum energy of the inflaton drives inflation in the early Universe and solves the cosmological problems, while at the same time the exponential expansion of space dilutes the matter and radiation that existed before inflation, and the Universe becomes highly non-equilibrium and very cold state.
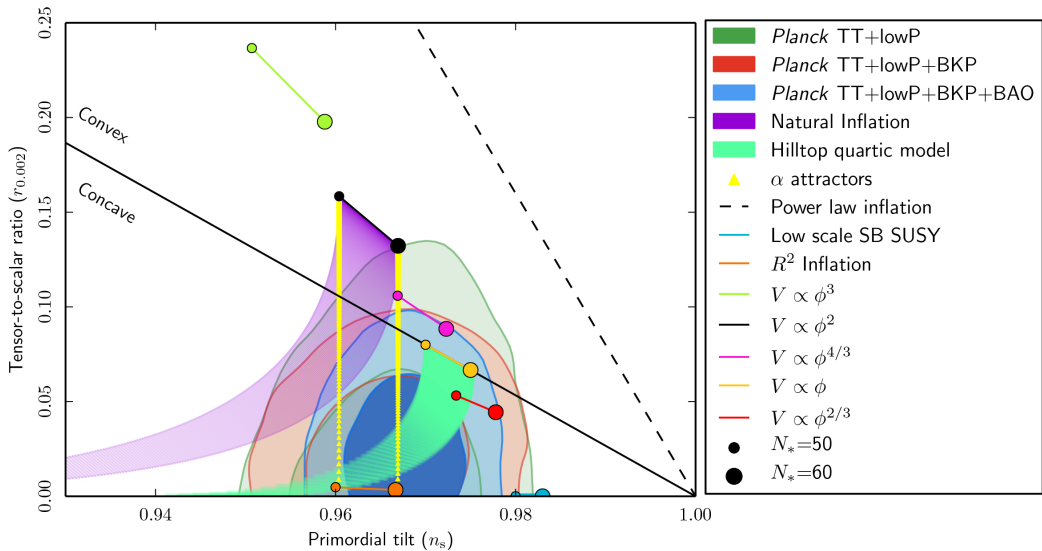
Figure 2.1: Marginalized joint 68% and 95% CL regions for n_s and r from Planck alone and in combination with its cross correlation with BICEP2/Keck Array and/or BAO data compared with the theoretical predictions of selected inflationary models [30].

After inflation, the inflaton decays into other particles, and the energy stored in the inflaton is transferred to them. At some time the inflaton decay is completed, and the decayed particles dominate the Universe making a thermal equilibrium state. This process is called reheating. Then, after the Universe cools down to a temperature of $\mathcal{O}(\text{MeV})$, BBN begins.

In many inflation models, it is considered that, after the end of inflation, the inflaton coherently oscillates around the minimum of the potential. The coherent oscillation of the inflaton can be treated as like particles with large occupation numbers stored in zero mode. In this case, the decay of the inflaton is calculated in the perturbative way [42, 43].

In addition to the perturbative decay, there occur other decay processes. The coherent oscillation acts as like a classical external force on other fields, which have interactions with the inflaton. This leads to an explosive decay of the inflaton in non-perturbative ways such as the parametric resonance [28, 29]. This non-perturbative process is called preheating.

In the non-perturbative decay, fluctuations of the fields are enhanced [28, 29]. After fluctuations grow comparable with the background field, re-scattering with the zero mode or with other modes starts, and the distribution of the energy density becomes highly inhomogeneous. [1] It is known that, in some class of potentials, scalar fields fragment into spherical objects such as Q-balls or I-balls. These objects are spatially localized stable or quasi-stable objects. Through the formation of these objects, the decay rate of the scalar field would be enhanced by the bose enhancement [27, 56] or would be suppressed

---

[1] Fermionic fields are not efficiently amplified for this mechanism due to the Pauli blocking [55].

by the Pauli blocking [22]. Thus, in order to estimate the decay rate precisely, we have to pay attention to the formation of these objects. We will explain these objects in the next chapter. In this chapter, we briefly review the dynamics of the reheating and comment about the preheating mainly following the reviews [45, 46].

2.4.1 Perturbative decay

First, we review the perturbative decay of the inflaton. As a simple example, we suppose that the inflaton ϕ decays into a scalar field χ and a fermion field ψ through interactions given by

$$\mathcal{L} \ni \nu_d \sigma \phi \chi^2, \; h_d \phi \bar{\psi} \psi, \tag{2.4.1}$$

where σ is a constant with mass dimension one, and ν_d and h_d are dimensionless coupling constants. For these interactions, the decay rates are calculated at tree-level as

$$\Gamma(\phi \to \chi\chi) \;\; = \frac{\nu_d^2 \sigma^2}{8\pi m_\phi} \left(1 - \frac{4m_\chi^2}{m_\phi^2}\right)^{1/2} \simeq \frac{\nu_d^2 \sigma^2}{8\pi m_\phi}, \tag{2.4.2}$$

$$\Gamma(\phi \to \psi\bar{\psi}) \;\; = \frac{h_d^2 m_\phi}{8\pi} \left(1 - \frac{4m_\psi^2}{m^2}\right)^{3/2} \simeq \frac{h_d^2 m_\phi}{8\pi}, \tag{2.4.3}$$

where $m_{\phi,\chi,\psi}$ is the mass of ϕ, χ or ψ, and the latter approximate equations are valid when the mass of the decay products is small. As the inflaton decays, its energy density decreases. We treat the damping of the energy density by adding a dissipation term into the equation of motion as

$$\dot{\rho}_\phi + (3H + \Gamma_{\rm tot}) \rho_\phi = 0, \tag{2.4.4}$$

where $\Gamma_{\rm tot}$ is the total decay rate of the inflaton:

$$\Gamma_{\rm tot} \equiv \Gamma(\phi \to \chi\chi) + \Gamma(\phi \to \psi\bar{\psi}). \tag{2.4.5}$$

Here we have assumed that the energy density of the inflaton is diluted as like non-relativistic particles.

Just after the end of inflation, as the Hubble parameter H is larger than the decay rate $\Gamma_{\rm tot}$, the dilution by the decay is negligible compared with that by the Hubble expansion. Thus, the decay products cannot be the dominant component of the Universe at first. However, as the Hubble parameter decreases and becomes below the decay rate $\Gamma_{\rm tot}$ (2.4.4), the energy density of the inflaton starts to decrease exponentially. Then, the Universe is dominated by decay products soon after $\Gamma_{\rm tot} \simeq H$. Here we assume that the thermalization of decay products occurs instantaneously just after $\Gamma_{\rm tot} = 3H$. Under this assumption, the Universe is dominated by relativistic particles in thermal equilibrium, and their energy density is given by

$$\rho_r = \frac{\pi^2}{30} g_* T^4 = 3M_p^2 H^2. \tag{2.4.6}$$

From this relation, we can estimate the temperature of relativistic particles at the completion of reheating, which is called reheating temperature:

$$T_R \simeq 0.4 \left(\frac{100}{g_*}\right)^{1/4} \sqrt{\Gamma_{\rm tot} M_p}. \tag{2.4.7}$$

19

Here we have assumed that the decay time is given by $3H = \Gamma_{\text{tot}}$.

2.4.2 Preheating

We have estimated the reheating temperature by the perturbative decay. Next, we consider non-perturbative decay processes of the inflaton.

For the sake of discussion, let us consider a specific interaction of the inflaton with another scalar field χ as $V_{\text{int}} = (g_i^2/2)\chi^2\phi^2$ where g_i is a coupling constant. Furthermore, we assume that the inflaton potential is dominated by a quadratic term $(m_\phi^2/2)\,\phi^2$ with inflaton mass m_ϕ. In this case, the equations of motion for χ and ϕ are given by

$$\ddot{\phi} + 3H\dot{\phi} - \frac{1}{a^2}\nabla^2\phi + m^2\phi + g_i^2\chi^2\phi = 0, \tag{2.4.8}$$

$$\ddot{\chi} + 3H\dot{\chi} - \frac{1}{a^2}\nabla^2\chi + g_i^2\phi^2\chi = 0, \tag{2.4.9}$$

where we have assumed that the mass of χ is negligibly small compared with m_ϕ.

During reheating, the inflaton coherently oscillates. By the oscillation, the frequency of χ is modulated through the interaction term $g_i^2\phi^2\chi^2$. In this case, the non-perturbative decay of the inflaton could enhance fluctuations of χ at particular scales. This dynamics is investigated by numerical simulations such as [57] by performing lattice simulations. One of the results is shown in fig. 2.2. From the figure, we can see that the rapid growth of fluctuations of χ at a particular scale $k \simeq 10m_\phi$. Furthermore, we can see that as the fluctuations grow, they start to re-scatter with other scales, and the spectrum of the fluctuations broadens for higher momenta. This non-perturbative and non-linear process is called preheating [28, 29].

By the rapid growth of the fluctuations of the χ field, the energy of the inflaton is transferred into χ. In many cases, after the sufficient growth, the coherent oscillation of inflaton is affected by backreactions, and the preheating terminates. Then, the decay process of the inflaton is completed in perturbative ways. However, in some class of potentials, enhanced fluctuations fragment into stable or quasi-stable objects. We consider this case in the next chapter.

2.5   Inflation model

We have explained the dynamics of inflation, and how the cosmological perturbations are produced in the inflationary Universe. Furthermore, we have explained the decay process of the inflaton. In this section, we briefly review a specific inflation model, i.e., R^2 inflation [5, 32].

The R^2 inflation is one of the oldest inflation models, which was proposed by Starobinsky [5, 32] even before the cosmological problems were claimed to be solved. The unique point of this inflation model is that we do not extend the matter contents in order to achieve inflation. On the other hand, we extend the gravitational sector adding an extra scalar freedom of the gravity. The extra scalar graviton achieves inflation, we call it inflaton. [2] By rescaling the metric, this scalar graviton behaves as if a scalar field minimally

---

[2] More strictly, it is called scalaron, but in this thesis, we call simply inflaton.
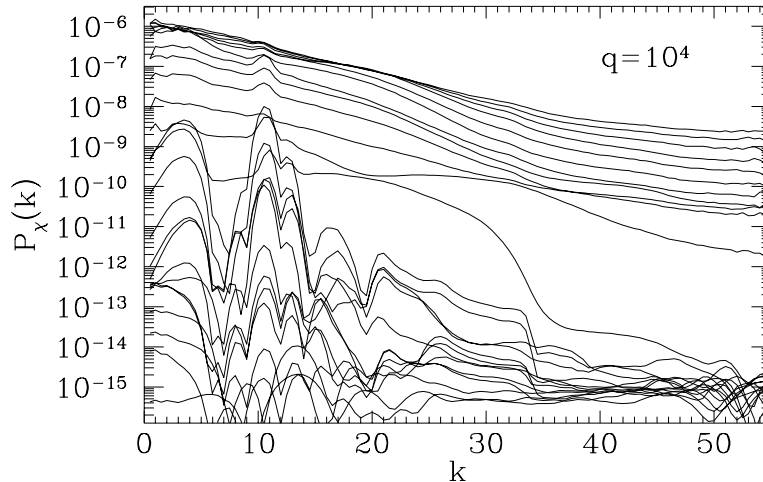
Figure 2.2: Evolution of the power spectrum of χ [57]. Each line is plotted when the inflaton ϕ takes the maximal value. k is the momentum of the χ field in unit of m_ϕ.

coupled to the Einstein gravity. We call this rescaled frame as the Einstein frame. In the Einstein frame, the dynamics of the R^2 inflation is similar to the ordinary slow-roll inflation model. After sufficient exponential expansion, the inflaton starts to oscillate around the minimum of the potential, and then decays into other particles [58, 59].

This inflation model is characterized by a single parameter M. Thus, the curvature perturbations, spectrum index and tensor-to-scalar ratio are determined only by this one parameter. As the origin of the inflaton for this inflation model is the scalar graviton, the inflaton interacts with elementary particles of the standard model only through gravitational interactions. Thus, the decay rate into the elementary particles is determined by M. Therefore, the predictions for temperature anisotropies are determined uniquely. In this section, we briefly review the dynamics of the R^2 inflation and its perturbative decay.

Dynamics of inflation

The action of the R^2 inflation is written as [5]

$$S = \int d^4 x \sqrt{-g} \left[\frac{M_p^2}{2} f(R) + \mathcal{L}_{\text{matter}} \right], \tag{2.5.1}$$

where $\mathcal{L}_{\text{matter}}$ is the Lagrangian of the standard model particles. Here $f(R)$ is a function of the Ricci scalar and is given by

$$f(R) = R + \frac{1}{6} \frac{R^2}{M^2}, \tag{2.5.2}$$

21

where M is a constant with mass dimension one. Compared with the Einstein-Hilbert action, the R^2 inflation model is extended with respect to the gravity sector by the quadratic term of the Ricci scalar. We can see that, by this additional quadratic Ricci scalar, the scalar freedom of the gravity becomes dynamical:

$$\ddot{R} + 3H\dot{R} + M^2 R = 0, \tag{2.5.3}$$

where we have neglected the matter contents and assumed the FRW Universe. In the case $H \gg M$, the dynamical evolution of the Ricci scalar is approximately time independent, and inflation is achieved. Rescaling the metric and re-defining the scalar freedom, we can treat this inflation dynamics as like the ordinary inflation model. In the rescaled frame, the scalar freedom behaves as a canonical scalar field with minimally coupled to the Einstein gravity [60,61], and its fluctuations give the curvature perturbations [62]. These curvature perturbations become the seeds of the matter fluctuations. We call this rescaled frame as the Einstein frame, and in this thesis we consider the dynamics of the R^2 inflation in the Einstein frame.

For convenience of discussions, let us take a Legendre transformation with respect to R as

$$\begin{cases} \varphi \equiv \dfrac{\partial f}{\partial R}, \\ U \equiv \varphi R - f. \end{cases} \tag{2.5.4}$$

$$\implies \begin{cases} \varphi = 1 + \dfrac{R}{3M^2}, \\ U = \dfrac{3}{2}M^2 \left(\phi - 1\right)^2. \end{cases} \tag{2.5.5}$$

The Lagrangian of the gravity sector is reduced to

$$\sqrt{-g}\,\mathcal{L}_{\text{grav}} = \sqrt{-g}\,\frac{M_p^2}{2}\left[\varphi R - U\right]. \tag{2.5.6}$$

We conformally transform the metric by Ω as

$$\tilde{g}_{\mu\nu} \equiv \Omega^2 g_{\mu\nu}. \tag{2.5.7}$$

With appropriate choice of Ω, we obtain the Einstein frame. For this rescaling, the determinant of the metric and Ricci scalar are transformed as

$$\begin{cases} \sqrt{-g} = \Omega^{-4}\sqrt{-\tilde{g}}, \\ R = \Omega^2 \left[\tilde{R} + 3\tilde{\Box}\ln\Omega^2 + \dfrac{3}{2}\tilde{g}^{\mu\nu}\tilde{\partial}_\mu \ln\Omega^2 \tilde{\partial}_\nu \ln\Omega^2\right], \end{cases} \tag{2.5.8}$$

where

$$\tilde{\Box} = \frac{1}{\sqrt{-\tilde{g}}}\tilde{\partial}_\mu \left(\sqrt{-\tilde{g}}\,\tilde{g}^{\mu\nu}\tilde{\partial}_\nu\right). \tag{2.5.9}$$

Here, the tilde means that the metric is $\tilde{g}_{\mu\nu}$. Substituting these forms into the Lagrangian, we obtain

$$\sqrt{-g}\,\mathcal{L}_{\text{grav}} = \sqrt{-\tilde{g}}\left\{(\Omega^{-2}\varphi)\left[\frac{M_p^2}{2}\tilde{R} + \frac{1}{2}\tilde{g}^{\mu\nu}\tilde{\partial}_\mu\left(\sqrt{\frac{3}{2}}M_p\ln\Omega^2\right)\tilde{\partial}_\nu\left(\sqrt{\frac{3}{2}}M_p\ln\Omega^2\right)\right.\right.$$
$$\left.\left. + \frac{\sqrt{6}}{2}\tilde{\Box}\left(\sqrt{\frac{3}{2}}M_p\ln\Omega^2\right)\right] - \frac{M_p^2}{2}\Omega^{-4}U\right\}. \tag{2.5.10}$$

Now we obtain the Einstein frame by taking

$$\Omega_E^2 \equiv \varphi. \tag{2.5.11}$$

In this frame, the action of the gravity sector is reduced to

$$S = \int d^4\sqrt{-g_E}\left[\frac{M_p^2}{2}R_E + \frac{1}{2}\left(\partial_{E,\mu}\sqrt{\frac{3}{2}}M_p\ln\varphi\right)^2 - \frac{M_p^2}{2}\frac{U}{\varphi^2}\right], \tag{2.5.12}$$

where the subscript E means that the metric is $g_{E,\mu\nu}$. Here we deleted the surface term:

$$\int d^4x\sqrt{-g_E}\frac{\sqrt{6}}{2}\Box_E\left(M_p\sqrt{\frac{3}{2}}\ln\Omega_E\right) = \frac{\sqrt{6}}{2}\int d^4x\,\partial_{E,\mu}\left(\sqrt{-g_E}g_E^{\mu\nu}\partial_{E,\nu}M_p\sqrt{\frac{3}{2}}\ln\Omega_E\right)$$
$$= 0. \tag{2.5.13}$$

Let us redefine the dynamical variable by

$$\phi \equiv \sqrt{\frac{3}{2}}M_p\ln\varphi. \tag{2.5.14}$$

Then, the actions is reduced to

$$S = \int d^4x\sqrt{-g_E}\left[\frac{M_p^2}{2}R_E + \frac{1}{2}(\partial_{E,\mu}\phi)^2 - \frac{3}{4}M^2M_p^2\left(1 - e^{-\sqrt{2/3}\phi/M_p}\right)^2\right]. \tag{2.5.15}$$

Thus, in the Einstein frame, the Lagrangian of the scalar freedom is written as

$$\mathcal{L}_{\text{grav}} = \sqrt{-g}\left[\frac{M_p^2}{2}\mathcal{R} + \frac{1}{2}\partial^\mu\phi\partial_\mu\phi - V(\phi)\right], \tag{2.5.16}$$

where

$$V(\phi) = \frac{3}{4}M^2M_p^2\left(1 - e^{-\sqrt{2/3}\,\phi/M_p}\right)^2. \tag{2.5.17}$$

Here for a while, we omit the index E. It is seen that the Lagrangian for ϕ is identical to that of a canonical scalar field minimally coupled to the Einstein gravity with the potential (2.5.17). The potential is plotted in fig. 2.3. Since the potential is flat for $\phi \gtrsim M_p$, ϕ slowly rolls down along the potential, and then inflation occurs. At $\phi \simeq M_p$, inflation ends and ϕ starts to oscillate. When the decay rate becomes comparable with the Hubble parameter,
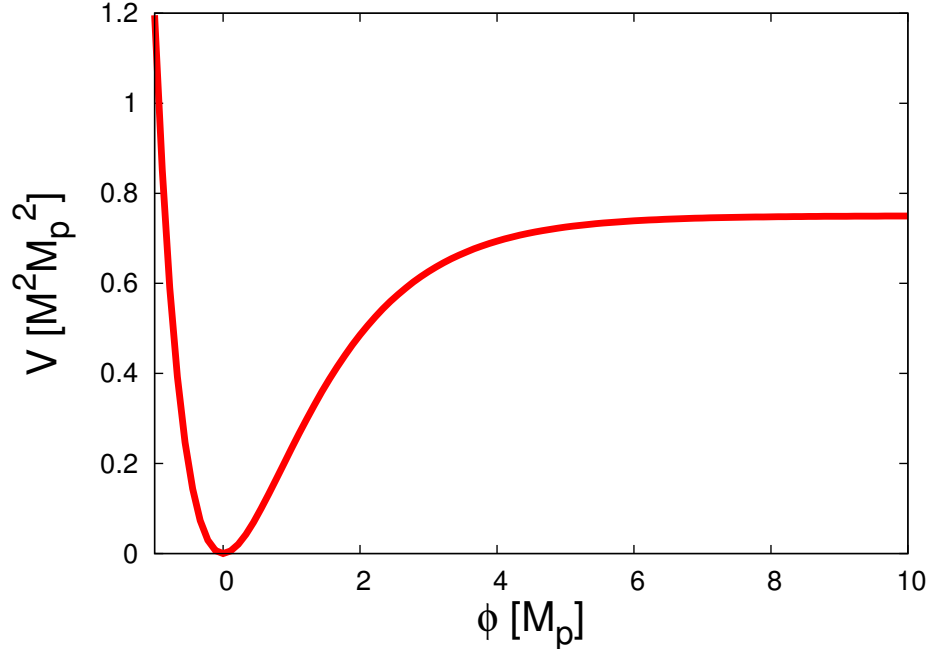
Figure 2.3: Inflaton potential of the R^2 inflation (2.5.17).

ϕ decays into the standard model particles efficiently. After the completion of reheating, ϕ settles down to the vacuum value $\phi = 0$.

For this inflaton potential, we can calculate the cosmological perturbations as explained in sec. 2.3. We can see in eqs. (2.5.1) and (2.5.2), that the action has only a single extra parameter M. Thus, the dynamics of the R^2 inflation is determined by M. First, let us calculate the e-folding number under the slow-roll approximation,

$$
\begin{aligned}
N_e = \int_{t_p}^{t_e} H dt &\simeq \int_{\phi_e}^{\phi_p} \frac{V}{M_p^2 V'} d\phi \\
&= \frac{\sqrt{3}}{2\sqrt{2}} \frac{1}{M_p} \int_{\phi_e}^{\phi_p} d\phi \left(e^{\sqrt{2/3}\phi/M_p} - 1 \right) \\
&\simeq \frac{3}{4} e^{\sqrt{2/3}\,\phi_p/M_p},
\end{aligned}
\tag{2.5.18}
$$

where t_p is the time that the pivot scale exits the horizon, and t_e is the one that inflation ends. Here we have assumed that the field value at the pivot scale is larger than the Planck mass: $\phi_p > M_p$. The field value at the end of inflation is estimated by the break down of the slow-roll condition $\epsilon_V = 1$ as $\phi_e \simeq 0.94 M_p$. Using this and eq. (2.3.41), we can estimate the power spectrum of the curvature perturbations at the pivot scale ($k^{-1} \simeq 0.002\,\mathrm{M_{pc}}^{-1}$)

as

$$\mathcal{P}_{\mathcal{R}_c} \simeq \frac{1}{12\pi^2} \frac{V^3}{M_p^6 V'^2} \simeq \frac{1}{12\pi^2} \frac{1}{2} \left(\frac{3}{4}\right)^2 \left(\frac{M}{M_p}\right)^2 e^{2\sqrt{2/3}\phi_p/M_p}$$

$$\simeq \frac{1}{24\pi^2} N_e^2 \left(\frac{M}{M_p}\right)^2. \tag{2.5.19}$$

By the observation of CMB, the amplitude is measured as $\mathcal{P}_{R_c} \simeq 2 \times 10^{-9}$ [30]. Thus, the mass parameter M is determined as

$$M \simeq 10^{-5} \frac{4\pi\sqrt{30}}{N_e} \left(\frac{\mathcal{P}_{\mathcal{R}_c}}{2 \times 10^{-9}}\right)^{1/2} M_p$$

$$\simeq 1.3 \times 10^{-5} \left(\frac{N_e}{55}\right)^{-1} \left(\frac{\mathcal{P}_{\mathcal{R}_c}}{2 \times 10^{-9}}\right)^{1/2} M_p. \tag{2.5.20}$$

Let us also calculate the values of the slow-roll parameters ϵ_V and η_V at the pivot scale,

$$\begin{cases} \epsilon_V = \frac{M_p^2}{2} \left(\frac{V'}{V}\right)^2 \simeq \frac{4}{3} e^{-2\sqrt{2/3}\phi_p/M_p} \simeq \frac{3}{4} \frac{1}{N_e^2}, \\ \eta_V = M_p^2 \frac{V''}{V} \simeq -\frac{4}{3} e^{-\sqrt{2/3}\phi_p/M_p} \simeq -\frac{1}{N_e}. \end{cases} \tag{2.5.21}$$

In sec. 2.3, we have explained that the spectral index n_s and tensor to scalar ratio r are written by the slow-roll parameters. Thus, for the R^2 inflation, those are determined by N_e as

$$n_s - 1 \quad \simeq \quad -6\epsilon_V + 2\eta_V \simeq -\frac{2}{N_e}, \tag{2.5.22}$$

$$r \quad \simeq \quad 16\epsilon_V \simeq \frac{12}{N_e^2}. \tag{2.5.23}$$

By estimating the e-folding number, we can predict these parameters theoretically.

The theoretical prediction of N_e is related to the reheating temperature T_R. Its relation is obtained by comparing the present comoving horizon $(a_0 H_0)^{-1}$ to the comoving horizon scale when the corresponding scale exits the horizon $(a_p H_p)^{-1}$ during inflation:

$$1 = \frac{a_p H_p}{a_0 H_0} = \frac{a_p}{a_e} \frac{a_e}{a_R} \frac{a_R}{a_0} \frac{H_p}{H_0}$$

$$= e^{-N_e} \left(\frac{V(\phi_e)}{\frac{\pi^2}{30} g_* T_R^4}\right)^{-1/3} \left(\frac{T_R}{T_0}\right)^{-1} \frac{\sqrt{V(\phi_e)/3M_p^2}}{\sqrt{\rho_c/3M_p^2}}. \tag{2.5.24}$$

Here ρ_c is the present critical density $\rho_c \simeq \left(3. \times 10^{-3}\text{eV}\right)^4 0.67^2$, T_0 is the present CMB temperature $T_0 \simeq 2.7K$, and g_* is the relativistic freedom at the reheating $g_* \simeq 106.75$. Substituting these parameters and the energy scale of the inflation $V(\phi_e) \simeq (3/4)M^2 M_p^2$, we obtain the relation between the e-folding number and reheating temperature as

$$N_e \simeq 54 + \frac{1}{3} \ln \frac{T_R}{10^9 \text{GeV}}. \tag{2.5.25}$$

The reheating temperature is determined by the decay rate of the inflaton as explained in sec. 2.4.

Perturbative decay

Since the inflaton of the R^2 inflation is the scalar graviton, it has gravitational interactions with other particles. Thus, without supposing additional interactions, it decays into the standard model particles [32, 58]. In order to define the Einstein frame, we have rescaled the metric. By this rescaling, the metric of the matter sector is also modified. In the Einstein frame, we can explicitly write down the interactions between the inflaton ϕ and other particles [33–35]. Here we review the decay process of the inflaton in the Einstein frame, mainly following [34].

The Lagrangian of the standard model contains a scalar filed(=Higgs) χ and fermion fields(=leptons and quarks) ψ. To make physics clear, consider a $U(1)$ charge for those fields with a gauge field A_μ. Furthermore, we assume that the vacuum expectation value of the Higgs field during the reheating is small, and then the mass of the standard model particles are smaller than the inflaton mass. The Lagrangian of the matter sector is written as

$$
\begin{aligned}
\mathcal{L}_{\text{matter}} &= \mathcal{L}_\chi + \mathcal{L}_\psi + \mathcal{L}_{A_\mu} \\
&= \sum_{s=1}^{N_\chi} \left[(D_\mu \chi_s)^* D^\mu \chi_s - m_s^2 |\chi_s|^2 \right] + \sum_{f=1}^{N_\psi} \bar{\psi}_f \left(i \, \slashed{D} - m_f \right) \psi_f \\
&\quad - \frac{1}{4} F_{\mu\nu} F^{\mu\nu},
\end{aligned}
\tag{2.5.26}
$$

where N_χ and N_ψ are the number of degrees of freedom of the scalar and fermion fields. Here $F^{\mu\nu}$ is the field strength of the gauge field:

$$
F^{\mu\nu} \equiv g^{\mu\rho} g^{\nu\sigma} \left(A_{\sigma;\rho} - A_{\rho;\sigma} \right) = g^{\mu\rho} g^{\nu\sigma} \left(\partial_\rho A_\sigma - \partial_\sigma A_\rho \right).
\tag{2.5.27}
$$

We have defined covariant derivatives:

$$
\begin{cases}
D^\mu \chi \equiv g^{\mu\nu} \left(\partial_\mu - i g_a A_\nu \right) \chi, \\
\slashed{D} \psi \equiv e_\alpha^\mu \gamma^\alpha \left(\partial_\mu - \Gamma_\mu - i g_a A_\mu \right) \psi,
\end{cases}
\tag{2.5.28}
$$

where γ^α is the Gamma matrix, e_α^μ is the tetrad with Lorentz indices: $\alpha, \beta, \cdots$ and coordinate indices: $\mu, \nu, \cdots$, and Γ_μ is the spin connection defined as $\Gamma_\mu \equiv (1/8) \left[\gamma^\alpha, \gamma^\beta \right] e_\alpha^\lambda e_{\lambda\beta:\mu}$. By the rescale of the metric (2.5.7), the kinetic terms of the fields are also rescaled. In order to keep them canonical, we rescale the fields:

$$
\begin{cases}
\chi_E \equiv \Omega_E^{-1} \chi, \\
\psi_E \equiv \Omega_E^{-3/2} \psi, \\
A_{E,\mu} \equiv A_\mu \to A_E^\mu = \Omega_E^{-2} A^\mu.
\end{cases}
\tag{2.5.29}
$$

For these transformations, the Lagrangians are reduced to

$$\sqrt{-g}\,\mathcal{L}_\chi \;=\; \sqrt{-g_E}\sum_{s=1}^{N_\chi}\left[g_E^{\mu\nu}\left(D_{E,\mu}\chi_{E,s}\right)^* D_{E,\nu}\chi_{E,s} - \Omega_E^{-2}m_s^2|\chi_{E,s}|^2\right], \quad (2.5.30)$$

$$\sqrt{-g}\,\mathcal{L}_\psi \;=\; \sqrt{-g_E}\sum_{f=1}^{N_\psi}\bar\psi_{E,f}\left[i\,\slashed{D}_E - \Omega_E^{-1}m_f\right]\psi_{E,f}, \quad (2.5.31)$$

$$\sqrt{-g}\,\mathcal{L}_{A_\mu} \;=\; -\frac{1}{4}\sqrt{-g_E}\,g_E^{\mu\rho}g_E^{\nu\sigma}F_{E,\mu\nu}F_{E,\rho\sigma}. \quad (2.5.32)$$

Here the covariant derivatives in the Einstein frame are defined as

$$\begin{cases} D_{E,\nu}\,\chi_E = \partial_{E,\mu}\,\chi_E + \chi_E\,\partial_{E,\mu}\ln\Omega_E - ig_a A_{E,\mu}\chi_E, \\ \slashed{D}_E\,\psi_E = ie_{E,\alpha}^\mu\gamma^\alpha\left(\partial_{E,\mu} - \Gamma_{E,\mu} - ig_a A_{E,\mu}\right)\psi_E. \end{cases} \quad (2.5.33)$$

We have defined the Einstein frame by

$$\Omega_E^2 = \varphi = e^{-\sqrt{2/3}\phi/M_p}. \quad (2.5.34)$$

Thus, through the conformal factor Ω_E^2, the scalars and fermions have the interactions with the inflaton ϕ. By these interactions, the inflaton decays into those fields. On the other hands, as the gauge fields are conformally invariant, the inflaton does not have direct interactions with them. However, if we consider quantum effects, the inflaton decays into the gauge fields by loop effect. In the case that the mass of particles is larger than the inflaton mass, breakings of the conformal invariance become significant, and then the inflaton decays into gauge fields more copiously. In this section, let us limit the discussion for the smaller mass of fields.

First, let us consider interactions with χ. Expanding the covariant derivative and mass terms with respect to ϕ, we can obtain the following interactions:

$$\begin{cases} D_\mu\chi_E = \partial_{E,\mu}\chi_E - \sqrt{\frac{1}{6}}\frac{\phi}{M_p}\chi_E - ig_a A_{E,\mu}\chi_E, \\ -\Omega_E^{-2}m_s^2|\chi_E|^2 \simeq -m_s^2\left[1 - \sqrt{\frac{2}{3}}\frac{\phi}{M_p}\right]|\chi_E|^2. \end{cases} \quad (2.5.35)$$

$$\Longrightarrow \mathcal{L}_{\text{int},\phi\chi\chi} \simeq \frac{1}{\sqrt{6}M_p}\left[\chi_E\partial_E^\mu\chi_E^*\partial_{E,\mu}\phi + \partial_E^\mu\chi_E\chi_E^*\partial_{E,\mu}\phi 2m_\chi^2|\chi_E|^2\phi\right],$$

$$= -\frac{2}{\sqrt{6}M_p}\phi\partial^\mu\chi^*\partial_\mu\chi + \frac{4m_{\chi^2}}{\sqrt{6}M_p}\phi|\chi_E|^2, \quad (2.5.36)$$

where we have only considered leading terms in the expansion. Thus, from the above interactions, the decay rate of the inflaton into χ is given by

$$\Gamma(\phi \to \chi\chi) = \frac{N_\chi\left[M^2 + 2m_\chi^2\right]^2}{96\pi M M_p^2}\sqrt{1 - \frac{4m_\chi^2}{M^2}} \simeq \frac{N_\chi}{96\pi}\left(\frac{M}{M_p}\right)^2 M. \quad (2.5.37)$$

As for ψ, the interactions arise from the mass term as

$$\bar{\psi}_E \Omega_E^{-1} m_f \psi_E \simeq \left(1 - \frac{1}{\sqrt{6}} \frac{\phi}{M_p}\right) m_f \bar{\psi}_E \psi_E. \tag{2.5.38}$$

$$\implies \mathcal{L}_{\text{int},\phi\bar{\psi}\psi} \simeq \frac{m_\psi}{\sqrt{6} M_p} \phi \bar{\psi}_E \psi_E. \tag{2.5.39}$$

Thus, for these interactions, the decay rate is given by

$$\Gamma\left(\phi \to \bar{\psi}\psi\right) = \frac{N_\psi M m_\psi^2}{48\pi M_p^2}\left(1 - 4\frac{m_\psi^2}{M^2}\right)^{3/2} \simeq \frac{N_\psi}{48\pi}\left(\frac{m_\psi}{M_p}\right)^2 M. \tag{2.5.40}$$

Since the gauge field is conformally invariant, the inflaton does not have interactions with it. However, by the propagation of the fermion or the scalar field in the loop as shown in fig. 2.4, the inflaton can decay into the gauge field at the quantum level. In the diagrams in fig. 2.4, the relevant interactions between the gauge field and ψ or χ are give by $\simeq g_a A \bar{\psi}\psi$ or $\simeq g_a^2 A^2 \chi^2$, and hence the interactions between inflation and ψ or χ are given by $\simeq (m_\psi/M_p)\phi\bar{\psi}\psi$ or $\simeq (m_\chi^2/M_p)\phi\chi\chi$ and $\simeq (1/M_p)\phi|\partial\chi|^2$. Thus, the decay rates are estimated as [34]

$$\Gamma_f\left(\phi \to 2A\right) = \frac{\alpha^2 N_\psi^2}{384\pi^3}\left(\frac{M}{M_p}\right)^2 M \left|I_f\left(\frac{m_\phi^2}{m_\psi^2}\right)\right|^2, \tag{2.5.41}$$

$$\Gamma_s\left(\phi \to 2A\right) = \frac{\alpha^2}{1536\pi^3}\left(\frac{M}{M_p}\right)^2 M \left(2 + \frac{M^2}{M_\chi^2}\right)^2 \left|I_s\left(\frac{m_\phi^2}{m_\chi^2}\right)\right|^2, \tag{2.5.42}$$

where the functions $I_f(\xi)$ and $I_s(\xi)$ are defined as

$$I_f(\xi) = \int_0^1 dx \int_0^{1-x} df \frac{1 - 4xy}{1 - \xi xy}, \tag{2.5.43}$$

$$I_s(\xi) = \int_0^1 dx \int_0^{1-x} dy \frac{4xy}{1 - \xi xy}. \tag{2.5.44}$$

Here α is a gauge coupling constant $\alpha \equiv g_a^2/(4\pi) \ll 1$. We are now considering that the inflaton mass $m_\phi \simeq M \simeq 10^{-5} M_p$ is much heavier than m_ψ and m_χ, $m_\phi \gg m_\psi$ and $m_\phi \gg m_\chi$. For this limit, the functions behave as $I_f(\xi) \to 0$ and $I_s(\xi) \to 0$ while $(2 + \xi)I_s(\xi) \to 2$ in the limit of $\xi \to \infty$. Hence, in the limit of $m_\phi \gg m_\psi$, m_χ, the decay rates are reduced to $\Gamma_f \to 0$ and $\Gamma_s \to \alpha^2/(768)(M/M_p)^2 M$. Thus, the total decay rate is given by

$$\Gamma_{\text{tot}} \simeq \Gamma\left(\phi \to \chi\chi\right) + \Gamma\left(\phi \to \bar{\psi}\psi\right) + \Gamma_f\left(\phi \to 2A\right) + \Gamma_s\left(\phi \to 2A\right)$$
$$\simeq \Gamma\left(\phi \to \chi\chi\right) \simeq \frac{N_\chi}{96\pi}\left(\frac{M}{M_p}\right)^2 M. \tag{2.5.45}$$

Note that, in the standard model, χ is the Higgs boson and $N_\chi = 4$.

Now we have determined the decay rate by the mass parameter M. Thus, using eq. (2.4.7), we can calculate the reheating temperature:

$$T_R \simeq 0.4\sqrt{\Gamma_{\text{tot}} M_p} \simeq 0.4 \left(\frac{N_\chi}{96\pi}\right)^{1/2} \frac{M}{M_p}\sqrt{MM_p} \simeq 10^{-9} M_p. \qquad (2.5.46)$$

Using this, we can give the prediction for the e-folding number corresponding to the pivot scale for the R^2 inflation model:

$$N_e \simeq 54 + \frac{1}{3}\left(\frac{T_R}{10^{-9}\,\text{M}_\text{p}}\right). \qquad (2.5.47)$$
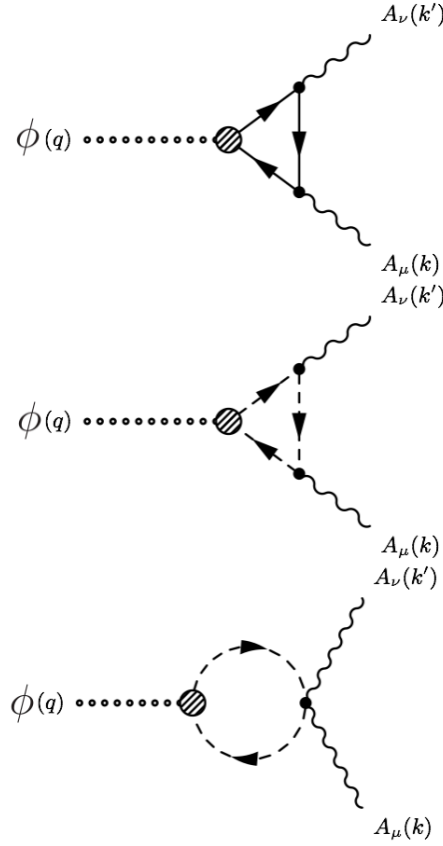

Figure 2.4: 1-loop diagram for the decay of the inflaton into the gauge field [34]. Note, we have changed the notion from [34] such as $\sigma \to \phi$. In the upper panel (lower two panels), the fermion ψ (scalar ϕ) is propagating in the loop.

Chapter 3

Review of I-balls

It is known that some of scalar fields could form stable and localized objects such as topological defects or Q-balls. By the formation of such objects, the dynamics of the field such as the decay process or dilution rate of the energy density due to the Hubble expansion would be affected. Thus, to study the scenario of the Universe, we have to pay attention to the formation of the objects.

The stability of such objects are guaranteed by a conserved quantity such as a topological number for topological defects or a $U(1)$ charge for Q-balls. Based on the conserved quantities, the formation of the objects and their longevity are explained. However, there is some objects whose formation and stability are not yet clarified analytically. One of such objects is I-balls. I-balls are spatially localized objects, which consist of a real scalar field. Inside I-balls, the field is oscillating periodically, and its period is approximately given by the inverse mass of the field. By numerical simulations, the natures of I-balls have been investigated, and it is found that the lifetime of the objects is significantly larger than the period of the oscillation. However, the longevity has not yet been explained very well. As I-balls are formed by an oscillating real scalar field, it seems difficult to consider some conserved quantities like topological defects or Q-balls. Thus, if we want to study whether I-balls are formed or not for a specific potential, numerical simulations are required.

I-balls were first discovered in [23, 24] when the authors were studying elementary particles of a finite size, and after a while, I-balls were rediscovered in [25] when the author was studying a spontaneous symmetry breaking. By further investigations, especially by numerical simulations, the properties of I-balls have been revealed. It is heuristically known that for the formation of I-balls, the potential of the field should be flatter than the quadratic one. If the initial state of the field is a coherent oscillation, the formation occurs after significant oscillations. After the formation, for some potentials, I-balls emit radiations from the surface and then gradually decay [63,64].

As I-balls are spatially localized objects, if the initial field is nearly homogeneous, for the formation of I-balls, small fluctuations around the homogeneous distribution should be enhanced by some mechanism such as the parametric resonance. By the parametric resonance, fluctuations grow at a particular scale exponentially at first. Then, after they grow and become comparable with the background field, the interactions of fluctuations with other mode become efficient. For some class of potentials with flatter shape, the field may fragment into I-balls through the non-linear process. The formation is also confirmed

even in the expanding Universe [65]. In [66–68], it is verified by numerical simulations that for the formation in the expanding Universe, the growth rate of fluctuations should be larger than the Hubble parameter. First, we review the mechanism of the enhancement of fluctuations, and then review the heuristic condition on the growth rate.

As mentioned above, the stability of I-balls are yet not understood, but there're some proposals for the stability of I-balls. It was conjectured in [26] that the stability of I-balls is due to an existence of some conserved quantity like Q-balls and topological defects, which we call as adiabatic charge. The adiabatic charge comes from the adiabatic invariance known in a classical mechanical system extended to a classical field theory. The adiabatic invariant is briefly explained as follows. Let us here consider a periodic oscillation of a point particle in a classical mechanical system. In the system, the motion of the particle on the phase space is periodic and closed. Thus, evidently, the area surrounded by the trajectory of the motion is time independent. In the case that there is an external force on the system, the trajectory is not closed, and the oscillation is quasi-periodic. It is known that, even for the quasi-periodic oscillation, the area is approximately time independent. This area is called adiabatic invariant. In [26], the authors showed that the adiabatic invariant (or charge) exists even for a classical field theory, and they showed that the nature of I-balls could be understood by it. If the adiabatic charge is conserved for an oscillating field, we can consider the lowest energy state for a fixed value of the adiabatic charge. In this case, it is verified that a localized configuration of the field exists for potentials that are flatter than the quadratic one. Thus, by the adiabatic charge, we can derive the heuristic condition on the shape of potentials for I-balls to form.

In [26], the conservation of the adiabatic charge was proved in a certain case where the spatial gradient energy is negligible. In this chapter, we give a more general and rigorous proof that the adiabatic charge is conserved for a potential that allows a periodic motion of the field. In contrast to the previous work [26], this argument does not rely on the assumption that the spatial gradient energy is negligible. After the proof, we derive the condition on the shape of potentials for the formation of I-balls.

3.1 Growth of fluctuations

Let us consider a scalar field χ interacting with another scalar field ϕ, and assume that ϕ is oscillating coherently. In this case, fluctuations of χ might be enhanced by the motion of ϕ through the interaction. We describe the mechanism of the enhancement.

As ϕ is oscillating, the interaction term of χ with it oscillates periodically. Thus, the frequency of the mode function of χ would become a periodic function. We denote the time dependent frequency by $f(t, k)$. Then, the equation of motion for the mode function of χ, χ_k is written as

$$\frac{d^2}{dt^2}\chi_k + f(t, k)\chi_k = 0. \tag{3.1.1}$$

The above equation is a linear one with respect to χ_k with a periodically oscillating coefficient $f(t, k)$. According to the Floquet theorem, the solution of such equation is written by a complex parameter $\mathcal{M}_k$ and stationary periodic function $P_{\pm}(t)$ as

$$\chi_k(t) = c_+ P_+(t)e^{\mathcal{M}_k t} + c_- P_-(t)e^{-\mathcal{M}_k t}, \tag{3.1.2}$$

where c_+ and c_- are arbitrary constants. The stability/instability of the solution is determined by the parameter $\mathcal{M}_k$. When the real part of $\mathcal{M}_k$ is non-zero as $\mu_k \equiv \mathrm{Re}(\mathcal{M}_k) \neq 0$, the solution exponentially increases. The explicit form of the parameter $\mathcal{M}_k$ and function $P_\pm(t)$ depend on the potential of the scalar fields and their interactions. If the potentials allow the parametric resonance to take place, μ_k is non-zero at particular momentum. If the potentials are such as a double well potential, which allows the spontaneous symmetry breaking, μ_k is non-zero for momenta lower than the mass of the field. In this case, fluctuations grow more violently than the parametric resonance, which is called tachyonic resonance.

The parametric resonance or other mechanisms gives a rapid growth of fluctuations, and they re-scatter with the background field or other modes. When this backreaction becomes efficient, the dynamics of the coherent mode is affected, and then the resonance terminates. In this stage, the spatial distribution of the energy density is highly inhomogeneous. Through the non-linear state, for some class of potentials, the field fragments and forms I-balls, which is described later.

3.1.1 Parametric resonance

As analytically solvable examples, we explain the parametric resonance. For simplicity, we assume that a scalar field ϕ only couples to another scalar field χ, the Lagrangian of which is given by

$$\mathcal{L} = \frac{1}{2}(\partial_\mu\phi)^2 - V(\phi) + \frac{1}{2}(\partial_\mu\chi)^2 - \frac{1}{2}m_\chi^2\chi^2 - V_{\mathrm{int}}(\phi, \chi), \tag{3.1.3}$$

where $V(\phi)$ is the potential of ϕ, m_χ is the mass of χ and $V_{\mathrm{int}}(\phi, \chi)$ is the interaction between the two fields. In this subsection, we assume that the mass of χ is sufficiently small compared with the mass of ϕ and set it to zero. (If we identify χ with fluctuations of ϕ as $\chi = \delta\phi$ and choose an appropriate interaction, we can analyze the amplification of fluctuations of ϕ itself.)

Instabilities of the mode function χ_k depend on $V(\phi)$ and V_{int}. For the convenience, in this sub-section, we mainly consider a quartic interaction and a quadratic or quartic potential for $V(\phi)$. In the case that ϕ oscillates with a quadratic potential, the equation of motion for χ_k is reduced to the Mathieu equation [69]. On the other hand, in the case that ϕ oscillates with a quartic potential, the equation of motion is reduced to the Lamé equation [28, 29, 70, 71]. Considering the two cases, we calculate the growth rate μ_k.

Quadratic potential

First, we consider the scalar field ϕ with a quadratic potential,

$$V(\phi) = \frac{1}{2}m_\phi^2\phi^2, \tag{3.1.4}$$

and a quartic interaction,

$$V_{\mathrm{int}} = \frac{1}{2}g^2\phi^2\chi^2, \tag{3.1.5}$$

where g is a dimensionless coupling constant. By the interaction term, the effective mass of χ depends on ϕ. Here we assume that ϕ oscillates with a time independent amplitude Φ. In this case, the effective mass of χ oscillates periodically:

$$m_{\chi,\text{eff}}^2 = g^2 \Phi^2 \sin^2(m_\phi t), \tag{3.1.6}$$

where we have neglected an arbitrary phase of ϕ's oscillation. Thus, the frequency of χ_k is time dependent:

$$\omega_k^2 = k^2 + g^2 \Phi^2 \sin^2(m_\phi t). \tag{3.1.7}$$

Normalizing the time variable by the mass of ϕ as $z \equiv m_\phi t$, we can reduce the equation of motion for χ_k to the Mathieu equation [69], which is characterized by two parameters q and A_k as

$$\frac{d^2}{dz^2}\chi_k + (A_k - 2q\cos(2z))\chi_k = 0, \tag{3.1.8}$$

where q and A_k are defined as

$$\begin{cases} q \equiv \dfrac{g^2}{4}\left(\dfrac{\Phi}{m_\phi}\right)^2, \\[2mm] A_k \equiv \left(\dfrac{k}{m_\phi}\right)^2 + 2q. \end{cases} \tag{3.1.9}$$

In most parameter regions of (A, q), the solution of the Mathieu equation is stationary with a periodic oscillation, in other words, the growth rate is zero, which is presented as the white region in fig. 3.1. However, if the set of parameters (A, q) is in the blue region in fig. 3.1, the solution grows exponentially,

$$\chi_k \propto e^{\mu_k z} = e^{\mu_k m_\phi t}. \tag{3.1.10}$$

Here, μ_k is non-zero when (A_k, q) is located in the instability region. This exponential growth of χ_k corresponds to the rapid production of particles by the oscillation of ϕ. For this mode, the occupation number is defined by the Hamiltonian divided by the frequency ω_k as

$$n_k \equiv \frac{\omega_k}{2}\left(\frac{|\dot{\chi}_k|^2}{\omega_k^2} + |\chi_k|^2\right) - \frac{1}{2}. \tag{3.1.11}$$

Thus, the rapid growth of the occupation number at the instability mode is given by

$$n_k \propto e^{2\mu_k m_\phi t}. \tag{3.1.12}$$

The instability region shown in fig. 3.1 is divided into two regions according to the typical width of the instability band and to the behavior of the amplification. The two regions are classified by q as

$$\begin{cases} q < 1 \rightarrow \text{narrow resonance} \\ q > 1 \rightarrow \text{broad resonance.} \end{cases} \tag{3.1.13}$$

In the case $q < 1$, the enhancement of the fluctuations is called narrow resonance, and in the other case $q > 1$, the enhancement is called broad resonance.

The feature of the narrow resonance is that the instability occurs for a narrow range of A, and its width is described by an integer n and q up to numerical factors as

$$|A - n^2| < q^n. \tag{3.1.14}$$

The growth rate in the instability region μ_k is characterized by n and q. The most efficient one is for $n = 1$, and for larger n, it becomes smaller. Here we show the explicit relation for the largest growth rate, i.e., μ_k for $n = 1$ (first band) as [28,37]

$$\mu_k|_{n=1} = \left[\left(\frac{q}{2} \right)^2 - \frac{1}{4}(A_k - 1)^2 \right]^{1/2} \simeq \frac{q}{2}. \tag{3.1.15}$$

At this first band, the mode function and the occupation number increase as shown in the left panel of fig. 3.2 [70], where the parameters are set to $(A, q) = (1, 0.1)$. From this figure, we can see that the resonance occurs continuously through the oscillation of ϕ.

In the case of the broad resonance $q > 1$, the instability occurs for a broad range of A. The instability is characterized by breakdown of the adiabatic condition:

$$\frac{|\dot{\omega}_k|}{\omega_k^2} \gg 1. \tag{3.1.16}$$

Left hand side of eq. (3.1.16) is evaluated as

$$\frac{|\dot{\omega}_k|}{\omega_k^2} \simeq \frac{|\dot{\phi}|}{g\phi^2} \simeq \frac{m_\phi}{g\phi}. \tag{3.1.17}$$

Thus, the breakdown of the adiabatic condition occurs when the velocity of ϕ becomes large, and amplitude does small, i.e., around the minimum of the potential. The increase of the mode function by the broad resonance is shown in the right panel of fig. 3.2 [70], where parameters are set as $(A, q) = (1, 200)$. Since the broad resonance occurs for q larger than unity, the frequency ω_k at the resonance band is larger than the mass of ϕ. Thus, χ_k experiences lots of oscillations during one oscillation of ϕ, and as ϕ passes around the minimum of the potential, it is amplified. This mechanism is explained as bellow.

For the convenience of discussion, suppose that ϕ passes the bottom of the potential at time t_j $(j = 1, 2, ...)$. Most region between t_{j-1} and t_j, the adiabatic condition is satisfied: $|\dot{\omega}_k|/\omega_k^2 < 1$, and χ_k oscillates stationary. In this region, the solution of the equation of motion

$$\ddot{\chi}_k + \omega_k^2 \chi_k = 0, \tag{3.1.18}$$

is given by the WKB approximation as

$$\chi_k(t) = \frac{\alpha_k^j}{\sqrt{2\omega_k}} e^{i \int \omega_k dt} + \frac{\beta_k^j}{\sqrt{2\omega_k}} e^{i \int \omega_k dt}. \tag{3.1.19}$$

Here the coefficients α_k^j and β_k^j are called Bogolyubov coefficients, which satisfy the following normalization:

$$|\alpha_k^j|^2 - |\beta_k^j|^2 = 1. \tag{3.1.20}$$

34

The occupation number is calculated using the Bogolyubov coefficients as

$$n_k = |\beta_k|^2. \tag{3.1.21}$$

As ϕ reaches the bottom of the potential, the adiabatic condition breaks down, and the solution of the mode equation cannot be approximated by the WKB solution. However, we can obtain the solution of the equation of motion using the approximation form of $\phi^2(t)$. When ϕ oscillate around the minimum of potential, the argument of ϕ modulo $\pi/2$ is nearly zero. Thus, we can approximate $\phi^2(t)$ by a quadratical function of the time as

$$\phi^2(t) \simeq \Phi^2 m_\phi^2 (t - t_j)^2. \tag{3.1.22}$$

By this approximation, we can reduce the mode equation to the Weber's equation as

$$\frac{d^2}{d\tau^2} \chi_k + (\kappa^2 + \tau^2)\chi_k = 0, \tag{3.1.23}$$

where we have normalized the time variable as $\tau \equiv g\,\Phi\,m_\phi(t - t_j)$, and the momentum as $\kappa^2 \equiv k^2/(g\,\Phi\,m_\phi)$. The exact solution of this Weber's equation is given by the parabolic cylinder function $W(-\kappa^2/2; \pm\tau)$.

Connecting the asymptotic form of the cylinder function to the WKB solution (3.1.19), we obtain the transformation matrix of the Bogolyubov coefficients:

$$\begin{pmatrix} \alpha_k^{j+1} \\ \beta_k^{j+1} \end{pmatrix} = \begin{pmatrix} \sqrt{1 + e^{-\pi\kappa^2}}\, e^{i\varphi_k} & i e^{-\frac{\pi}{2}\kappa^2 + 2i\theta_k^j} \\ -i e^{-\frac{\pi}{2}\kappa^2 - 2i\theta_k^j} & \sqrt{1 + e^{-\pi\kappa^2}}\, e^{i\varphi_k} \end{pmatrix} \begin{pmatrix} \alpha_k^j \\ \beta_k^j \end{pmatrix}. \tag{3.1.24}$$

Here θ_k^j is the phase variation from $t = 0$ to $t = t_j$ and is given by

$$\theta_k^j = \int_0^{t_j} \omega_k dt, \tag{3.1.25}$$

and φ_k is given by

$$\varphi_k \equiv \arg\left\{ \Gamma\left(\frac{1 + i\kappa^2}{2} \right) \right\} + \frac{\kappa^2}{2}\left(1 + \ln\frac{2}{\kappa^2} \right), \tag{3.1.26}$$

where Γ is the Gamma function. Using the transformation matrix, we can calculate the occupation number n_k^{j+1} after ϕ passes through the bottom of the potential as

$$n_k^{j+1} = e^{-\pi\kappa^2} + (1 + 2e^{-\pi\kappa^2})n_k^j - 2e^{-\frac{\pi}{2}\kappa^2}\sqrt{1 + e^{-\pi\kappa^2}}\sqrt{n_k^j(1 + n_k^j)}\sin\theta_{\text{tot}}^j, \tag{3.1.27}$$

where the total phase θ_{tot}^j is given by

$$\theta_{\text{tot}}^j = 2\theta_k^j - \varphi_k + \arg\beta_k^j - \arg\alpha_k^j. \tag{3.1.28}$$

From the relation between n_k^{j+1} and n_k^j (3.1.27), we can see that for the increase of the occupation number by the broad resonance, κ needs to be smaller than $1/\sqrt{\pi}$. Thus, the instability band of the broad resonance is given by

$$k < \sqrt{g\,\Phi\,m_\phi}. \tag{3.1.29}$$

35

After several oscillations, the occupation number becomes larger than unity, and (3.1.27) is approximately reduced to

$$n_k^{j+1} = \left(1 + 2\mathrm{e}^{-\pi\kappa^2} - 2\mathrm{e}^{-\frac{\pi}{2}\kappa^2}\sqrt{1 + \mathrm{e}^{-\pi\kappa^2}}\sin\theta_{\mathrm{tot}}^j \right) n_k^j. \tag{3.1.30}$$

Thus, by the relation, we obtain the growth rate for the broad resonance:

$$\mu_k^j = \frac{1}{2\pi}\ln\left(1 + 2\mathrm{e}^{-\pi\kappa^2} - 2\mathrm{e}^{-\frac{\pi}{2}\kappa^2}\sqrt{1 + \mathrm{e}^{-\pi\kappa^2}}\sin\theta_{\mathrm{tot}}^j \right). \tag{3.1.31}$$

Quartic potential

We have seen that the oscillation of ϕ with the quadratic potential induces the instability of χ with the quartic interaction. Reducing the mode equation for χ to the Mathieu equation, we have calculated the growth rate, which is shown by (3.1.15) for the narrow resonance and by (3.1.31) for the broad resonance. Not only the quadratic oscillation, but a quartic oscillation of ϕ with a potential

$$V = \frac{\lambda}{4}\phi^4, \tag{3.1.32}$$

also induces the instability of χ with the quartic interaction $V_{\mathrm{int}} = (g^2/2)\phi^2\chi^2$. Furthermore, in this case, the quartic oscillation induces the instability in fluctuations of ϕ itself. For the quartic oscillation of ϕ with a time independent amplitude Φ, we can reduce the equation of motion for χ_k to the Lamé equation:

$$\frac{d^2}{dz^2}\chi_k + \left[\kappa^2 + \frac{g^2}{\lambda}\mathrm{cn}\left(z; \frac{1}{\sqrt{2}} \right) \right]\chi_k = 0, \tag{3.1.33}$$

where we have normalized the time variable as $z \equiv \sqrt{\lambda}\,\Phi t$ and the momentum as $\kappa^2 \equiv k^2/(\lambda\Phi^2)$, and $\mathrm{cn}(x; 1/\sqrt{2})$ is the elliptic function. As for fluctuations of ϕ, the equation of motion for the mode function is also reduced to the Lamé equation as

$$\frac{d^2}{dz^2}\delta\phi_k + \left[\kappa^2 + 3\mathrm{cn}\left(z; \frac{1}{\sqrt{2}} \right) \right]\delta\phi_k = 0. \tag{3.1.34}$$

Here we have divided the scalar field ϕ as $\phi(t, \vec{x}) = \phi_0(t) + \delta\phi(t, \vec{x})$. In the same way as the Mathieu equation, in some region in $(\kappa, g^2/\lambda)$ plane the growth rate is non-zero, and then the solution increases exponentially. The instability chart is shown in fig. 3.3 [71].

Expanding Universe

In the early Universe, the cosmic expansion rate is large due to the high energy density of the Universe. For the large expansion rate comparable with the mass of the oscillating field, the parametric resonance would be suppressed to some extent. Even in this case, by rescaling the field variables and space-time coordinates, we can reduce the equation of motion for the mode function to the Mathieu equation or Lamé equation, and then we can discuss the effects of the parametric resonance.
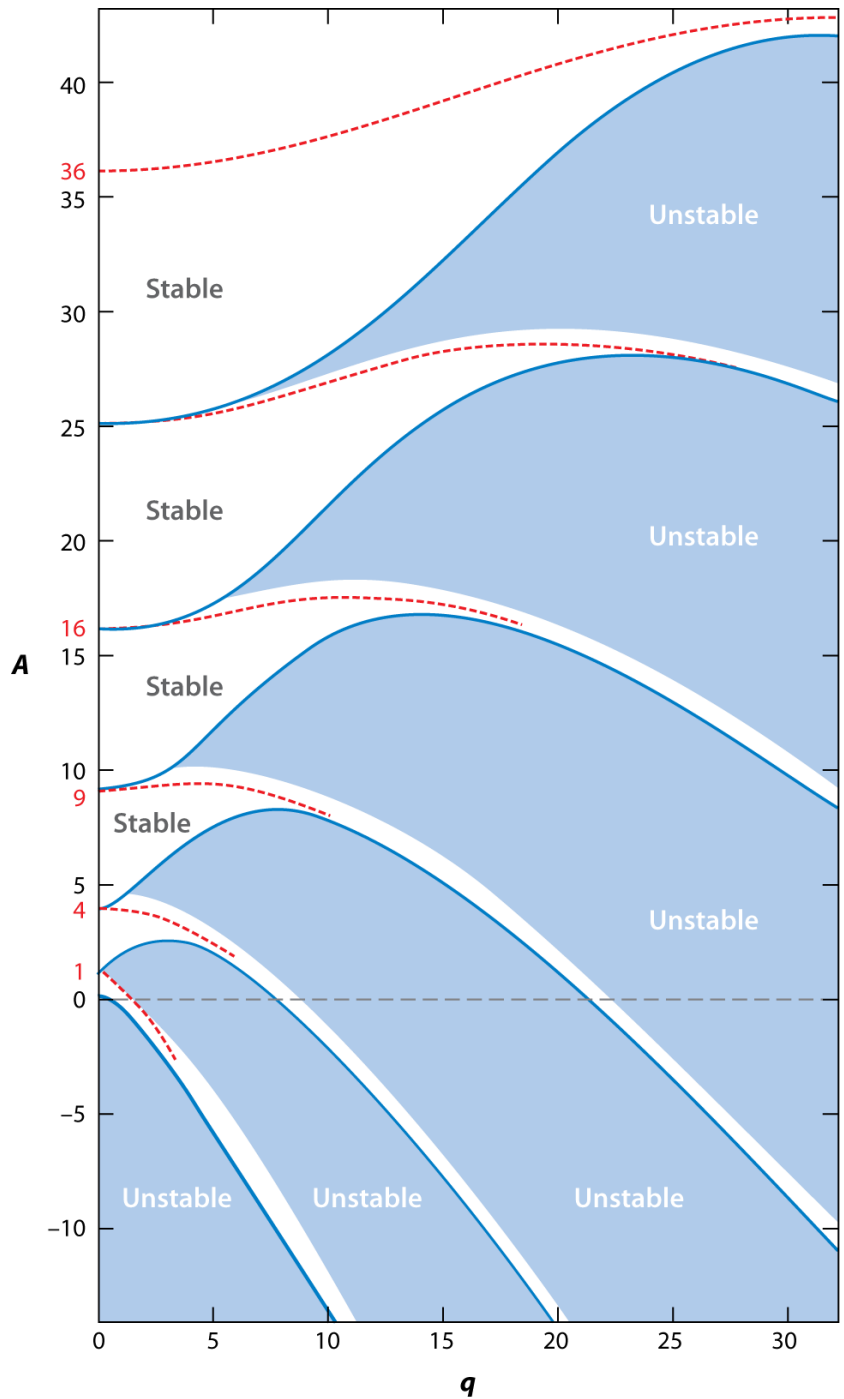
Figure 3.1: Stability and instability chart for Mathieu equation [45]. In the blue region, the solution is stationary, and in the white region the solution grows exponentially.
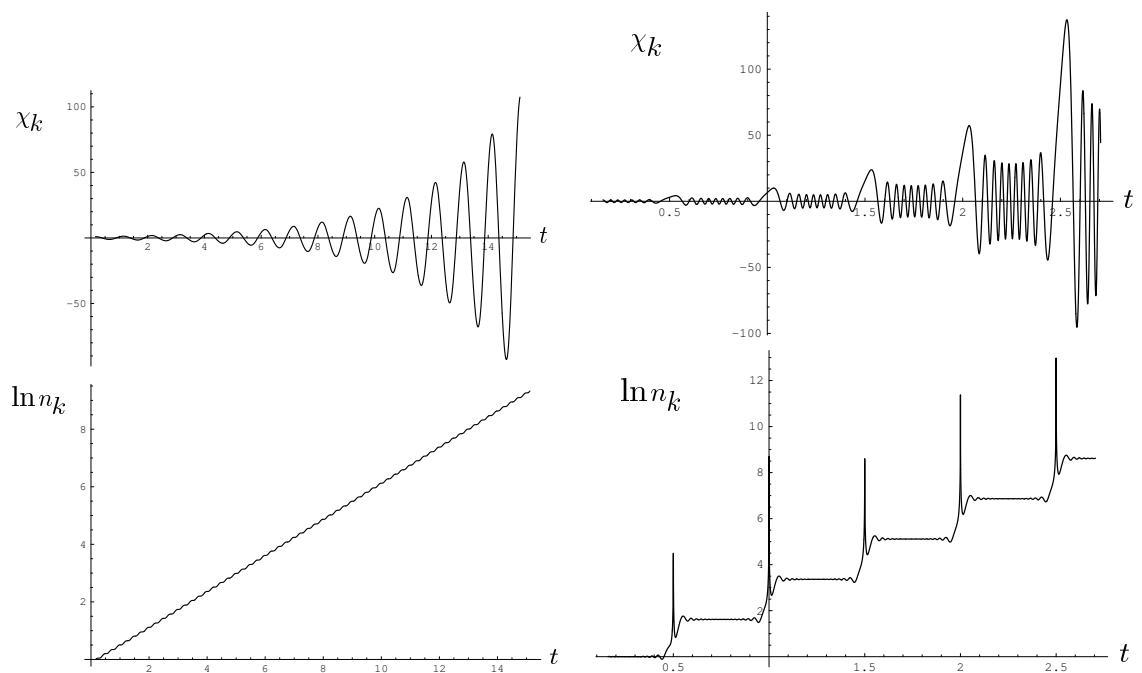
Figure 3.2: Evolution of the mode function χ_k and its occupation number n_k for narrow and broad resonances [70] in the Minkowski spacetime. The left panel shows the narrow resonance for $(A, q) = (1, 0.1)$. The right panel shows the broad resonance for $(A, q) = (1, 200)$. The unit of the time is the mass of the ϕ as m_ϕ with the division by 2π as $m_\phi/2\pi$.
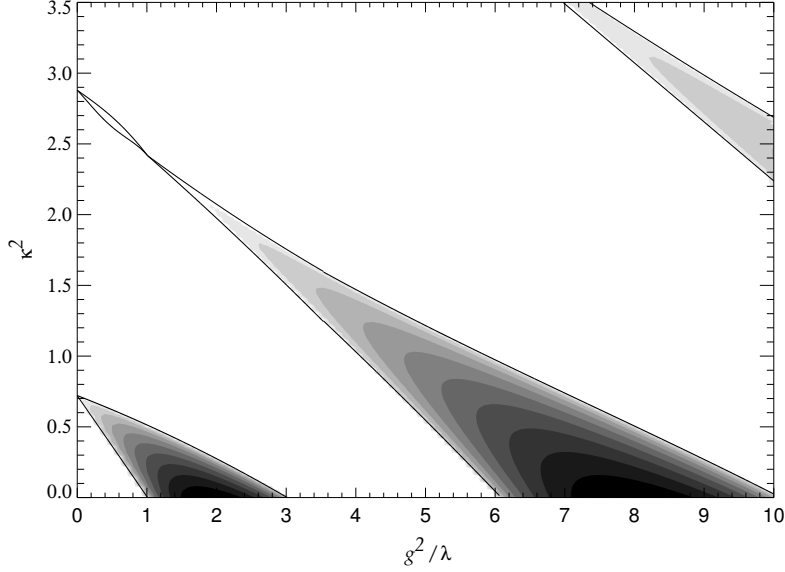
Figure 3.3: The stability-instability chart for the Lamé equation [71]. Shaded areas are regions of instability. In the instability bands, the darker shade means the larger Floquet index μ_k. One color step corresponds to the increment $\Delta\mu_k = 0.0237$.

In the FRW universe with zero curvature, the equation of motion for χ_k at a comoving momentum k is written as

$$\ddot{\chi}_k + 3H\dot{\chi}_k + \left[\frac{k^2}{a^2} + g^2\phi^2(t)\right]\chi_k = 0, \qquad (3.1.35)$$

where H is the Hubble parameter and a is the scale factor, and we assumed the quartic interaction.

Due to the Hubble expansion, the amplitude of the field damps adiabatically, and then the energy density of ϕ decreases. In the case of the quadratic potential, the energy density damps like non-relativistic particles, and the amplitude of the field scales as $\Phi \propto a^{-3/2}$. In the case of the quartic potential, the energy density damps as like relativistic particles, and the amplitude scales as $\Phi \propto a^{-1}$.

First, we consider the quadratic potential $V = m_\phi^2\phi^2/2$. In this case, we rescale the fields as $\tilde{\phi} = a^{3/2}\phi$ and $\tilde{\chi} = a^{3/2}\chi$. Then, the equation of motion is reduced to the Mathieu equation as

$$\frac{d^2}{dz^2}\tilde{\chi}_k + \left(\tilde{A}_k - 2\tilde{q}\cos(2z)\right)\tilde{\chi}_k = 0, \qquad (3.1.36)$$

where we have normalized the cosmic time as $z \equiv m_\phi t$. The parameters $\tilde{q}$ and $\tilde{A}_k$ are

39

given by

$$\begin{cases} \tilde{q} \equiv a^{-3} \dfrac{g^2}{4} \left(\dfrac{\tilde{\Phi}}{m_\phi} \right)^2, \\[4mm] \tilde{A}_k = 2\tilde{q} + \dfrac{(k/m_\phi)^2}{a^2} - \dfrac{9}{4}\dfrac{H^2}{m_\phi^2} - \dfrac{3}{2}\dfrac{\dot{H}}{m_\phi^2}, \end{cases} \qquad (3.1.37)$$

where $\tilde{\Phi}$ is the rescaled amplitude as $\tilde{\Phi} \equiv a^{3/2}\Phi$ to be time-independent. In the case that $\tilde{q}$ is smaller than unity, the narrow resonance occurs, and the resonance band is given by $|\tilde{A} - n^2| < \tilde{q}^n$. As is seen from the above equation, in the expanding Universe, the parameters $\tilde{q}$ and $\tilde{A}$ depend on the scale factor. Thus, the resonance band changes as the scale factor evolves by the redshift of the momentum and decrease of the amplitude of the background field.[1] In the case that $\tilde{q}$ is larger than unity, the broad resonance occurs, a numerical result of which is shown in fig. 3.4 [29]. There appears a characteristic feature of the resonance in the expanding Universe. Compared to the instability in the Minkowski space-time shown in fig. 3.2, the mode function and the occupation number either increase or decrease, but on average they increase. This stochastic nature is due to the time dependence of the accumulated phase of the mode function for one oscillation of ϕ as $\Delta\theta_k^j = \int_{t_{j-1}}^{t_j} dt\,\omega_k(t)$. Since in the expanding Universe, the momentum is red-shifted as k/a, and the effective mass of the mode function $g^2\phi^2$ damps as $\propto a^{-3}$, the accumulated phase for a single oscillation varies. This variation of the phase accumulation makes the stochastic change of the total accumulated phase (3.1.28) modulo 2π, and then the growth rate (3.1.31) becomes either negative or positive. Even though fluctuations decrease at one time, at most times they increase because the enhancement is realized for $0 < \theta_{\rm tot}^j(\mathrm{mod}\ 2\pi) < \pi/4$ and $3\pi/4 < \theta_{\rm tot}^j(\mathrm{mod}\ 2\pi) < 2\pi$. Thus, on average, fluctuations are enhanced.

In the case of the quartic potential $V = (\lambda/4)\phi^4$, we choose other rescaling of the fields and the time as $\tilde{\phi} = a\phi$, $X = a\chi$ and $d\eta = dt/a$. By this rescaling, the equation of motion for χ_k is reduced to

$$\frac{d^2}{d\eta^2}X_k + \left[k^2 + g^2\tilde{\phi}^2 - a^{-1}\frac{d^2}{d\eta^2}a \right] X_k = 0. \qquad (3.1.38)$$

The structure of the resonance depends on the last term in the bracket. If ϕ dominates the Universe, the expansion is as like the domination of relativistic particles as $a \propto t^{1/2}$. Then, the last term vanishes, and the equation of motion is reduced to the Lamé equation.

3.1.2 Tachyonic resonance

We have shown that, by the oscillation of the scalar field, the parametric resonance occurs, and fluctuations increase. The key point of this resonance is that the frequency of the mode function becomes a periodic function by the interaction with the oscillating field. In

---

[1]The growth of χ_k is given by $\chi_k \propto a^{-3/2}\mathrm{e}^{(\tilde{q}/2)m_\phi t} = \exp\left[\ln a\left(-3/2 + a^{-3}\tilde{q}_0/(2\gamma)m_\phi t_0\right)\right]$, where we have parametrized the evolution of the scale factor by γ as $a = (t/t_0)^\gamma$, and the initial value of $\tilde{q}$ as $\tilde{q}_0$. From this expression, we can see that, in the case that $\tilde{q}_0$ is smaller than unity, the resonance effect is smaller than the dilution effect by the cosmic expansion.
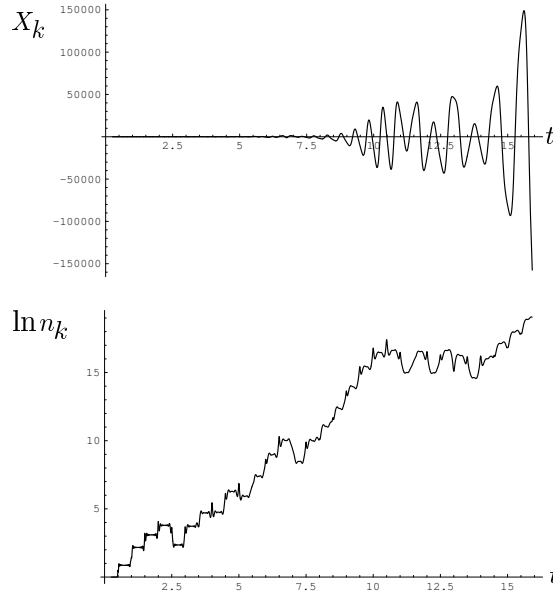
Figure 3.4: Evolution of mode function χ_k and occupation number n_k for broad resonance in the expanding Universe [29]. The unit of the time is the mass of the ϕ as m_ϕ with the division by 2π as $m_\phi/2\pi$.

the previous section, we have assumed the quartic interaction with $g^2 > 0$. On the other hand, in the case of $g^2 < 0$, there occurs more explosive enhancement of fluctuations [72].

As we have explained, the broad resonance occurs when the adiabatic condition breaks down. At that time, the mode function deviates from the WKB solution, and then the mixing of the Bogolyubov coefficients occurs, which corresponds to the creation of particles. The deviation from the WKB solution is crucial for the broad resonance, but the square of the frequency itself is always positive. By the negative coupling, the square of the mass directly becomes negative (tachyonic), and hence the square of the frequency of the mode function becomes negative for lower momenta. As the square of the frequency becomes negative, the enhancement of the mode function occurs, which is called tachyonic resonance. This tachyonic resonance is also induced by cubic interactions [73–75]. At a spontaneous symmetry breaking, the tachyonic resonance also occurs [76, 77]

As one example, we consider a scalar field ϕ with a double well potential:

$$V = \frac{\lambda}{4}\left(\phi^2 - v^2\right)^2, \tag{3.1.39}$$

where λ is a positive constant, and v is the vacuum expectation value of ϕ. In the case that ϕ starts to oscillate near the local maximum of the potential $\phi \simeq 0$, its effective mass becomes tachyonic up to the inflection point, and then the equation of motion for the mode function is given by

$$\ddot{\phi}_k + (k^2 + m^2)\phi_k = 0, \tag{3.1.40}$$

41

where we have defined the tachyonic mass as $m^2 \equiv -\lambda v^2 < 0$. From this equation, we can see that the solution of the mode equation for lower momenta $k^2 < -m^2$ grows with $\mu_k \lesssim 1$. With this rate fluctuations grow exponentially, and then re-scattering becomes efficient within only several oscillations. Assumed the initial fluctuations $\delta\phi_k(t_0) = (1/\sqrt{2k})e^{-ikt_0 + i\vec{k}\vec{x}}$, the variance of fluctuations at t becomes

$$\langle \delta\phi^2 \rangle = \int_0^{|m^2|} \frac{dk^2}{8\pi^2} e^{2t\sqrt{|m^2|-k^2}}. \tag{3.1.41}$$

3.1.3 Backreaction

We have seen that the coherent oscillation of the scalar field ϕ makes the modulation of the frequency of fluctuations, and then triggers the explosive particle productions at particular momenta. The growth rate of the fluctuations is calculated explicitly for some potentials as shown in (3.1.15), (3.1.31) and (3.1.41). As the particle production proceeds, the fluctuations trigger non-liner processes such as the re-scattering of the fluctuations with the coherent mode or other modes of the fluctuations. Thus, by the growth of the fluctuations, the dynamics of the background field is affected, and at some time the resonance becomes inefficient. In order to investigate the non-linear processes extensively, we have to perform numerical simulations, but the typical time scale that the back-reactions become non-negligible can be estimated using the Hartree approximation [29, 70, 78].

For convenience of discussions, we consider the quartic interaction. We deal with the back reaction effect by the Hartree approximation:

$$\ddot{\phi} + 3H\dot{\phi} + \frac{\partial V}{\partial \phi} + g^2 \langle \chi^2 \rangle \phi = 0, \tag{3.1.42}$$

where the variance is calculated by the mode function as

$$\langle \chi^2 \rangle = \frac{1}{2\pi^2} \int dk \ k^2 |\chi_k|^2. \tag{3.1.43}$$

The effective mass of ϕ depends on the variance $\langle \chi^2 \rangle$. At the beginning of the resonance, the induced mass due to the fluctuations is negligible compared to the bare mass of ϕ, but after the sufficient production of particles, it becomes comparable with the bare mass, and then the field amplitude Φ_t adiabatically decreases as

$$\Phi_t \simeq \frac{m_\phi}{m_{\text{eff}}} \Phi_0, \tag{3.1.44}$$

where Φ_0 is the initial amplitude of ϕ, m_ϕ is the bare mass of ϕ and m_{eff} is the effective mass of ϕ given by

$$m_{\text{eff}}^2 = m_\phi^2 + g^2 \langle \chi^2 \rangle. \tag{3.1.45}$$

By the decrease of the amplitude, the parameter q of the Mathieu equation (3.1.9) also decreases as

$$q = \frac{g^2}{4} \frac{\Phi_t^2}{m_{\text{eff}}^2} \simeq \frac{g^2}{4} \frac{m_\phi^2 \Phi_0^2}{m_{\text{eff}}^4} \simeq \frac{1}{4g^2} \frac{m_\phi^2 \Phi_0^2}{\langle \chi^2 \rangle^2}. \tag{3.1.46}$$

Since the absolute value of q determines the strength of the resonance, by the damping, the resonance of χ becomes gradually inefficient. The typical time scale that the backreaction becomes efficient can be estimated by the time when the induced mass becomes comparable with the bare mass. Assumed the parametric resonance with growth rate μ_k for the resonance band $k^2 \lesssim g\,\Phi_0\,m_\phi \equiv k_*^2$, the variance of the fluctuations is calculated as

$$\langle \chi^2 \rangle = \frac{1}{2\pi^2} \int dk \; k^2 |\chi_k|^2 \simeq k_*^3 \frac{1}{k_*} e^{2\mu_k m_\phi t} = g\,\Phi_0\,m_\phi\,e^{2\mu_k m_\phi t}. \tag{3.1.47}$$

Then, the induced mass is approximately estimated as $g^2 \langle \chi^2 \rangle \simeq g^3 \Phi_0 m_\phi \exp(2\mu_k m_\phi t)$. Thus, the time that the induced mass becomes comparable with the bare mass $g^2 \langle \chi^2 \rangle \simeq m_\phi^2$ is estimated as

$$t_{\rm bk} \simeq \frac{1}{2\mu_{k_*} m_\phi} \ln\left(\frac{1}{g^2 \Phi_0}\right) \simeq \frac{1}{\mu_k m_\phi}. \tag{3.1.48}$$

3.2 I-ball formation

We have explained that, by the oscillation of the scalar field, its fluctuations are enhanced through the self-coupling, and they evolve non-linearly. Then some scalar fields fragment into stable objects such as the topological defects or Q-balls. The stability of the objects is guaranteed by conserved quantities such as the topological or $U(1)$ charge, respectively. On the other hand, there is a case that, without explicit conserved quantities, stable objects are formed. It is known that an oscillating real scalar field could fragment into localized objects called I-balls, oscillons or pulsons.

The formation process of I-balls is yet to be revealed analytically. However, some heuristic natures have been found by performing numerical simulations. In [23, 25, 25] it is found that, when the initial configuration of a scalar field is a spherical bubble, I-balls are formed through the collapse of a bubble. More extensive investigations of the I-balls revealed that I-balls emit radiations from their tail and that within I-balls amplitude at multi frequencies around the mass of the field is excited [64, 79–81].

Numerical simulations also revealed that I-balls are formed from a nearly homogeneous field with small fluctuations, even under the expansion of the Universe [65–68, 82, 83]. Due to the expansion, fluctuations are diluted, and their momenta are red-shifted. Thus, the expansion of the Universe would suppress the resonance, and it would affect the formation of I-balls. In [66–68], the heuristic conditions for the formation of I-balls are obtained by lattice simulations.

3.2.1 I-ball by the collapse of Gaussian bubble

In the relativistic field theory, the I-ball was first discovered in [23, 24] by using numerical simulations when the classical models of finite-size particles were investigated. Then after a while, the I-ball was rediscovered in [25] when a dynamical symmetry breaking was studied with a double well potential $V = (\lambda/4)(\phi^2 - v^2)^2$. The authors in [25] studied an evolution of a Gaussian bubble configuration, and then found that the configuration settles down to a quasi-stable state (I-ball) by rapid emission of radiations. The quasi-stable state is studied more expensively in [64, 79–81]. Then, it was found that the I-ball

is formed for a slightly flatter potential than the quadratic one, and the lifetime is larger than the inverse of the mass of the scalar field. Here we briefly review the collapse of the Gaussian bubble for several potentials following [64].

As one example, we consider the double well potential $V = (\lambda/4)(\phi^2 - v^2)^2$. We set a Gaussian bubble configuration as the initial condition:

$$\phi(t = 0, r) = v(1 + \exp(-r^2/r_0^2)), \tag{3.2.1}$$

where r_0 it the initial radius of the bubble. At first, the bubble emits radiations, and then the energy of the bubble decreases. However, after a while, the bubble settles down to a stationary state, called I-ball. In order to confirm this collapse, [64] has performed lattice simulations with the initial condition (3.2.1) with $r_0 = 3.0/\sqrt{2\lambda}v$. In the simulations, the spherical symmetry is assumed for the field. By this assumption, the equation of motion is reduced to

$$\ddot{\phi} - \frac{d^2}{dr^2}\phi - \frac{D-1}{r}\frac{d}{dr}\phi + V'(\phi) = 0, \tag{3.2.2}$$

where D is the dimension of space. In [64], the numerical simulations were performed in $D = 2$ and $D = 3$ cases. In the simulation, the energy inside the shell of radius $r = 5r_0$ was calculated, which is shown in fig. 3.5 [64]. The figure shows the result of $D = 3$. The energy inside the shell rapidly decreases at the beginning, and after a while, the energy stabilizes to $E \simeq 40\sqrt{2\lambda}v$. Then, after the steady decrease of the energy, the I-ball abruptly breaks down at $t \simeq 7200/\sqrt{2\lambda}v$.

The stationary state after the collapse of the Gaussian bubble also appears for other potentials such as the axion like potential $V = (m^2\alpha^2)/\pi^2 [1 + \cos(\pi\phi/\alpha)]$. In the case of this potential, [64] performed simulations in $D = 2$.[2] For the axion like potential, the collapse to the stationary state is confirmed by numerical simulations, where the initial Gaussian bubble is set as

$$\phi(r, t = 0) = \alpha \left[1 - \exp(-r^2/r_0^2)\right], \tag{3.2.3}$$

with $r_0 = 2.9/m$. The time evolution of the energy inside the shell of radius $r = 5r_0$ is calculated and shown in fig. 3.6 [64]. From this figure, we can see that the Gaussian bubble with the axion like potential also collapses to the stationary state.

By the numerical simulations, some natures of I-balls have been revealed. The energy density of the I-ball is approximately time independent, while the field is oscillating within it. Without the localized objects, the oscillation of the field is described by one frequency. However, the frequency of I-balls has some multiplicity, and higher modes are excited. In order to see the excitations, [64] performed Fourier transformation for the amplitude at the center of an I-ball as

$$\phi(t, r = 0) = \int d\omega \ \Phi(\omega)e^{i\omega t}. \tag{3.2.4}$$

The power spectrum of $\Phi(\omega)$ is calculated for the double well potential and the axion like potential. The results of simulations are shown in fig. 3.7 for the double well potential and in fig. 3.8 for the axion like potential. For the double well potential, the Fourier

---

[2]Note that in $D = 2$ space, mass dimension of ϕ is one half, and then α is a constant of mass dimension one half.

transformation is performed over the interval $\Delta t = 200/(\sqrt{2\lambda}v)$ from $t = 4000/(\sqrt{2\lambda}v)$. For the axion like potential it is performed over the interval $\Delta t = 500/m$ from $t = 5.12 \times 10^7/m$. From the figures, we can see that the spectrum has several peaks and that the largest peak is located just below the mass of the field $\omega \lesssim m$. Even at higher frequencies than the mass, the spectrum has also peaks. The I-ball loses its energy gradually as shown in fig. 3.5 and in fig. 3.6. It is suggested that this decay of the I-ball is related to the excitation of the power spectrum at the higher frequencies.

3.2.2 I-balls from homogeneous mode

An I-ball is a spatially localized object. In the previous subsection, we have explained that the I-ball is formed after the collapse of the Gaussian bubble for slightly flatter potentials. On the other hand, it is know that, without the initial bubble configuration, I-balls are also formed. In the case that the scalar field is oscillating homogeneously with small fluctuations, the formation could also take place. As I-balls are the spatially localized objects, in this case, the growth of fluctuations is necessary. After the enhancement of the fluctuations, through the non-linear process, the fluctuations fragment into I-balls. The formation is also confirmed in other cases such as a rapid quench of a potential from a quadratic potential to a double well potential with thermal fluctuations [84–86].

In the early Universe, the expansion rate may be comparable with the oscillation scale of the scalar field, and then the enhancement of fluctuations would be suppressed by the dilution of the Hubble expansion. Thus, the expansion rate of the Universe is related to the formation of I-balls. The formation under the expansion is studied in [66–68,82,83]. As the formation process proceeds through the parametric resonance, I-balls would be formed for the growth rate larger than the Hubble expansion rate. This threshold is expected to be order unity. By numerical simulations, the threshold is investigated in [66–68] for a generic class of inflaton potentials. In this subsection, we review the formation of I-balls in the expanding Universe, and explain that, for the formation, the growth rate of the fluctuations need to exceed the expansion rate.

First, we consider the formation of I-balls for a scalar field ϕ not restricting to the inflaton, but we assume that ϕ dominates the Universe. We suppose the potential of ϕ by

$$V = \frac{1}{2}m^2\phi^2 - \frac{\lambda}{4}\phi^4 + \frac{g_6^2}{6m^2}\phi^6. \tag{3.2.5}$$

Here we assume that the ratio of the dimension less coupling λ to g_6 is smaller than unity $(\lambda/g_6)^2 \ll 1$ and λ is positive. The expansion rate of the Universe is determined by the Friedmann equation:

$$H^2 = \frac{1}{3M_p^2}\left[\frac{1}{2}\dot{\phi}^2 + \frac{1}{2}(\nabla\phi)^2 + V(\phi)\right]. \tag{3.2.6}$$

Here we assume that the scalar field is oscillating with an initial amplitude ϕ_i with small fluctuations $\delta\phi$. As we have explained, the fluctuations are enhanced by the parametric resonance with a growth rate μ_k. In this case, the growth rate is analytically estimated as

$$\mu_k \simeq \frac{1}{2}\frac{k/a}{m}\left[\frac{3\lambda}{2}\left(\frac{\Phi}{m}\right)^2\left(1 - \frac{\Phi^2}{\phi_{\rm ins}^2}\right) - \left(\frac{k/a}{m}\right)^2\right]^{1/2}. \tag{3.2.7}$$
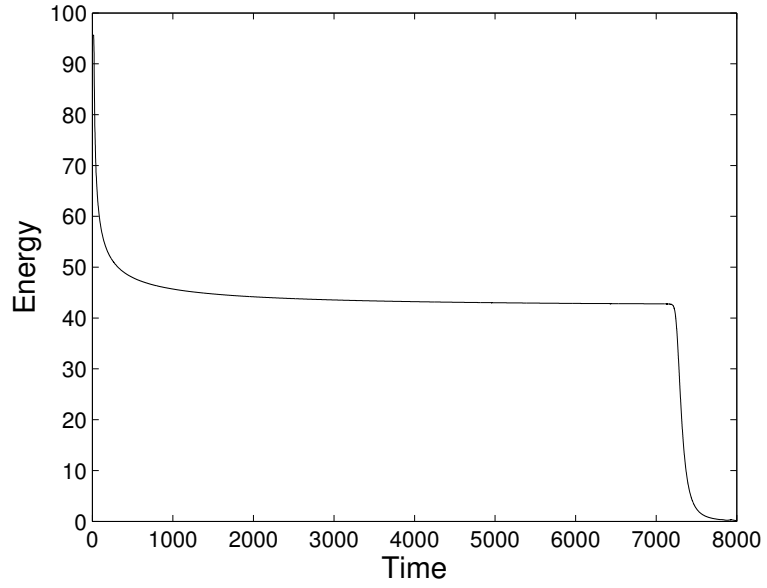
Figure 3.5: Evolution of the energy inside a shell of radius $r = 5r_0$ for the double well potential [64]. Unit of the energy is $\sqrt{2\lambda}v$, and the unit of time is its inverse.
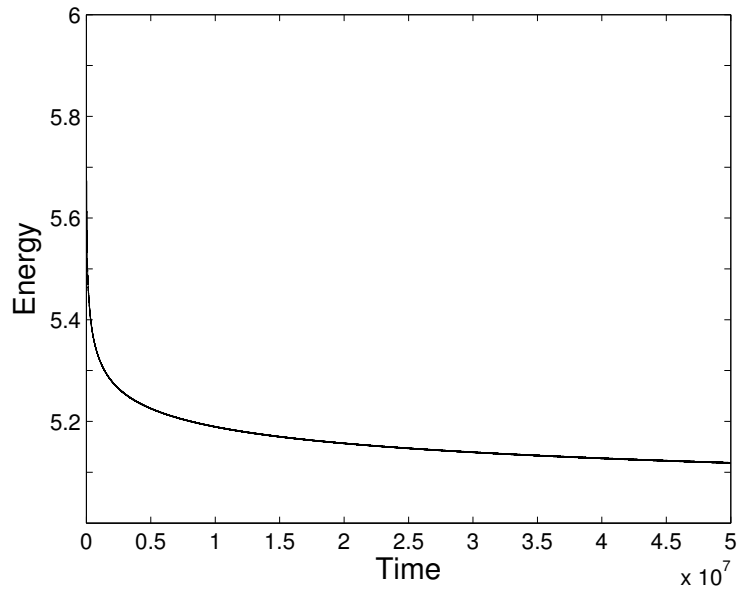

Figure 3.6: Evolution of the energy inside a shell of radius $r = 5r_0$ for the axion like potential [64]. Unit of the energy is α^2, and time is $1/m$.
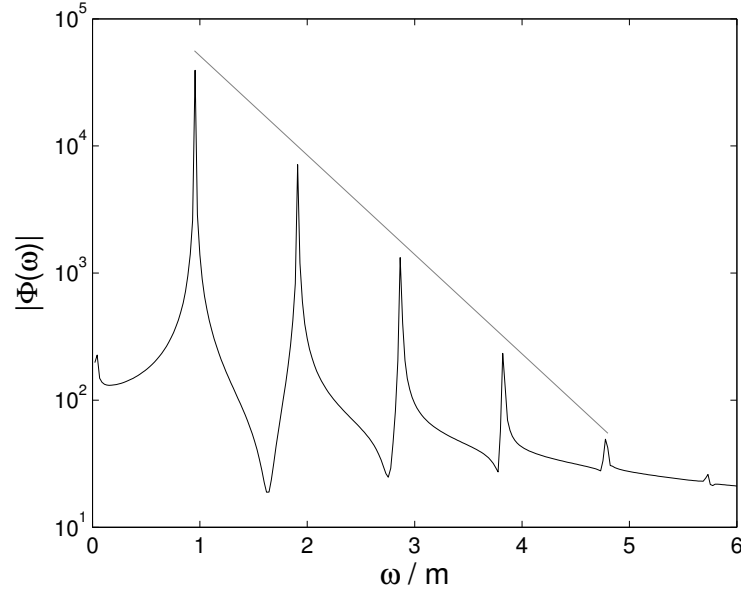
Figure 3.7: The power spectrum of the field at the center of the I-ball, $r = 0$, in the double well potential [64], where mass is defined as $m = \sqrt{2\lambda}v$. The straight solid line is the fit by the exponential function $\propto \exp(-1.8\omega)$.
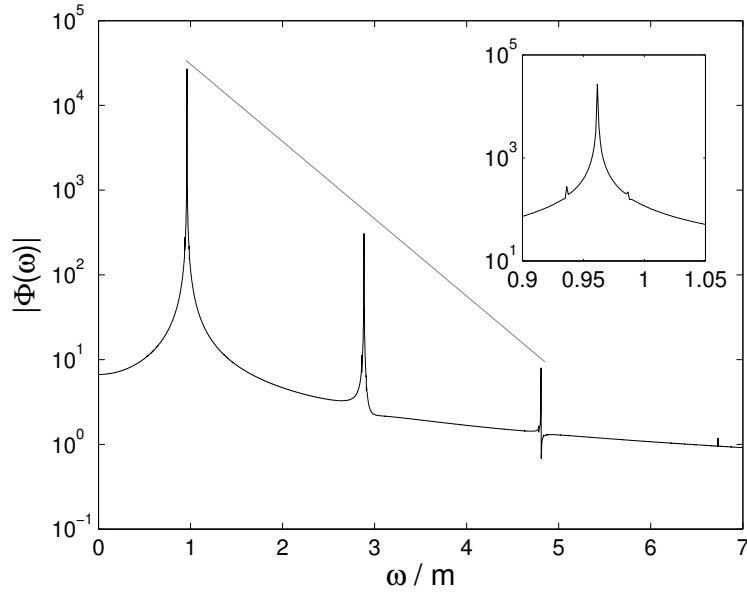

Figure 3.8: The power spectrum of the field at the center of the I-ball, $r = 0$, in the axion like potential [64]. The straight solid line is the fit by the exponential function $\propto \exp(-2.1\omega)$.

47

Here a is the scale factor, which is set to unity at $t = t_i$, Φ is the amplitude of ϕ adiabatically damping as $\Phi = \phi_i a^{-3/2}$ and ϕ_{ins} is defined as

$$\phi_{\text{ins}} = \left(\frac{3\lambda}{5g^2}\right)^{1/2} m. \tag{3.2.8}$$

With the growth rate, the amplitude of fluctuations grows as

$$\delta\phi_k = \frac{\delta\phi_{k,i}}{a^{3/2}} \exp\left(\int \mu_k(t)dt\right) = \delta\phi_{k,i} \exp\left[\int\left(\frac{\mu_k}{H} - \frac{3}{2}\right)d\ln a\right], \tag{3.2.9}$$

where $\delta\phi_k$ is the Fourier mode of the fluctuations of ϕ. By the parametric resonance, fluctuations are amplified when their momentum passes through the instability band. On the other hand, the Hubble expansion suppresses the fluctuations. For the value $\mu_k/H = 3/2$, the enhancement and suppression of fluctuations are balanced, and then the fluctuations do not decrease nor also increase. The suppression rate estimated by the Hubble parameter is given by

$$H \simeq a^{-3/2}\frac{\phi_i}{\sqrt{6}M_p}m. \tag{3.2.10}$$

We set the initial amplitude of the homogeneous mode to $\phi_i = \phi_{\text{ins}}$. By this, the ratio of the growth rate to the expansion rate is reduced to

$$\frac{\mu_k}{H/m} = \beta_1\tilde{k}\sqrt{\frac{9}{4a^2}\left(1 - \frac{1}{a^3}\right) - \frac{\tilde{k}^2}{a}}. \tag{3.2.11}$$

Here we have rescaled the comoving momentum as

$$\tilde{k} \equiv \frac{g_6}{\lambda}\frac{k}{m}, \tag{3.2.12}$$

and defined β_1 as

$$\beta_1 = \sqrt{\lambda}\frac{\lambda}{g_6}\frac{M_p}{m}. \tag{3.2.13}$$

The enhancement of the instability is most efficient at $\tilde{k} \sim 0.4$, which gives the ratio maximally as $\mu_k m/H \simeq 0.5\beta_1$. In [68], the formation of I-balls is simulated for various β_1, and then it is verified that the formation occurs for $\beta_1 > 50$ as shown in fig. 3.9, where the left panel shows the ratio of the energy in I-balls to the total energy, and the right panel shows the mean energy per an I-ball. As the momentum which experiences the enhancement passes through the instability bands due to the redshift, the growth rate is smaller than the case without the expansion of the Universe. Thus, the typical ratio of the growth rate to the expansion rate is smaller than β.

From (3.2.9), we can estimate the typical ratio of the growth rate to the expansion rate as

$$\langle\frac{\mu_k\, m}{H}\rangle \simeq \frac{\ln\left(\delta\phi_k/\delta\phi_{i,k}\right)}{\Delta\ln a} + \frac{3}{2}. \tag{3.2.14}$$

Here $\langle\mu_k/H\rangle$ is the average value of the ratio from $a = a_1$ to a evaluated from

$$\int \mu_k dt = \int \frac{\mu_k}{H}d\ln a = \langle\frac{\mu_k}{H}\rangle\Delta\ln a, \tag{3.2.15}$$

48

where $\Delta \ln a = \ln a - \ln a_i$. For the value $\beta_1 = 50$, we evaluate the typical growth ratio. For this parameter, we have numerically calculated the fluctuations with linear perturbation method from $a = 1$ to $a = 5$, by solving the following coupled equations

$$\ddot{\phi}_0 + 3H\dot{\phi}_0 + \frac{\partial V(\phi_0)}{\partial \phi_0} = 0, \tag{3.2.16}$$

$$\delta\ddot{\phi}_k + 3H\delta\dot{\phi}_k + \left[\left(\frac{k}{a}\right)^2 + \frac{\partial^2 V(\phi_0)}{\partial \phi_0^2}\right]\delta\phi_k = 0. \tag{3.2.17}$$

In fig. 3.10, we show the growth of N_k which is defined by

$$N_k = \frac{\omega_k}{2}\left[\frac{|\delta\dot{\phi}_k|^2}{\omega_k^2} + |\delta\phi_k|^2\right], \tag{3.2.18}$$

where ω_k is defined by $\omega_k = \sqrt{|\partial^2 V/\partial \phi^2| + (k/a)^2}$. We set the initial value of ϕ_0 to $\phi_{0,i} = \phi_{\text{ins}}$. In the figure, we normalized the vertical axis by the initial value of $N_{k,i}$. From this result, the typical ratio is estimated as

$$\langle\frac{\mu_k m}{H}\rangle \simeq \frac{\ln 10^{\sqrt{11/2}}}{\ln 5} + \frac{3}{2} \simeq 5. \tag{3.2.19}$$

This result means that for the formation of I-balls, the amplitude of fluctuations need to grow against cosmic expansion (i.e. $\langle\frac{\mu_k m}{H}\rangle \gg \frac{3}{2}$).
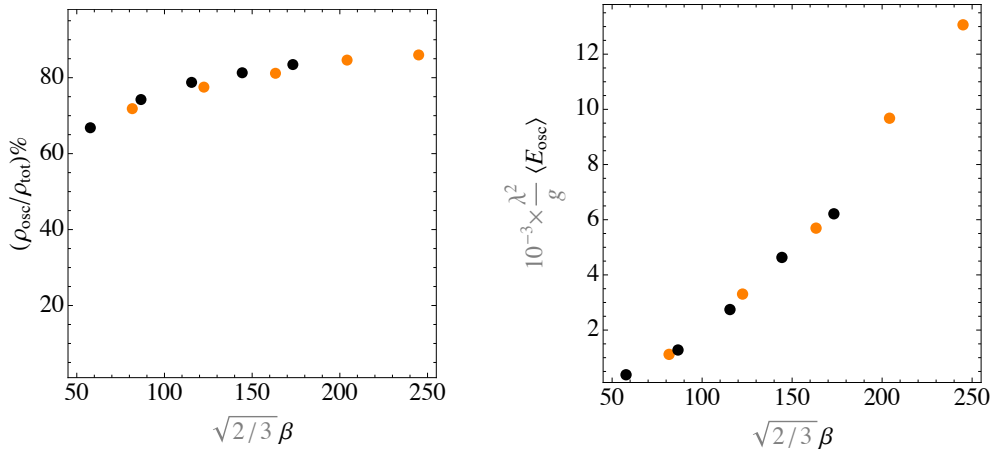

Figure 3.9: The left panel shows the ratio of the energy in I-balls to the total energy. The right panel shows the mean energy per an I-ball [68]. The black and orange points correspond to simulations with parameters $(\lambda/g)^2 = 0.2$ and 0.1.

Next we explain the formation of I-balls for an inflaton potential following [66]. As we have noted that the formation of I-balls could occur for a slightly flatter potential than
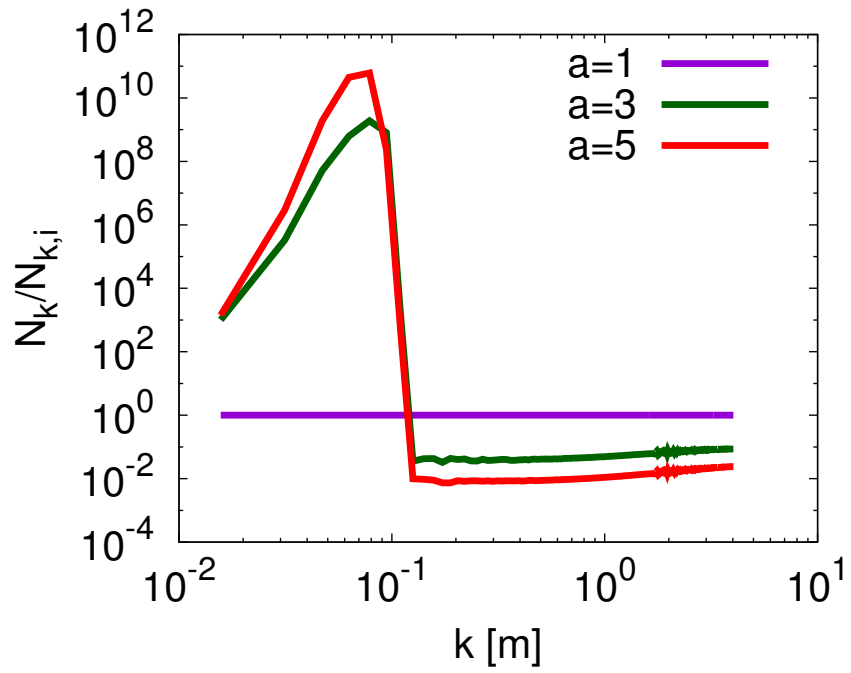
Figure 3.10: Evolution of N_k for the potential (3.2.5) from $a = 1$ to $a = 5$. In the simulation, we set the parameters to $m = 5 \times 10^{-6} M_p$, $\lambda = 2.81 \times 10^{-6}$ and $\beta = 50 \times \sqrt{3/2}$.

the quadratic one. For this potential, the scalar field is oscillating around the minimum of the potential with a quadratic term $\sim m^2\phi^2/2$, but the curvature of the potential is suppressed far away from the minimum as $V_I \sim \phi^{2\alpha}$, where α is smaller than unity. In order to capture this nature, we set the potential as

$$V_I = \frac{m^2 M^2}{2\alpha}\left[\left(1 + \frac{\phi^2}{M^2}\right)^\alpha - 1\right], \tag{3.2.20}$$

where M is a constant with mass dimension one. Here we suppose that ϕ is an inflaton. $\alpha = 1$ corresponds to the quadratic chaotic inflation. For this inflation potential, we can calculate the curvature perturbation at the pivot scale:

$$\mathcal{P}_{\mathcal{R}_c} = \frac{1}{96\pi^2\alpha^3}\left(\frac{m}{M_{\rm pl}}\right)^2\left(\frac{M}{M_{\rm pl}}\right)^{2-2\alpha}(220\alpha)^{1+\alpha}, \tag{3.2.21}$$

where we have assumed the 55 e-folds and used the slow-roll approximation. By the observation of CMB, it is determined as $\mathcal{P}_{\mathcal{R}_c} = 2.9 \times 10^{-10}$ [30]. In the investigation, the parameters are chosen to satisfy this value.

When we neglect the redshift effects on the momentum, the maximal ratio of the growth rate to the expansion rate is approximately given using α and M as [66]

$$\frac{\mu_k}{H/M} \simeq \frac{M_{\rm pl}}{M}\frac{1}{2}\left[(1-\alpha) - 0.1(1-\alpha)^2\right] = \beta_2\frac{1}{2}\left[(1-\alpha) - 0.1(1-\alpha)^2\right], \tag{3.2.22}$$

where we have defined a parameter as $\beta_2 = M_{\rm p}/M$. We assume that the typical value of α is $\mathcal{O}(0.1)$. Thus, β_2 is typically equals to the ratio of the growth rate to the cosmic expansion rate (i.e. $\beta_2 \simeq \mu_k M/H$). However if we include the redshift effects on the momentum, the instability band and the growth rate change due to the Hubble expansion, and the typical ratio is smaller than β.

Using β_2, we can reduce the curvature perturbation (3.2.21) to

$$\mathcal{P}_{\mathcal{R}_c} = \frac{(220\alpha)^{1+\alpha}}{96\pi^2\alpha^3}\left(\frac{m}{M_{\rm pl}}\right)^2\beta_2^{2\alpha-2}. \tag{3.2.23}$$

For several sets of parameters (α, β_2), the formation of I-balls just after inflation are investigated in [66] using lattice simulations. Then, the fraction of the energy of I-balls to the total energy

$$f = \frac{\int_{\rho>2\langle\rho\rangle}\rho dV}{\int \rho dV} \tag{3.2.24}$$

is calculated as shown in fig. 3.11 [66]. Here $\langle\rho\rangle$ is the spatial average of the energy density. From the figure, we can see that the significant production of I-balls occurs for $\beta_2 \gtrsim 20$, where the fraction f can be larger than 0.3. Thus, for the formation of I-balls, the growth rate neglected the redshift effect should be tens of times larger than the Hubble expansion rate $\mu_k M/H \gtrsim 10$ (without redshift). In the figure, the black thick contour denotes $\mu_k M/H > 7$ (without redshift). For these parameters, we numerically evaluate the typical ratio including the redshift effects as (3.2.14).

As fiducial values, we evaluate the ratio for the parameters $(\alpha, \beta) = (0.5,\ 29.5)$ and $(0.6,\ 36.5)$, which are the thresholds for the formation of I-balls as shown in 3.11. We have numerically solved following coupled equations as

$$\ddot{\phi}_0 + 3H\dot{\phi}_0 + \frac{\partial V_I(\phi_0)}{\partial \phi_0} = 0, \tag{3.2.25}$$

$$\delta\ddot{\phi}_k + 3H\delta\dot{\phi}_k + \left[\left(\frac{k}{a}\right)^2 + \frac{\partial^2 V_I(\phi_0)}{\partial^2 \phi_0}\right]\delta\phi_k = 0 \tag{3.2.26}$$

from $a = 1$ to $a = 7$. We set the initial field values of the inflaton by which the time derivative of the inflaton first becomes zero, $\dot{\phi}_0 = 0$ after inflation as the same way in [66]. In fig. 3.12, we show the evolution of N_k, where we define ω_k by $\omega_k = \sqrt{|\partial^2 V_I/\partial\phi^2| + (k/a)^2}$. From the results, the typical ratio is estimated as

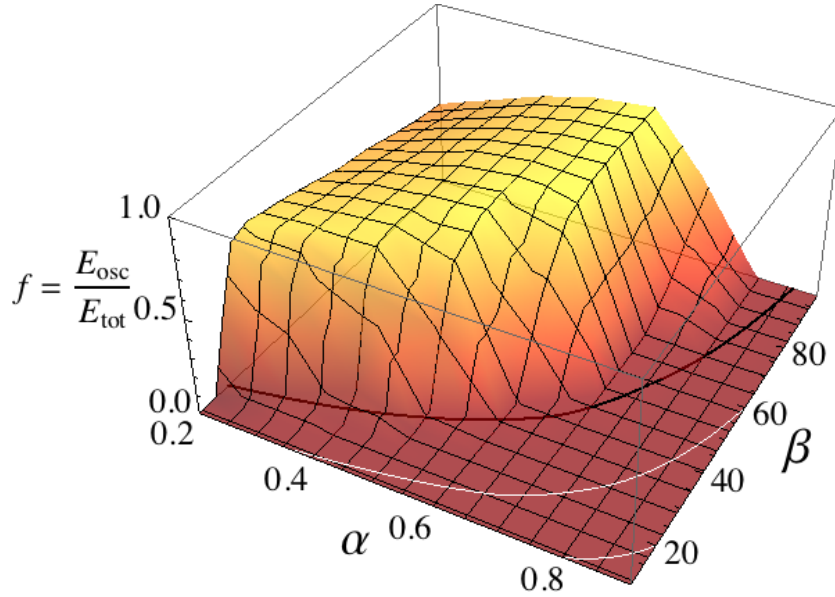$$\langle\frac{\mu_k m}{H}\rangle \simeq \frac{\ln 10^{\sqrt{4/2}}}{\ln 7} + \frac{3}{2} \simeq 4. \tag{3.2.27}$$

Figure 3.11: The distribution of f on (α, β) at $a = 7$ [66]. The black thick contour denotes $(\mu_k m/H)_{\max} = 7$, and the white ones correspond to $(\mu_k m/H)_{\max} = 1$ and 3.

We have reviewed that for the formation of I-balls in the expanding Universe the growth rate of fluctuations needs to exceed the Hubble expansion rate. The ratio is evaluated by numerical simulations in [66–68]. As shown by (3.2.19) and (3.2.27), the ratio is order unity, but should be larger $3/2$, which means that for the formation of I-balls, the amplitude of the fluctuations need to grow against cosmic expansion.
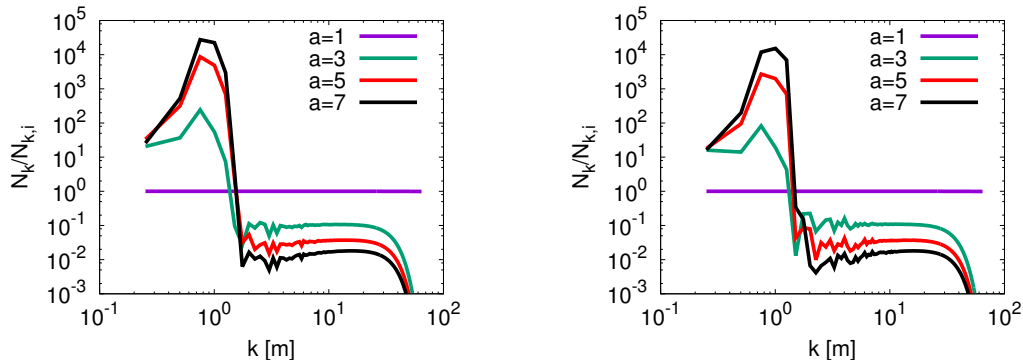
Figure 3.12: Evolution of N_k for the potential (3.2.20) from $a = 1$ to $a = 7$. We set the parameters to $(\alpha, \beta) = (0.5, 29.5)$ on the left panel and $(\alpha, \beta) = (0.6, 36.5)$ on the right panel.

3.3 Adiabatic charge

As we have noted, in most cases, the stability of solitons is guaranteed by some conserved quantities such as $U(1)$ charge corresponding to Q-balls or topological charge corresponding to topological defects. As for I-balls, it seems that there is no explicit conserved quantity. However, in the previous study [26], it is conjectured that an adiabatic charge can be the candidate to guarantee the stability of I-balls. The study showed that, if we consider the lowest energy state for a fixed value of the adiabatic charge, the configuration of the scalar field for flatter potentials becomes a localized one, i.e., I-ball. In this section, we prove the conservation of the adiabatic charge. This proof is based on my work collaborated with Masahiro Kawasaki and Fuminobu Takahashi [87], which is the improved version of [26].

3.3.1 Adiabatic invariant in classical mechanics

The proof of the conservation of the adiabatic charge is based on the ways in a classical mechanical system. First we briefly review the conservation of the adiabatic invariant in a classical mechanical system [37, 38], especially following the argument by Tomonaga.

We consider a point particle with a Hamiltonian:

$$H = \frac{p^2}{2m^2} + V(q, \lambda_f(t/T)), \tag{3.3.1}$$

where $\lambda_f(t/T)$ is an external parameter that changes sufficiently slowly compared to the typical time scale of the point particle. T defines the time scale over which the external parameter changes from $\lambda_{f,i} \equiv \lambda_f(0)$ to $\lambda_{f,f} \equiv \lambda_f(1)$, and it will be set to be infinity in the end. We suppose that the point particle is oscillating quasi-periodically. Since the external parameter is time dependent in this case, the Hamiltonian is not time independent as

$$\frac{d}{dt}H = \frac{\partial H}{\partial \lambda_f}\frac{d\lambda_f(t/T)}{dt}. \tag{3.3.2}$$

Let us consider a hypothetical system for one period of the motion from $t = \tau$ until $t = \tau + 1/\nu_\tau$, while the external parameter $\lambda_f(t/T)$ is fixed to be the value at $t = \tau$, i.e., $\lambda_f(t/T) = \lambda_f(\tau/T)$. Here ν_τ is the frequency for $\lambda_f = \lambda_f(\tau/T)$. In such a hypothetical system, the trajectory on the phase space is periodic and closed. We denote the trajectory of $(q(t), p(t))$ in the hypothetical system by $(q_\tau(t), p_\tau(t))$. For this hypothetical system, the Hamiltonian is time independent with a constant energy:

$$H(p_\tau(t), q_\tau(t), \lambda_f(\tau/T)) = E(\tau). \tag{3.3.3}$$

Solving this equation with respect to $p_\tau(t)$, we obtain

$$p_\tau = p_\tau(q_\tau(t), E(\tau), \lambda_f(\tau/T)). \tag{3.3.4}$$

Thus, the canonical momentum $p_\tau(t)$ can be regarded as a function of $q_\tau(t), E(\tau)$ and $\lambda_f(\tau/T)$. For later use, we differentiate eq. (3.3.3) with respect to E and λ_f:

$$\left(\frac{\partial H}{\partial p_\tau}\right)_{q_\tau, \lambda_f} \left(\frac{\partial p_\tau}{\partial E}\right)_{q_\tau, \lambda_f} = 1 \tag{3.3.5}$$

$$\iff \quad \left(\frac{\partial p_\tau}{\partial E}\right)_{q_\tau, \lambda_f} = \left(\frac{\partial H}{\partial p_\tau}\right)_{q_\tau, \lambda_f}^{-1} \tag{3.3.6}$$

$$\left(\frac{\partial H}{\partial \lambda_f}\right)_{p_\tau, q_\tau} + \left(\frac{\partial H}{\partial p_\tau}\right)_{q_\tau, \lambda_f} \left(\frac{\partial p_\tau}{\partial \lambda_f}\right)_{q_\tau, E} = 0 \tag{3.3.7}$$

$$\iff \quad \left(\frac{\partial p_\tau}{\partial \lambda_f}\right)_{q_\tau, E} = -\frac{\left(\frac{\partial H}{\partial \lambda_f}\right)_{p_\tau, q_\tau}}{\left(\frac{\partial H}{\partial p_\tau}\right)_{q_\tau, \lambda_f}}. \tag{3.3.8}$$

Now let us define the area surrounded by the closed trajectory:

$$I_T(\tau) = 2 \int_{q_\tau^{(1)}}^{q_\tau^{(2)}} p_\tau(q_\tau, E(\tau), \lambda(\tau/T)) dq_\tau,$$

where $q_\tau^{(1)}$ and $q_\tau^{(2)}$ are the roots of $p_\tau = 0$. In order to estimate the time variation of I_T, we differentiate $I_T(\tau)$ with respect to τ:

$$\frac{\partial I_T(\tau)}{\partial \tau} = 2 \left[p_\tau(q_\tau(t), E(\tau), \lambda_f(\tau/T)) \frac{dq_\tau}{d\tau} \right]_{q_\tau^{(1)}}^{q_\tau^{(2)}}$$

$$+ 2 \int_{q_\tau^{(1)}}^{q_\tau^{(2)}} \left[\left(\frac{\partial p_\tau}{\partial E(\tau)}\right)_{q_\tau, \lambda_f} \frac{\partial E(\tau)}{\partial \tau} + \left(\frac{\partial p_\tau}{\partial \lambda_f}\right)_{q_\tau, E} \frac{d\lambda_f(\tau/T)}{d\tau} \right] dq_\tau, \tag{3.3.9}$$

where the first term vanishes as p_τ vanishes at the end points. Using eqs. (3.3.6) and (3.3.8), we obtain

$$\frac{dI_T(\tau)}{d\tau} = 2 \int_{q_\tau^{(1)}}^{q_\tau^{(2)}} \left[\frac{\partial E(\tau)}{\partial \tau} - \left(\frac{\partial H}{\partial \lambda_f}\right)_{p_\tau, q_\tau} \frac{d\lambda_f(t/T)}{d\tau} \right] \left(\frac{\partial H}{\partial p_\tau}\right)_{q_\tau, \lambda_f}^{-1} dq_\tau$$

$$= \int_\tau^{\tau + 1/\nu_\tau} \left[\frac{\partial E(\tau)}{\partial \tau} - \left(\frac{\partial H}{\partial \lambda_f}\right)_{p_\tau, q_\tau} \frac{d\lambda_f(\tau/T)}{d\tau} \right] dt, \tag{3.3.10}$$

54

where we have used the Hamilton's equation:

$$\left(\frac{\partial H}{\partial p_\tau}\right)_{q_\tau, \lambda_f} = \frac{\partial q_\tau(t)}{\partial t}. \tag{3.3.11}$$

We can replace the time variable t in eq.(3.3.2) by τ, and substitute it into the above equation:

$$\frac{dI_T(\tau)}{d\tau} = \int_\tau^{\tau+1/\nu_\tau} \left[\left(\frac{\partial H(p(\tau), q(\tau), \lambda_f(\tau/T))}{\partial \lambda_f(\tau/T)}\right) \frac{d\lambda_f(\tau/T)}{d\tau}\right.$$
$$\left. - \left(\frac{\partial H(p_\tau(t), q_\tau(t), \lambda_f(\tau/T))}{\partial \lambda_f(\tau/T)}\right) \frac{d\lambda_f(\tau/T)}{d\tau}\right] dt. \tag{3.3.12}$$

As τ varies, the first term oscillates around some finite value. The second term is exactly subtracts the finite value from the first term. Thus, by the integration of $dI_T/d\tau$ over one oscillation, the oscillation term vanishes in the limit of $T \to \infty$, since in this limit, the trajectories q and q_τ become identical. Therefore, I_T is conserved if λ_f changes sufficiently slowly.

3.3.2 Adiabatic invariant (adiabatic charge) for a classical scalar field

In the previous sub-section, we have explained the conservation of the adiabatic invariant I in the classical mechanical system. As for the classical field theory, there also exists a conserved quantity, which we call as adiabatic charge, for a system that a scalar field is oscillating quasi-periodically. We explain the conservation of the adiabatic charge. The proof explained as bellow is based on [87].

We consider a real scalar field ϕ with a Lagrangian:

$$\mathcal{L} = \frac{1}{2}\partial_\mu \phi \partial^\mu \phi - V(\phi, \lambda_f(t/T)), \tag{3.3.13}$$

where $\lambda_f(t/T)$ is an external parameter as explained in the previous subsection. The Hamiltonian is given by

$$\mathcal{H} = \frac{1}{2}\dot{\phi}^2 + \frac{1}{2}(\partial_i \phi)^2 + V(\phi, \lambda_f(t/T)), \tag{3.3.14}$$

and the equation of motion is given by

$$\ddot{\phi}(x) - \partial_i^2 \phi + V'(\phi, \lambda_f(t/T)) = 0. \tag{3.3.15}$$

Using this equation of motion, we can write down a (non-)conservation law of the energy:

$$\partial_\mu j^\mu = \frac{\partial V}{\partial \lambda_f} \frac{d\partial \lambda_f(t/T)}{dt} = \frac{\partial \mathcal{H}}{\partial \lambda_f} \frac{d\lambda_f(t/T)}{dt}, \tag{3.3.16}$$

where the current density is given by

$$j^0 = \mathcal{H}, \ j^i = -\dot{\phi}(x)\partial_i \phi(x). \tag{3.3.17}$$

The energy is not conserved because of the external parameter $\lambda_f(t/T)$. As is clear from the derivation, spatial components of the current arises from the gradient term, which is the crucial differences from the case of the single degree of freedom in the classical mechanical system.

For later use, let us rewrite the above equation as

$$\frac{\partial \mathcal{H}}{\partial t} - \partial_i \left(\frac{\partial \phi(x)}{\partial t} \partial_i \phi(x) \right) = \frac{\partial \mathcal{H}}{\partial \lambda_f} \frac{d\lambda_f(t/T)}{dt}. \tag{3.3.18}$$

One can define another energy density $\tilde{\mathcal{H}}$ which differs from $\mathcal{H}$ by a total spatial derivative as

$$\tilde{\mathcal{H}} = \mathcal{H} - \frac{1}{2}\partial_i \left(\phi \partial_i \phi \right). \tag{3.3.19}$$

For a vanishing surface term, the spatial integrals of $\mathcal{H}$ and $\tilde{\mathcal{H}}$ are equal:

$$\int d^3 x \, \mathcal{H} = \int d^3 x \, \tilde{\mathcal{H}}. \tag{3.3.20}$$

Using $\tilde{\mathcal{H}}$, we can rewrite eq. (3.3.18) as

$$\frac{\partial \tilde{\mathcal{H}}}{\partial t} - \partial_i \left[\frac{1}{2} \left(\dot{\phi}(x)\partial_i \phi(x) - \phi(x)\partial_i \dot{\phi}(x) \right) \right] = \frac{\partial H}{\partial \lambda_f} \frac{d\lambda_f(t/T)}{dt} = \frac{\partial \tilde{\mathcal{H}}}{\partial \lambda_f} \frac{d\lambda_f(t/T)}{dt}. \tag{3.3.21}$$

This equation will be important in the following argument.

We limit ourselves to the case in which the dynamics of the scalar field is approximately periodic. In particular, we assume that, if $\lambda_f(t/T)$ is fixed to a constant value at $t = \tau$, the scalar dynamics is exactly periodic, and the scalar field has a solution in a separable form,

$$\phi(x) = \Phi(\vec{x})f(t, \lambda_f(\tau/T)), \tag{3.3.22}$$

where $f(t, \lambda_f(t/T))$ is a periodic function:

$$f(t, \lambda_f(\tau/T)) = f(t + 1/\nu_\tau, \lambda_f(\tau/T)). \tag{3.3.23}$$

Here ν_τ is the frequency of the scalar dynamics for $\lambda_f = \lambda_f(\tau/T)$, and the maximum value of $f(t, \lambda(\tau/T))$ is normalized to be unity. We emphasize here that such a periodic motion is not guaranteed at all for a generic form of the potential, and the scalar potential must be close to the quadratic one, as we shall see later in chap. 6. Here we do not specify the form of the potential in order to include a case in which the scalar dynamics can be approximated by the above separable form over a sufficiently long time scale of interest. Most importantly, $\tilde{\mathcal{H}}$ is a constant of motion for the separable solution (3.3.22) with a constant $\lambda_f = \lambda_f(t/T)$, because $\dot{\phi}(x)\partial_i \phi(x) = \phi(x)\partial_i \dot{\phi}(x)$ holds in this case (see eq.(3.3.21)).

As the external parameter $\lambda_f(t/T)$ depends on time, the dynamics of the scalar field is not strictly periodic. In particular, a significant amount of the energy can be transferred to other spatial points by scalar waves, in contrast to the case of one dynamical degree of freedom in the classical mechanical system. For a constant λ_f, the trajectory of

$(\phi(x), \pi(x))$ in the phase space is a closed one so that $\tilde{\mathcal{H}}$ at each spatial point is a constant of motion. Here $\pi(x) = \dot{\phi}(x)$ is the canonical momentum of $\phi(x)$.

Following the approach in the previous sub-section, we consider a hypothetical system for one period of the motion from $t = \tau$ to $\tau + 1/\nu_\tau$, while the external parameter $\lambda_f(t/T)$ is fixed to the value at $t = \tau$, i.e., $\lambda_f(t/T) = \lambda_f(\tau/T)$. We denote the trajectory of $(\phi(x), \pi(x))$ in such a hypothetical system by $(\phi_\tau(x), \pi_\tau(x))$. As we mentioned, for the separable form (3.3.22), $\tilde{\mathcal{H}}$ is a constant of motion at each point,

$$\tilde{\mathcal{H}}(\pi_\tau(x), \phi_\tau(x), \lambda_f(\tau/T)) = \tilde{\rho}(\tau, \vec{x}). \tag{3.3.24}$$

Solving this equation for $\pi_\tau(x)$, we obtain

$$\pi_\tau = \pi_\tau(\phi_\tau(x), \tilde{\rho}(\tau, \vec{x}), \lambda_f(\tau/T)). \tag{3.3.25}$$

Thus, π_τ can be regarded as a function of $\phi_\tau(x)$, $\tilde{\rho}(\tau, \vec{x})$ and $\lambda_f(\tau/T)$. The dependence of the spatial derivative dose not affect the following discussion. For later use, we differentiate eq. (3.3.24) with respect to $\tilde{\rho}$ and λ_f:[3]

$$\left(\frac{\partial \mathcal{H}}{\partial \pi_\tau}\right)_{\phi_\tau, \lambda_f} \left(\frac{\partial \pi_\tau}{\partial \tilde{\rho}}\right)_{\phi_\tau, \lambda_f} = 1 \tag{3.3.26}$$

$$\Longleftrightarrow \quad \left(\frac{\partial \pi_\tau}{\partial \tilde{\rho}}\right)_{\phi_\tau, \lambda_f} = \left(\frac{\partial \mathcal{H}}{\partial \pi_\tau}\right)_{\phi_\tau, \lambda_f}^{-1} \tag{3.3.27}$$

$$\left(\frac{\partial \mathcal{H}}{\partial \lambda_f}\right)_{\pi_\tau, \phi_\tau} + \left(\frac{\partial \mathcal{H}}{\partial \pi_\tau}\right)_{\phi_\tau, \lambda_f} \left(\frac{\partial \pi_\tau}{\partial \lambda_f}\right)_{\phi_\tau, \tilde{\rho}} = 0 \tag{3.3.28}$$

$$\Longleftrightarrow \quad \left(\frac{\partial \pi_\tau}{\partial \lambda_f}\right)_{\phi_\tau, \tilde{\rho}} = -\frac{\left(\frac{\partial \mathcal{H}}{\partial \lambda_f}\right)_{\pi_\tau, \phi_\tau}}{\left(\frac{\partial \mathcal{H}}{\partial \pi_\tau}\right)_{\phi_\tau \lambda_f}}. \tag{3.3.29}$$

In analogy with the argument in the classical mechanics, let us calculate the area in the phase space surrounded by the trajectory at each spatial point:

$$J_T^0(\tau, \vec{x}) = 2 \int_{\phi_\tau^{(1)}}^{\phi_\tau^{(2)}} \pi_\tau(\phi_\tau(x), \tilde{\rho}(\tau, \vec{x}), \lambda_f(\tau/T)) d\phi_\tau$$

$$= \int_\tau^{\tau + 1/\nu_\tau} \left(\dot{\phi}_\tau(t, \vec{x})\right)^2 dt, \tag{3.3.30}$$

where $\phi_\tau^{(1)}$ and $\phi_\tau^{(2)}$ are the two roots of $\pi_\tau = 0$, and we assume $\phi_\tau^{(1)} < \phi_\tau^{(2)}$. Here we note that x represents $(t, \vec{x})$ not $(\tau, \vec{x})$. Let us first differentiate $J_T^0(\tau, \vec{x})$ with respect to τ:

$$\frac{\partial J_T^0(\tau, \vec{x})}{\partial \tau} = 2 \left[\pi_\tau(\phi_\tau(x), \tilde{\rho}(\tau, \vec{x}), \lambda_f(\tau/T)) \frac{d\phi_\tau}{d\tau}\right]_{\phi_\tau^{(1)}}^{\phi_\tau^{(2)}}$$

$$+ 2 \int_{\phi_\tau^{(1)}}^{\phi_\tau^{(2)}} \left[\left(\frac{\partial \pi_\tau}{\partial \tilde{\rho}}\right)_{\phi_\tau, \lambda_f} \frac{\partial \tilde{\rho}(\tau, \vec{x})}{\partial \tau} + \left(\frac{\partial \pi_\tau}{\partial \lambda_f}\right)_{\phi_\tau, \tilde{\rho}} \frac{d\lambda_f(\tau/T)}{d\tau}\right] d\phi_\tau, \tag{3.3.31}$$

---

[3] With respect to $\tilde{\rho}$ and λ_f, the partial derivative of $\tilde{H}$ is identical to that of $\mathcal{H}$.

where the first term vanishes as π_τ vanishes at the end points. Using eq. (3.3.27) and (3.3.29), we can reduce the derivative to

$$
\begin{aligned}
\frac{\partial J_T^0(\tau, \vec{x})}{\partial \tau} &= 2 \int_{\phi_\tau^{(1)}}^{\phi_\tau^{(2)}} \left(\frac{\partial \tilde{\rho}(\tau, \vec{x})}{\partial \tau} - \left(\frac{\partial \mathcal{H}}{\partial \lambda_f} \right)_{\pi_\tau, \phi_\tau} \frac{d\lambda_f(\tau/T))}{d\tau} \right) \left(\frac{\partial \mathcal{H}}{\partial \pi_\tau} \right)_{\phi_\tau, \lambda_f}^{-1} d\phi_\tau \\
&= \int_\tau^{\tau+1/\nu_\tau} \left(\frac{\partial \tilde{\rho}(\tau, \vec{x})}{\partial \tau} - \left(\frac{\partial \mathcal{H}}{\partial \lambda_f} \right)_{\pi_\tau, \phi_\tau} \frac{d\lambda_f(\tau/T))}{d\tau} \right) dt,
\end{aligned}
\tag{3.3.32}
$$

where we have used the Hamilton's equation:

$$
\left(\frac{\partial \mathcal{H}}{\partial \pi_\tau} \right)_{\phi_\tau, \lambda_f} = \frac{\partial \phi_\tau(x)}{\partial t}
\tag{3.3.33}
$$

in the second equality. Compared with the one in the classical system (3.3.10), so far, there is no difference in the form but for the extra label, $\vec{x}$. The difference comes from that the energy is transferred to other spatial points by current. We replace the time variable t in eq. (3.3.21) with τ and substitute it into the above equation:

$$
\begin{aligned}
\frac{\partial J_T^0(\tau, \vec{x})}{\partial \tau} = \int_\tau^{\tau+1/\nu_\tau} &\left[\left(\frac{\partial \mathcal{H}(\pi(\tau, \vec{x}), \phi(\tau, \vec{x}), \lambda_f(\tau/T))}{\partial \lambda_f(\tau/T)} \right) \frac{d\lambda_f(\tau/T))}{d\tau} \right. \\
&\left. - \left(\frac{\partial \mathcal{H}(\pi_\tau(t, \vec{x}), \phi_\tau(t, \vec{x}), a(\tau/T))}{\partial \lambda_f(\tau/T)} \right) \frac{d\lambda_f(\tau/T))}{d\tau} \right] dt \\
+ \partial_i &\left(\frac{1}{2} \int_\tau^{\tau+1/\nu_\tau} \left[\frac{\partial \phi(\tau, \vec{x})}{\partial \tau} \partial_i \phi(\tau, \vec{x}) - \phi(\tau, \vec{x}) \partial_i \frac{\partial \phi(\tau, \vec{x})}{\partial \tau} \right] dt \right),
\end{aligned}
\tag{3.3.34}
$$

where it should be noted that the third integral over t is trivial and the integrand is independent of t. Let us now define the spatial component of the adiabatic current as

$$
J_T^i(\tau, \vec{x}) = -\frac{1}{2\nu_\tau} \left[\frac{\partial \phi(\tau, \vec{x})}{\partial \tau} \partial_i \phi(\tau, \vec{x}) - \phi(\tau, \vec{x}) \partial_i \frac{\partial \phi(\tau, \vec{x})}{\partial \tau} \right] dt,
\tag{3.3.35}
$$

and then eq. (3.3.34) can be rewritten as

$$
\begin{aligned}
\partial_\mu J_T^\mu(\tau, \vec{x}) = \int_\tau^{\tau+1/\nu_\tau} &\left[\left(\frac{\partial \mathcal{H}(\pi(\tau, \vec{x}), \phi(\tau, \vec{x}), \lambda_f(\tau/T))}{\partial \lambda_f(\tau/T)} \right) \frac{d\lambda_f(\tau/T))}{d\tau} \right. \\
&\left. - \left(\frac{\partial \mathcal{H}(\pi_\tau(t, \vec{x}), \phi_\tau(t, \vec{x}), a(\tau/T))}{\partial \lambda_f(\tau/T)} \right) \frac{d\lambda_f(\tau/T))}{d\tau} \right] dt.
\end{aligned}
\tag{3.3.36}
$$

In order to show the conservation of the adiabatic charge, let us integrate (3.3.35) over one period from $\tau = \tau_i$ to $\tau_i + 1/\nu_{\tau_i}$:

$$
\begin{aligned}
\int_{\tau_i}^{\tau_i+1/\nu_{\tau_i}} d\tau \, \partial_\mu J_T^\mu(\tau, \vec{x}) = \int_{\tau_i}^{\tau_i+1/\nu_{\tau_i}} d\tau &\left(\frac{\lambda_f(\tau/T)}{d\tau} \right) \int_\tau^{\tau+1/\nu_\tau} dt \\
\times \left[\left(\frac{\partial \mathcal{H}(\pi(\tau, \vec{x}), \phi(\tau, \vec{x}), \lambda_f(\tau/T))}{\partial \lambda_f(\tau/T)} \right) \right. &\left. - \left(\frac{\partial \mathcal{H}(\pi_\tau(t, \vec{x}), \phi_\tau(t, \vec{x}), a(\tau/T))}{\partial \lambda_f(\tau/T)} \right) \right].
\end{aligned}
\tag{3.3.37}
$$

As we explained in the previous subsection, in the case of the single degree of freedom, J_T^0 is conserved for the adiabatic change of λ_f, i.e., in the limit of $T \to \infty$. In the case of the field theory, we expect that the adiabatic current J_T^μ is also conserved in the limit of $T \to \infty$. This conservation is explained as bellow.

Now let us see that the above quantity approaches zero faster than $\mathcal{O}(1/T)$ as $T \to \infty$. One can see that the RHS of the above equation contains a factor $d\lambda_f(\tau/T)/d\tau$, which is proportional to $1/T$. In addition, as we shall see below, the first and second terms contain an additional factor which oscillates fast about zero; the first integrand in the RHS is independent of t, and it contains functions $\pi(\tau, \vec{x})$ and $\phi(\tau, \vec{x})$, which oscillate fast as τ varies. In general it oscillates fast about some finite value. The second integrand exactly subtracts the finite value, as it is obtained by averaging the first term over one period. (Note that, in the limit of $T \to \infty$, the difference between $\phi(\pi)$ and $\phi_\tau(\pi_\tau)$ becomes negligible.) Thus, when integrated over the period, the sum of the first and second terms approaches zero faster than $\mathcal{O}(1/T)$.

To summarize, we have proved that the adiabatic current is conserved,

$$\overline{\partial_\mu J^\mu} = 0 \tag{3.3.38}$$

with

$$J^0 \equiv \frac{2\pi}{\omega}\overline{\dot{\phi}^2}, \ \ J^i \equiv -\frac{\pi}{\omega}\left(\dot{\phi}\partial_i\phi - \phi\partial_i\dot{\phi}\right), \tag{3.3.39}$$

if the dynamics of the scalar field is periodic at each point, and if the external parameter varies sufficiently slowly. Here $\omega = 2\pi\nu$ is the angular frequency, and the overline represents the average over one period of the motion:

$$\overline{X}(t) \equiv \nu \int_t^{t+1/\nu} X(t')dt'. \tag{3.3.40}$$

Note that the spatial components of the adiabatic current are induced by the weak deviation from the separable form. This implies that the adiabatic charge is transferred to other spatial points gradually as the external parameter varies adiabatically, which allows the deformation of I-balls as we shall see later in chap. 6.

We define the adiabatic charge:

$$I \equiv \frac{1}{2\pi} \int d^D x \, J^0 = \int d^D x \frac{\overline{\dot{\phi}^2}}{\omega}, \tag{3.3.41}$$

where D denotes the spatial dimension, and the pre-factor $1/2\pi$ is just a convention. For a spatially localized configuration, the adiabatic charge is conserved:

$$I = \text{const.} \tag{3.3.42}$$

as long as the external parameter changes sufficiently slowly with time.

3.4 Lowest energy state under the conservation of I

In the previous section 3.3, we have proved that, for an oscillating scalar field, the adiabatic charge is conserved if λ_f changes slowly. If we consider the lowest energy state for a fixed

value of the adiabatic charge, the configuration of the field becomes spatially localized one for some class of potentials. In this section, we will derive a necessary condition for the potentials to have the localized solution.

3.4.1 Necessary condition

In the proof of the conservation of the adiabatic charge, we have assumed the separable form (3.3.22) for the field. As we show later in chap. 6, the form is satisfied for some class of potentials that are dominated by a quadratic term with slight modulation by higher terms

$$V = \frac{m^2}{2}\phi^2 + \delta V, \tag{3.4.1}$$

where m is the mass of the field ϕ and δV represents higher order terms. When δV is absent, the field just oscillates with a frequency m. In this subsection, we explain the condition for the modulation δV that the configuration of ϕ becomes a localized one.

As the quadratic term dominates the potential, ϕ oscillates with a frequency $\omega \simeq m$. Thus, we assume the oscillation by a separable form as

$$\phi(t, \vec{x}) = \Phi(t, \vec{x})\cos(mt). \tag{3.4.2}$$

As we explain later, the periodic oscillation of the field is established for the potential mainly dominated by the quadratic term with a logarithmic correction. In this case, Φ is a time-independent function. For potentials deviated from that, Φ has slight time dependence as

$$|\dot{\Phi}|/\Phi \ll m. \tag{3.4.3}$$

By the slight deviation from the separable form, the trajectory of the phase space would not be closed, and there would occur a violation of the conservation of the adiabatic charge at some amount. Noting that the adiabatic invariant in the classical mechanical system is a well conserved quantity, and its variation is exponentially suppressed for a small breaking of the adiabaticity [37]. Thus, it would be expected that the adiabatic charge is conserved approximately even for the field theory. Here we assume that the conservation is established, and its value is fixed to a value I.

We investigate the configuration of the field that the energy becomes the lowest one for a fixed I. For the investigation, let us minimize the following energy $\bar{E}_{\tilde{\omega}}$ of the field for the fixed I using a Lagrange multiplier:

$$\overline{E}_{\tilde{\omega}} \equiv \overline{E} + \tilde{\omega}\left(I - \int d^D x \frac{1}{\omega}\overline{\dot{\phi}^2}\right)$$

$$= \int d^D x \left[\frac{1}{2}\left(1 - 2\frac{\tilde{\omega}}{\omega}\right)\overline{\dot{\phi}^2} + \frac{1}{2}\overline{(\nabla\phi)^2} + \overline{V}\right] + \tilde{\omega}I. \tag{3.4.4}$$

Here E is the energy of the field, $\tilde{\omega}$ is a multiplier, ω is the frequency of the oscillation, which is estimated by the mass of the field, $\omega \simeq m$ and D is the dimension of space. As I is a variable defined by the time average for one oscillation, we have used the time-averaged energy. Since we have approximated the oscillation of the field by a harmonic

function (3.4.2), the time average of polynomials of the field and its time derivative are approximately given by

$$\overline{\phi^n} \simeq c_n \Phi^n, \ \overline{\dot{\phi}^2} \simeq \frac{\omega^2}{2} \Phi^2, \tag{3.4.5}$$

where c_n is real parameters:

$$\{c_2, c_4, c_6, ...\} = \left\{ \frac{1}{2}, \frac{3}{8}, \frac{5}{16}, ... \right\}. \tag{3.4.6}$$

Substituting the time averages (3.4.5) into (3.4.4), $\overline{E}_{\tilde{\omega}}$ is written as

$$\overline{E}_{\tilde{\omega}} \simeq \frac{1}{4} \int d^D x \left[(\nabla \Phi)^2 + \omega^2 \left(\left(1 - 2\frac{\tilde{\omega}}{\omega} \right) \Phi^2 + 4\overline{V} \right) \right] + \tilde{\omega} I. \tag{3.4.7}$$

Let us take a functional derivative of the above equation with respect to Φ:

$$\delta \overline{E}_{\tilde{\omega}} = -\frac{1}{2} \int d^D x \, \delta \Phi \left[\nabla^2 \Phi - \omega^2 \left[\left(1 - 2\frac{\tilde{\omega}}{\omega} \right) \Phi - 2\frac{\partial \overline{V}}{\partial \Phi} \right] \right]. \tag{3.4.8}$$

From the lowest energy condition $\delta \overline{E}_{\tilde{\omega}} = 0$ for the above equation, we obtain the following bounce equation for Φ:

$$\nabla^2 \Phi - \omega^2 \left(1 - 2\frac{\tilde{\omega}}{\omega} \right) \Phi - 2\frac{\partial \overline{V}}{\partial \Phi} = 0. \tag{3.4.9}$$

Now we assume that the bounce solution is spherically symmetric, $\Phi = \Phi(r)$, where r is the radial coordinate. Then the Laplacian can be written as

$$\nabla^2 = \frac{d^2}{dr^2} + \frac{D-1}{r} \frac{d}{dr}. \tag{3.4.10}$$

Thus, the differential equation for Φ is reduced to

$$\frac{d^2}{dr^2} \Phi + \frac{D-1}{r} \frac{d}{dr} \Phi + \frac{\partial}{\partial \Phi} U = 0, \tag{3.4.11}$$

where

$$U \equiv -2\overline{V} - \frac{\omega^2}{2} \left(1 - 2\frac{\tilde{\omega}}{\omega} \right) \Phi^2. \tag{3.4.12}$$

Since we have assumed that the potential is dominated by the quadratic term (3.4.1), the potential U is written as

$$U = -2\overline{\delta V} - \left[m^2 + \frac{\omega^2}{2} \left(1 - 2\frac{\tilde{\omega}}{\omega} \right) \right] \Phi^2. \tag{3.4.13}$$

Comparing the differential eq. (3.4.11) to the equation of motion for a point particle, we can regard r as like the time variable. By this identification, we can regard eq. (3.4.11) as the evolution equation for Φ from $r = 0$ to ∞ with a friction term $(D-1) d\Phi/dr$. In

order to evaluate the solution of this equation, we set boundary conditions at $r = 0$ and ∞ as

$$
\begin{cases}
\dfrac{d}{dr}\Phi(r = 0) = 0, \\[2mm]
\quad \Phi(r = \infty) = 0.
\end{cases}
\tag{3.4.14}
$$

As the object that we are now investigating is radially symmetric, the gradient of the field at the center vanishes, which is the first condition. As the object is the localized one, amplitude at infinity should be zero, which is the second condition. Above boundary conditions are satisfied for some shape of potentials, which is explained as follows. Since we have assumed that the potential is dominated by the quadratic one around minimum, the curvature of U near $\Phi \simeq 0$ is determined by the quadratic one, and its sign is negative as shown in fig. 3.13. On the other hand, far away from the minimum, the potential is dominated by the higher term δV. The sign of δV is important whether the bounce solution becomes a localized one or not. In the case that the sign of it is positive $\delta V > 0$, U is not supported from the bellow as shown by the blue line in fig. 3.13. For this unstable potential, the boundary condition (3.4.14) is not satisfied. On the other hand, in the case that the sign of the higher term is negative $\delta V < 0$, U looks as shown by the red line in fig. 3.13, and a bounce solution exists. Thus, from above arguments, we can obtain a necessary condition for the potential to have the solution of the localized configuration,

$$
\delta V < 0. \tag{3.4.15}
$$

This necessary condition is identical to the heuristically known condition that, the slightly flatter potential is necessary for the formation of I-balls [23–25].
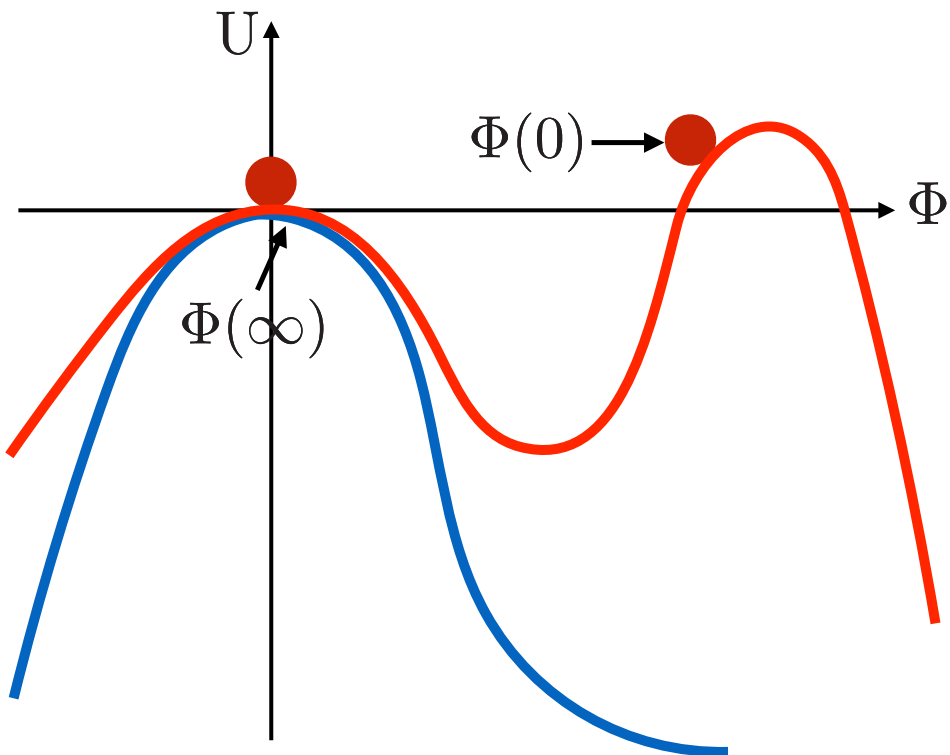
Figure 3.13: The condition for the existence of I-ball. The red line corresponds to $\delta V < 0$, and the blue one is for $\delta V > 0$.

Chapter 4

The possibility of the formation of I-balls in the R^2 inflation

We have briefly reviewed the dynamics of the R^2 inflation in sec. 2.5. A distinctive feature of this model is that the dynamics of inflation is determined only by one additional mass parameter M to the ones of the standard model. The interactions of the inflaton with standard model particles are given by the gravitational ones, and their strength is determined by the mass parameter. Thus, the mass parameter also determines the decay rate of the inflaton uniquely. Therefore, if we can evaluate the decay rate, we can determine the e-folding number at the pivot scale only by M, and then give the predictions of n_s and r uniquely, which can be tested by the future observations.

As we have reviewed in sec. 2.5, within the perturbative regime, the decay rate of the inflaton is estimated as $\Gamma_{\rm tot} \simeq (N_\chi/96\pi)\,(M/M_p)^2\,M$ [33–35]. Thus, the reheating temperature of this inflation model is estimated as $T_R \simeq 0.4\,(N_\chi/96\pi)^{1/2}\,(M/M_p)\sqrt{MM_p} \simeq 10^{-9}M_p$, and then the e-folding number is determined as $N_e \simeq 54 + (1/3)T_R/10^9{\rm GeV}$. However, the formation of I-balls might change the above estimation of the decay rate.

After inflation, the inflaton of the R^2 inflation coherently oscillates around the minimum of the potential. As we have explained in sec. 3.1, fluctuations of the particles that couple with the inflaton could be enhanced by the parametric resonance. By the resonance, the fluctuations would grow exponentially, and then at some time, they start to interact with other modes. As we have explained in sec. 3.2, by the non-linear dynamics after the non-perturbative evolution of the fluctuations, the inflaton might lead to the formation of I-balls. If I-balls are formed after inflation, the energy density of the inflaton would localize at finite regions, and then the decay process of it would be changed. Thus, to validate the estimation of the decay rate, we investigate the formation of I-balls.

It is heuristically known that the formation of I-balls could occur if the potential of the field is flatter than the quadratic one. Indeed, the shape of the potential of the R^2 inflation

$$V = \frac{3}{4}M^2 M_p^2 \left[1 - \exp\left(-\sqrt{2/3}\phi/M_p\right)\right]^2 \tag{4.0.1}$$

is flatter where the field value of the inflaton is larger than the Planck mass $\phi \gtrsim M_p$, and inflation occurs in this region. If fluctuations are sufficiently enhanced after the R^2 inflation, there might occur the formation of I-balls. As explained in sec. 3.2, a necessary

condition for the formation is heuristically obtained; the growth rate of fluctuations need to exceed the Hubble expansion rate [66–68].

In this chapter, we investigate whether the inflaton of the R^2 inflation forms I-balls during reheating. In particular, we study the growth rate of fluctuations during reheating, and compare it with the Hubble parameter. This chapter is based on the author's work [88] collaborated with Yuki Watanabe.

4.1 Instability ($H = 0$)

Just after inflation, the inflaton is coherently oscillating with small fluctuations. If a sufficient growth of the fluctuations takes place, the I-balls may be formed. As we explained in sec. 3.2, the growth rate should be larger than the Hubble expansion rate (Numerical value is given by $\langle \mu_k M/H \rangle \gtrsim 4-5$ in (3.2.19) and (3.2.27)). Thus, in order to investigate the possibility of the formation of I-balls, we study the resonance structure of the potential. First of all, to clarify the resonance structure, we consider the Minkowski space-time ($H = 0$). In this space-time, we study the growth rate of the fluctuations numerically and understand it analytically.

In the Minkowski space-time, the equation of motion for the inflaton field ϕ is given by

$$\ddot{\phi}(\mathbf{x}, t) - \nabla^2 \phi(\mathbf{x}, t) + V'(\phi) = 0. \tag{4.1.1}$$

In order to study the stability of fluctuations, we divide $\phi(\mathbf{x}, t)$ into the background and fluctuations as $\phi(t, \vec{x}) = \phi_0(t) + \delta\phi(t, \vec{x})$, and then we obtain coupled equations as

$$\ddot{\phi}_0 + V'(\phi_0) = 0, \tag{4.1.2}$$

and

$$\delta\ddot{\phi}_k + \left[k^2 + V''(\phi_0) \right] \delta\phi_k = 0, \tag{4.1.3}$$

where

$$V'(\phi) = \sqrt{\frac{3}{2}} M^2 M_p \left[1 - e^{-\sqrt{\frac{2}{3}} \frac{\phi}{M_p}} \right] e^{-\sqrt{\frac{2}{3}} \frac{\phi}{M_p}}, \tag{4.1.4}$$

$$V''(\phi) = M^2 \left[-1 + 2 e^{-\sqrt{\frac{2}{3}} \frac{\phi}{M_p}} \right] e^{-\sqrt{\frac{2}{3}} \frac{\phi}{M_p}}. \tag{4.1.5}$$

Here, we defined $\delta\phi_k$ by the Fourier mode of $\delta\phi(t, \vec{x})$. Numerically solving above coupled equations, we study the instabilities and understand them analytically by reducing the equations to the Mathieu equation.

4.1.1 Numerical result

We assume that ϕ_0 is oscillating with a constant amplitude Φ. In this case, we can see that the frequency of $\delta\phi_k$ in (4.1.3) is periodically oscillating one $\omega_k^2 = k^2 + V''(\phi_0)$. As we explained in sec. 3.1, by this periodic oscillation of the frequency, the parametric resonance occurs, and then fluctuations are enhanced at a particular resonance band. In order to

investigate this resonance band, first we numerically solve the coupled equations (4.1.2) and (4.1.3) with the method of the 4-th order Runge-Kutta.

We set the initial conditions for the background field as

$$\phi_0(t_0) = \Phi, \quad \dot{\phi}_0(t_0) = 0. \tag{4.1.6}$$

The field value of inflaton at the end of inflation is comparable with the Planck mass. Thus, we performed simulations for the initial value of the amplitude around the Planck mass: $\Phi/M_p = 2$, 0.5, 0.1 and 0.01. Since eq. (4.1.3) is a linear equation with respect to $\delta\phi$, the ratio of the fluctuation at t to the one at the initial $\delta\phi_k(t)/\delta\phi_k(t_0)$ is independent on the initial amplitude. Thus, in order to know the resonance structure of the potential, i.e., the growth rate of fluctuations, we set the initial amplitude by hands with a flat spectrum as

$$\delta\phi_k(t_0) = 10^{-5} M_p M^{-3}. \tag{4.1.7}$$

We show the results of simulations in fig. 4.1, which show the time evolution of fluctuations for different Φ. Each panel shows the power spectrum of $\delta\phi_k$ at four or five time slices. From the figure we can see that, for $\Phi \gtrsim 0.1 M_p$, fluctuations are amplified around a particular scale $k \sim 0.1\ M$, and for $\Phi \lesssim 0.01 M_p$, they are amplified around $k \sim 0.01\ M$. We find that the typical time scale of the amplification, if it happens, is larger than hundred unit times $\Delta t \gtrsim 100/M$. Parametrizing this enhancement as $\delta\phi_k(t) = \delta\phi_k(t_0)\exp(\mu_k Mt)$, we can estimate the typical growth rate at the resonance band as

$$\begin{aligned} \mu_k &= \ln\left(\delta\phi_k(t_0 + \Delta T)/\delta\phi_k(t_0)\right)\frac{1}{M\Delta t} \\ &\lesssim 0.01. \end{aligned} \tag{4.1.8}$$

Thus, in the Minkowski space-time, the growth rate of the R^2 inflation's potential is typically smaller than 10^{-2}. In the expanding Universe, the expansion would affect the resonance, and it is expected that by the dilution and red-shift, the growth rate would be more suppressed.

4.1.2   Analytical understanding

The self-resonance of ϕ can be understood analytically, based on the Mathieu equation as we have reviewed in sec. 3.1.

Let us approximate the oscillation of the background field by the harmonic function with a constant amplitude as

$$\phi_0 \simeq \Phi\cos(Mt). \tag{4.1.9}$$

In order to clarify the resonance band, we expand eq. (4.1.5) up to quadratic terms:

$$V'' \simeq M^2\left[1 - \sqrt{6}\frac{\phi}{M_p} + \frac{7}{3}\left(\frac{\phi}{M_p}\right)^2\right]. \tag{4.1.10}$$

By this expansion, the equation of motion for $\delta\phi_k$ is written as

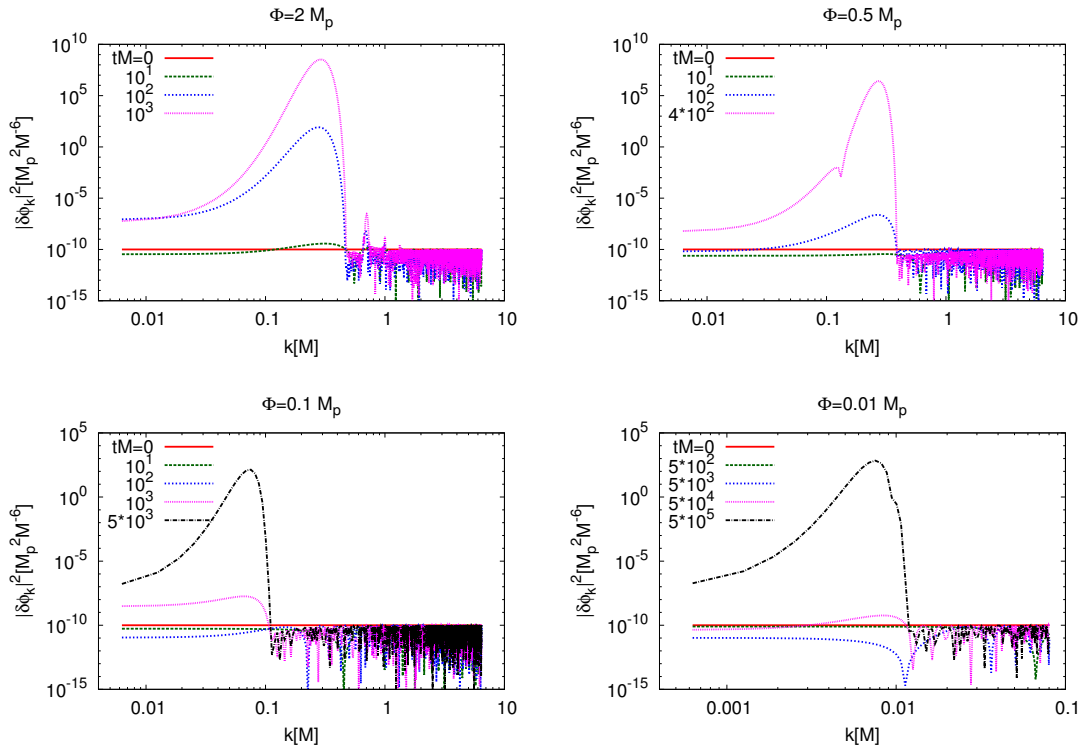$$\delta\ddot{\phi}_k + \omega_k^2\delta\phi_k = 0, \tag{4.1.11}$$

Figure 4.1: Time evolution of fluctuations from $t = 0$ for each initial amplitude of the background field $\Phi/M_p = 2$, 0.5, 0.1 and 0.01. Each line is the snapshot of the spectrum of the fluctuations at several time. The vertical axis $\delta\phi_k$ is the Fourier mode of the fluctuation $\delta\phi(x)$, and the horizontal axis k is the corresponding momentum.

where

$$\omega_k^2 = k^2 + M^2 \left[1 + \frac{7}{6} \left(\frac{\Phi}{M_p} \right)^2 \right]$$
$$- \sqrt{6} M^2 \frac{\Phi}{M_p} \cos(Mt) + \frac{7}{6} M^2 \left(\frac{\Phi}{M_p} \right)^2 \cos(2Mt). \tag{4.1.12}$$

For smaller Φ, the time dependence of the frequency (4.1.12) is dominated by $\cos(Mt)$, while for larger Φ, it is also contributed by higher harmonics such as $\cos(2Mt)$. We parametrize the contribution of the higher harmonic terms by defining the ratio of the two coefficients of $\cos(Mt)$ and $\cos(2Mt)$ as

$$\alpha_r \equiv \frac{7}{6\sqrt{6}} \frac{\Phi}{M_p}. \tag{4.1.13}$$

In order to clarify the resonance structure, we consider the contribution of the oscillating terms respectively.

Resonance by $\cos(Mt)$ term

When $\alpha_r \lesssim 1$, the expansion of the potential makes sense. This condition corresponds to $\Phi \lesssim 2M_p$, and the lower harmonic term $\propto \cos(Mt)$ dominates the frequency:

$$\omega_k^2 \simeq k^2 + M^2 \left[1 + \frac{7}{6} \left(\frac{\Phi}{M_p} \right)^2 \right] - \sqrt{6} M^2 \frac{\Phi}{M_p} \cos(Mt). \tag{4.1.14}$$

With this time dependent frequency, the equation of motion is reduced to the Mathieu equation as

$$\frac{d^2}{dz^2} \delta\phi_k + [A_{1k} - 2q_1 \cos(2z)] \delta\phi_k = 0, \tag{4.1.15}$$

where we rescaled the time variable as $z \equiv Mt$. Here, the parameters q_1 and A_{1k} are given by

$$q_1 \equiv 2\sqrt{6} \frac{\Phi}{M_p}, \tag{4.1.16}$$

$$A_{1k} \equiv 4 + 4 \left(\frac{k}{M} \right)^2 + \frac{7}{36} q_1^2. \tag{4.1.17}$$

As we explained in sec. 3.1, the solution of the Mathieu equation has growing mode solution depending on the two parameters. In the case $q_1 \lesssim 1$, the narrow resonance occurs, and the resonance band is estimated by the relation $A_{1k} \simeq n^2$. In the case $q_1 \gtrsim 1$, the broad resonance occurs, and the resonance band is estimated by considering the parameters that break the adiabatic condition $|d\omega_k/dt|/\omega_k^2 > 1$.

First consider the broad resonance $q_1 \gtrsim 1$, i.e., $0.2M_p \lesssim \Phi \lesssim 2M_p$. In this case, the growth of fluctuations occurs when the adiabatic condition breaks down $|d\omega_k/dt|/\omega_k^2 > 1$.
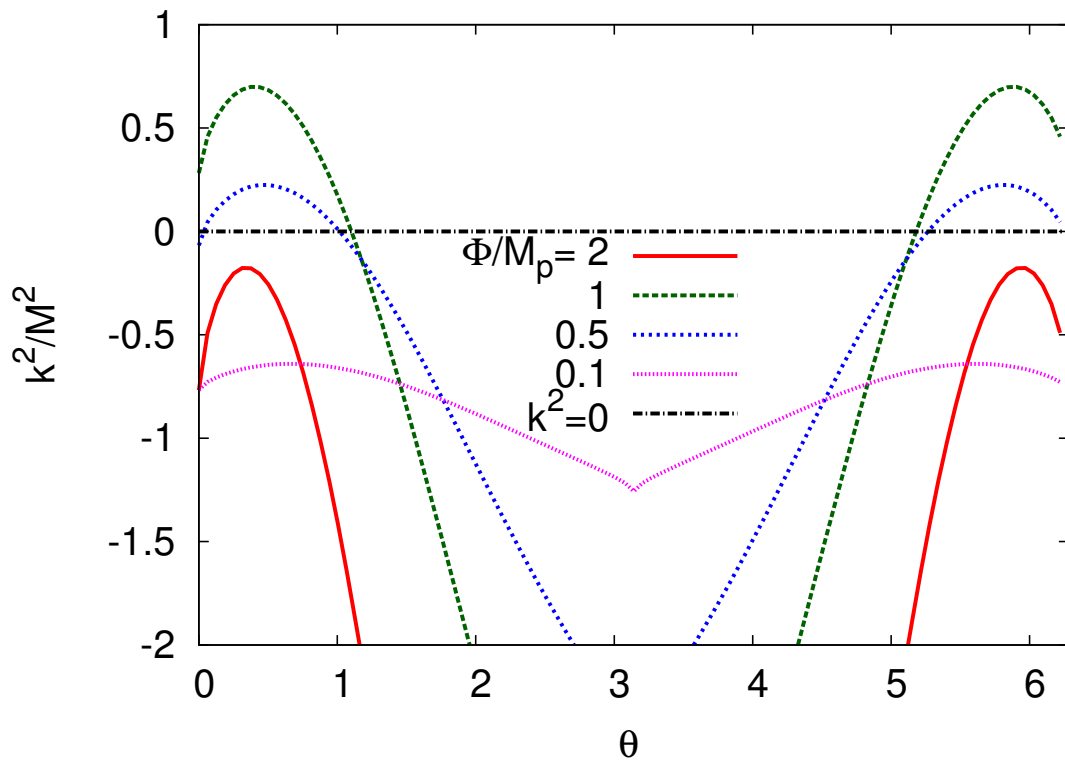
Figure 4.2:   Non-adiabatic condition triggered by the harmonic term $\propto \cos(Mt)$ for the initial amplitude $\Phi/M_p = 2$, 1, 0.5 and 0.1. The vertical axis is momentum. The horizontal axis is the time variable which is defined as $\theta \equiv Mt$ (modulo 2π). The curved lines in the figure are the right hand side of the resonance condition (4.1.18) for different Φ. The broad resonance occurs when each line locates over the $k = 0$ line.

Substituting the frequency (4.1.14) into this condition, we obtain the instability band of the broad resonance triggered by $\propto \cos(Mt)$ term as

$$\left(\frac{k}{M}\right)^2 < -1 - \frac{7}{6}\left(\frac{\Phi}{M_p}\right)^2 + \sqrt{6}\frac{\Phi}{M_p}\cos(Mt) + \left(\frac{3}{2}\right)^{\frac{1}{3}}\left(\frac{\Phi}{M_p}\right)^{\frac{2}{3}}|\sin(Mt)|^{\frac{2}{3}}. \qquad (4.1.18)$$

Fluctuations whose momenta satisfy the above equation are enhanced by the broad resonance. We numerically solved the right hand side of (4.1.18) and then plot the results in fig. 4.2. In the figure, the region above $k = 0$ and bellow each line is the instability mode for each Φ. Hence we can see that the broad resonance does not occur for $\Phi = 2M_p$ and $0.1M_p$ cases, but occurs for $\Phi = 0.5M_p$ and $1M_p$ for a resonance band. Thus, we expect that the resonance for $\Phi = 2M_p$ and $0.1M_p$ observed in fig. 4.1 would be triggered by higher harmonic terms or by the narrow resonance. On the other hand, for $\Phi = 0.5M_p$ case, we can see that the resonance occurs for $0 < k < 0.47M$, which explains the enhancement shown in the upper right panel of fig. 4.1.

Next let us consider the narrow resonance $q_1 \lesssim 1$, i.e. $\Phi < 0.2M_p$. For the narrow resonance, the instability band is given up to numerical factors by

$$-q^n \lesssim A_k - n^2 \lesssim q^n, \qquad (4.1.19)$$

where n is an integer. The band width of the narrow resonance shrinks as q^n for larger n, and the growth rate decreases. Thus, the resonance at lower bands is more important. Since now there is no real solution for $n = 1$ and $A_k = A_{1k}$, the second band is most important. In this case, the condition (4.1.19) can be given more precisely by (Sec. 20.2.25 of [69])

$$-\frac{1}{12}q^2 < A_k - 4 < \frac{5}{12}q^2. \qquad (4.1.20)$$

Thus the instability at the 2nd band for $q = q_1$ and $A_k = A_{1k}$ is given by

$$0 \leq \frac{k}{M} < \frac{1}{3\sqrt{2}}q_1. \qquad (4.1.21)$$

The condition for the narrow resonance shows that, for $\Phi = 0.1M_p$ and $10^{-2}M_p$, instabilities occur within $0 \leq k/M < 1/(5\sqrt{3}) \approx 0.115$ and $0 \leq k/M < 1/(50\sqrt{3}) \approx 0.0115$, respectively. This explains the enhancement of fluctuations for $\Phi = 0.1M_p$ and $10^{-2}M_p$ shown in the bottom two panels of fig. 4.1.

Resonance by $\cos(2Mt)$ term

Next, we consider the effect of the higher harmonic term $\propto \cos(2Mt)$ in the frequency ω_k (4.1.12). When $\alpha_r \gtrsim 1$, higher order terms of the potential affects the dynamics of the fluctuations and would change the structure of the resonance. To see the effect of the higher terms, as a reference, we consider the effect of the $\cos(2Mt)$ term.

In order to clarify the effect of $\cos(2Mt)$ term, we neglect $\cos(Mt)$ term in the frequency:

$$\omega_k^2 \simeq k^2 + M^2\left[1 + \frac{7}{6}\left(\frac{\Phi}{M_p}\right)^2\right] + \frac{7}{6}M^2\left(\frac{\Phi}{M_p}\right)^2\cos(2Mt). \qquad (4.1.22)$$

For this approximation, we can reduce the equation of motion for $\delta\phi_k$ to the Mathieu equation:

$$\frac{d^2}{dz^2}\delta\phi_k + [A_{2k} - 2q_2\cos(2z)]\,\delta\phi_k = 0. \tag{4.1.23}$$

Here, the parameters q_2 and A_{2k} are given by

$$q_2 \equiv \frac{7}{12}\left(\frac{\Phi}{M_p}\right)^2, \tag{4.1.24}$$

$$A_{2k} \equiv 1 + \left(\frac{k}{M}\right)^2 + 2q_2. \tag{4.1.25}$$

Substituting the frequency (4.1.22) into the non-adiabatic condition $|d\omega/dt|/\omega^2 > 1$, we obtain the instability band of the broad resonance triggered by $\propto \cos(2Mt)$ as

$$\left(\frac{k}{M}\right)^2 < -1 - \frac{7}{6}\left(\frac{\Phi}{M_p}\right)^2[1 + \cos(2Mt)] + \left(\frac{7}{6}\right)^{\frac{2}{3}}\left(\frac{\Phi}{M_p}\right)^{\frac{4}{3}}|\sin(2Mt)|^{\frac{2}{3}}. \tag{4.1.26}$$

Fluctuations whose momenta satisfy the above condition (4.1.26) exponentially grow. We have numerically solved the right hand side of (4.1.26) for $\Phi/M_p = 2$, 1 and 10 and then plot the result in fig. 4.3. Instabilities occur if the lines lie above zero for some time. For $\Phi = 2M_p$, the broad resonance is induced within $0 \leq k < 0.37M$. These k-modes explain the enhancement of fluctuations for $\Phi = 2M_p$ shown in the upper left panel of fig. 4.1. We have also studied the instability band for $\Phi = 10M_p$. The result of the simulation in fig. 4.3 shows the breakdown of the adiabatic condition for $0 \leq k < 2.2M$. For this case, amplitude of the higher terms are comparable to the lowest one $\propto \cos(Mt)$. Thus, we can expect that the broad resonance effects would be achieved by the multi higher harmonic terms $\propto \cos(nMt)$. This multi resonance bands can be seen by the numerical simulations shown in fig. 4.4.

In this section, we have investigated the resonance structure of the R^2 inflation's potential in the Minkowski space-time. We have found that the narrow and broad parametric resonances are induced by the oscillation of the background field with self-interactions (4.1.12). For smaller amplitude of the background field $\Phi < 0.2M_p$, fluctuations are enhanced by the narrow resonance at 2nd band. On the other hand, for larger amplitude $\Phi \gtrsim 0.2M_p$, the enhancement is induced by the broad resonance. In the case of $\Phi < 2M_p$, this broad resonance is achieved by a harmonic term $\cos(Mt)$ in the frequency. For $\Phi > 2M_p$, the resonance is triggered by multi harmonic terms in the potential, and then the enhancement occurs at multi resonance modes.

We have investigated the enhancement of fluctuations of the inflaton in the Minkowski space-time. In order to investigate the formation of I-balls, next, we study the growth rate in the expanding Universe, i.e., during reheating. In the expanding Universe, the redshift of the momenta of fluctuations would change the structure of the resonance, and the Hubble expansion would dilute fluctuations. In order to study these effects, again we perform calculations numerically and understand the results analytically.
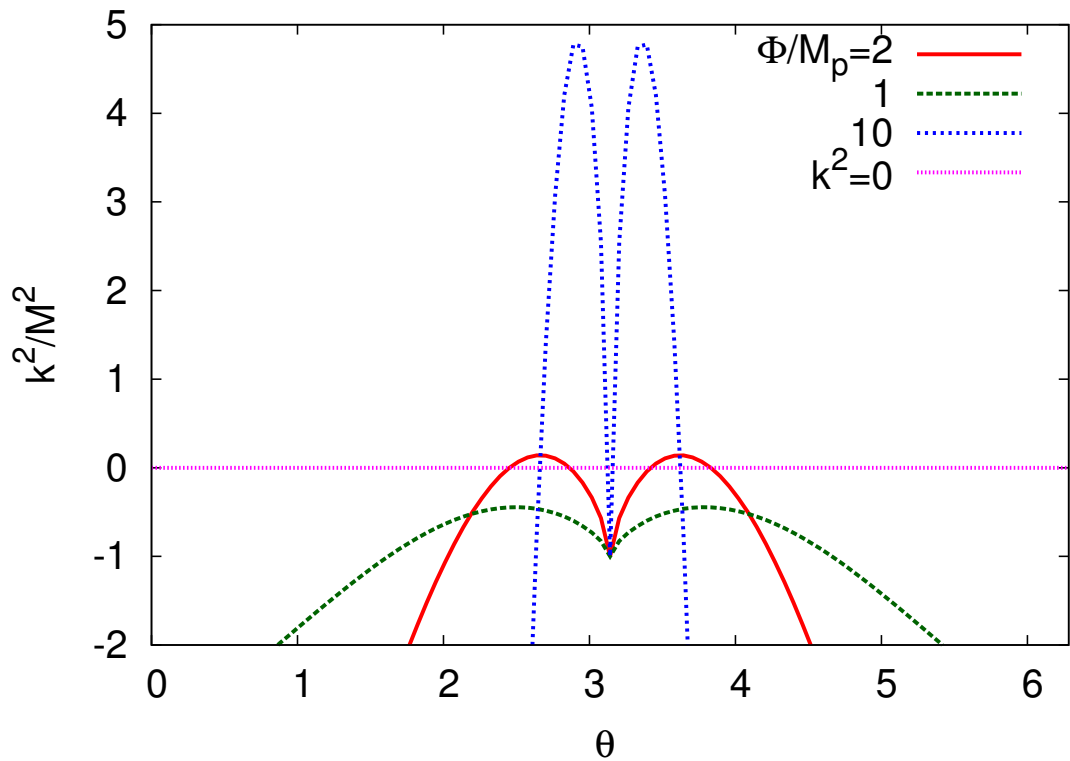
Figure 4.3: Non-adiabatic condition triggered by the higher harmonic term $\propto \cos(2Mt)$ for initial amplitude $\Phi/M_p = 10$, 2 and 1. The vertical axis is momentum. The horizontal axis is the time variable which is defined as $\theta \equiv Mt$ (modulo 2π). The curved lines are the right hand side of the resonance condition (4.1.26) for different Φ. The broad resonance occurs when each line locates over the $k = 0$ line.
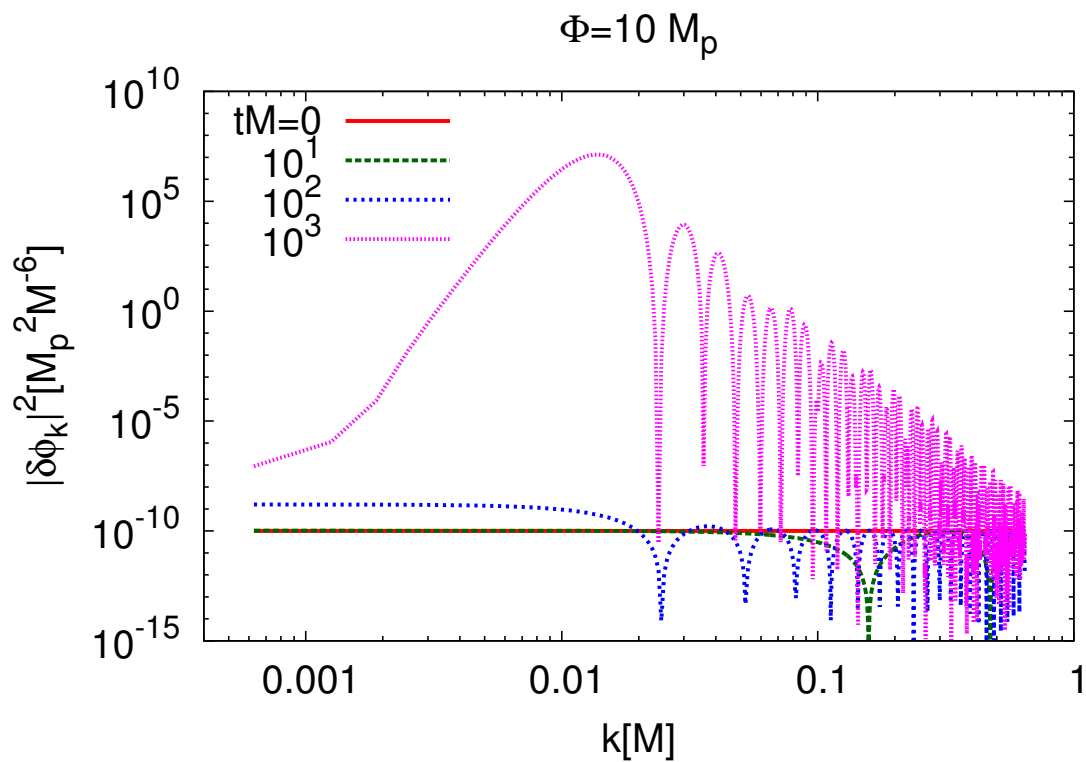
Figure 4.4: Time evolution of fluctuations from $t = 0$ to $10^3/M$ for $\Phi = 10\,M_p$. Each line is the snapshot of the spectrum of the fluctuations at several time. The vertical axis $\delta\phi_k$ is the Fourier mode of the fluctuation $\delta\phi(x)$, and the horizontal axis k is the corresponding momentum.

4.2 Instability ($H \neq 0$)

So far, we have ignored the Hubble expansion, which triggers the redshift of momentum and dilutes fluctuations. Structures of the parametric resonance would be affected by the Hubble expansion. Thus, in this section, we investigate the enhancement of fluctuations including the effect of the expansion.

4.2.1 Rigid Friedmann background

Let us consider the FRW metric. For this metric, the equation of motion for the inflaton is given by

$$\ddot{\phi} + 3H\dot{\phi} - \frac{\nabla^2}{a^2}\phi + V'(\phi) = 0. \tag{4.2.1}$$

Just after inflation, the Universe is dominated by the inflaton, and the Hubble parameter is dominantly determined by the energy density of the inflaton as

$$H^2 = \frac{1}{3M_p^2}\left(\frac{1}{2}\dot{\phi}^2 + V(\phi)\right). \tag{4.2.2}$$

To investigate the structure of the resonance, we divide ϕ into the background and fluctuations as $\phi(x,t) = \phi_0(t) + \delta\phi(x,t)$, and we write the equation as

$$\ddot{\phi}_0 + 3H\dot{\phi}_0 + V'(\phi_0) = 0, \tag{4.2.3}$$

$$\delta\ddot{\phi}_k + 3H\delta\dot{\phi}_k + \frac{k^2}{a^2}\delta\phi_k + V''(\phi_0)\delta\phi_k = 0. \tag{4.2.4}$$

Here we evaluate the Hubble parameter approximately by the background field as $H^2 \simeq [\dot{\phi}_0^2/2 + V(\phi_0)]/(3M_p^2)$. We denote the time when inflation ends by t_e. This time is estimated by the breaking of the slow-roll condition, which is determined by that the slow-roll parameter becomes unity $\epsilon_V = 1$, which gives $\phi_0(t_e) = 0.94M_p$.

In the previous section, we have found that the growth rate of the inflaton in the Minkowski space-time is typically $\mu_k \lesssim 10^{-2}$ if the background field is oscillating with a amplitude of the Planck mass. Thus, for the significant growth of fluctuations, it takes more than hundred unit times $\Delta t \gtrsim 100/M$. In the expanding Universe, the expansion would suppress the growth of fluctuations. Due to the expansion, the amplitude of the background field damps as $\phi_0 \propto a^{-3/2} \propto t^{-1}$. By this damping, the amplitude of the background ϕ_0 becomes too small to induce the growth of the fluctuations after a hundred unit times or a few tens of oscillations: $\phi_0(t_e + \Delta t) \approx 0.94M_p/100 \sim \mathcal{O}(10^{-2})M_p$. Therefore, the enhancement by the parametric resonance would not be efficient after the R^2 inflation.

We have studied the evolution of the background field and fluctuations, numerically solving the equations (4.2.3) and (4.2.4). The result of the simulation for the evolution of the amplitude of the background is shown in fig. 4.5. The initial value of the field is set to $\phi_0(t_{\text{ini}}) = 1M_p$. The amplitude of ϕ_0 is indeed decreasing as t^{-1}. From this figure, we can see that inflation ends at $t \approx 4/M$ and $\phi_0 \approx 0.9M_p$, and that $\phi_0 \sim \mathcal{O}(10^{-2})M_p$ after a hundred unit times $t \sim 100/M$ as was expected.
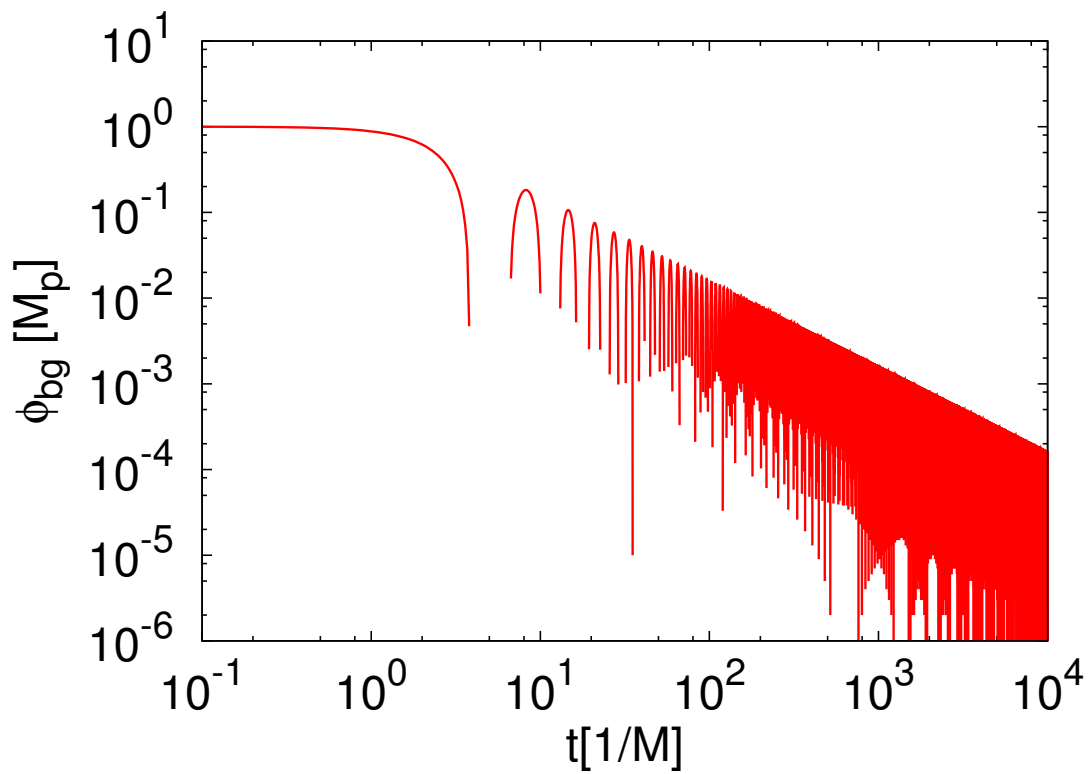
74

Figure 4.5: Time evolution of the background field from $t = 10^{-1}/M$ to $10^4/M$. The vertical axis $\phi_{\mathrm{bg}} = \phi_0$ is the amplitude of the background field, and the horizontal axis t is cosmic time in unit of M^{-1}.
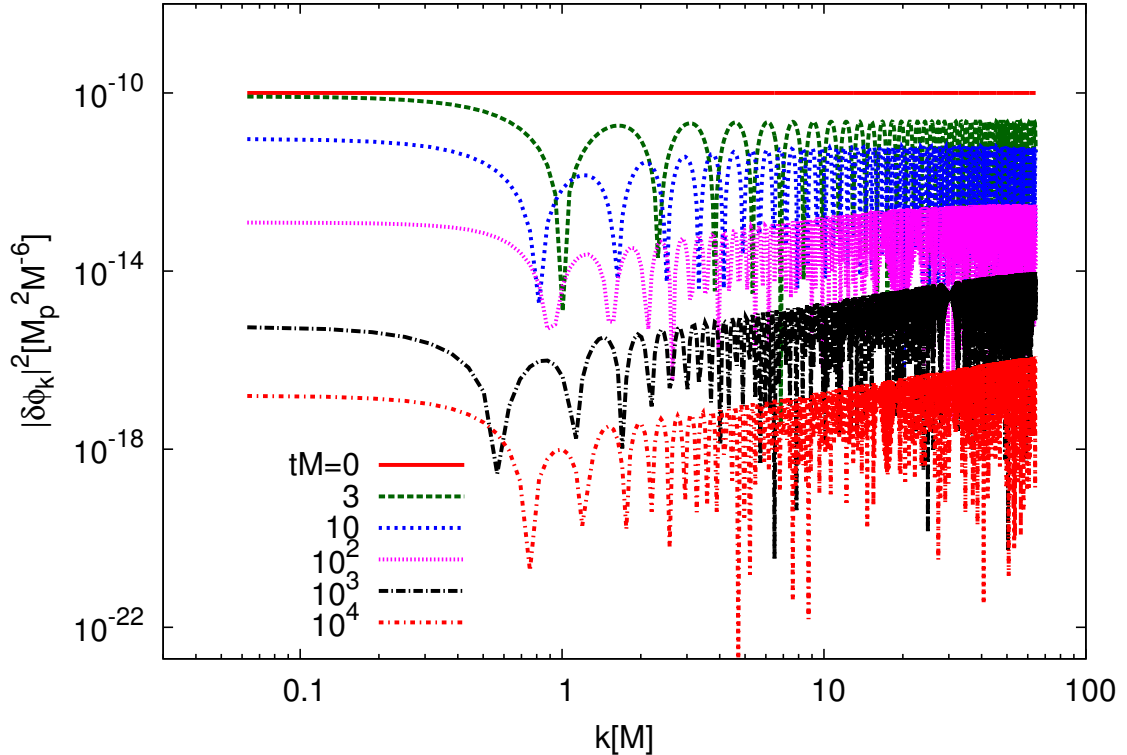
Figure 4.6: Time evolution of fluctuations in the expanding Universe from $t = 0$ to $10^4/M$. Each line is the snapshot of the spectrum of the fluctuations at $Mt = 0$, 10, 10^2, 10^3 and 10^4. The vertical axis $\delta\phi_k$ is the Fourier mode of the fluctuation $\delta\phi(x)$, and the horizontal axis k is the corresponding momentum.

Figure 4.6 shows the time evolution of fluctuations $\delta\phi_k$ for comoving wave numbers k from $2\pi \times 10^{-2}M$ to $2\pi \times 10M$. This simulation covers resonance bands studied in fig. 4.1. Since the eq. (4.2.4) is a linear one for the fluctuation, the growth rate of that to the initial one $\delta\phi_k(t)/\delta\phi_k(t_0)$ is independent of the initial value. In order to investigate the structure of the growth rate μ_k in the expanding Universe, we set the initial value by a flat spectrum as $\delta\phi_k = 10^{-5}M^{-3}M_p$ for every k-mode. From the result of the simulation, we can see that fluctuations are indeed decreased by the expansion of the Universe. This means that the growth rate in the expanding Universe is smaller than the Hubble expansion rate as $\mu_k M/H < 1$. By using lattice simulations [66–68], the heuristic condition for the sufficient production of I-balls in the expanding Universe is investigated, and it is shown that for the formation the amplitude of fluctuations need to grow as robustly $\langle \mu_k M/H \rangle > 3/2$ as explained in sec. 3.2. (Numerical value is given by $\langle \mu_k M/H \rangle \simeq 4 - 5$ in (3.2.19) and (3.2.27)). Following this heuristic condition, we can see that the enhancement of the fluctuations for the R^2 inflation is not sufficient to produce I-balls.

4.2.2 Metric preheating

As we have explained in sec. 2.3, the evolution of fluctuations is correlated with the metric perturbation by the Einstein equation. We have neglected this effect in the previous subsection. In order to include this effect, we construct gauge invariant variables or choose some specific gauge. The comoving gauge curvature perturbation $\mathcal{R}_c$ (2.3.10) is one of the gauge invariant variables. This gauge invariant variable becomes time independent after the exit of the horizon. After the re-enter of the horizon, it gives the initial fluctuations of the relativistic fluids. By theoretically calculating $\mathcal{R}_c$ and constraining it observationally, we can test inflation models. However, it is not useful to calculate this variable within the horizon during reheating because, since by the oscillation of inflaton $\mathcal{R}_c$ has a singular behavior as seen by (2.3.13):

$$\mathcal{R}_c \equiv \frac{H}{\dot{\phi}}\,\delta\phi_{\psi_g}. \tag{4.2.5}$$

Thus $\mathcal{R}_c$ becomes ill-defined. In order to avoid this difficulty, we use the Sasaki-Mukanov variable [50] and then can avoid the singular behavior [89–94]. As we have shown in (2.3.29), at the flat gauge $\psi_g = 0$, the Sasaki-Mukanov equation is given by

$$\delta\ddot{\phi}_{\psi_g} + 3H\delta\dot{\phi}_{\psi_g} + \left[\frac{k^2}{a^2} + V''(\phi_0) + \Delta F\right]\delta\phi_{\psi_g} = 0. \tag{4.2.6}$$

Here we denote the back-reaction from the metric perturbations by ΔF as

$$\Delta F \equiv \frac{2\dot{\phi}_0}{M_p^2 H}V'(\phi_0) + \frac{\dot{\phi}_0^2}{M_p^4 H^2}V(\phi_0). \tag{4.2.7}$$

We have numerically integrated the coupled eqs. (4.2.3) and (4.2.6). Initial conditions for the background and fluctuations are set to the same values as in the subsection 4.2.1. In fig. 4.7, we show the evolution of fluctuations from $t = 0$ to $10^4/M$ for comoving momentum between $k = 2\pi \times 10^{-2}M$ and $2\pi \times 10M$. From this figure, we can see that the fluctuations damp for larger momenta due to the Hubble expansion. For smaller momenta, on the other hand, we find the growth of the fluctuations. The instability occurs near the horizon scale $k \sim 1M$. This enhancement is explained as following. Just after the end of inflation, the enhancement is achieved by the breakdown of slow-roll. Slowly rolling inflaton suddenly starts to oscillates, and then by this rapid change of the velocity, fluctuations with low momenta are enhanced slightly, but this enhancement occurs just at the end of inflation only once. After inflation, the growth is balanced with the Hubble expansion. This result agrees with the previous works [91–94], in which the evolution of the Sasaki-Mukhanov variable for momentum bellow the horizon sale is calculated during reheating with a quadratic potential.

In fig. 4.7, one may notice that there is a decrease of fluctuations at low momenta $k \lesssim M$ at $t = 100/M$. This damping is caused simply by the phase dependence of fluctuations $\delta\phi_k \approx f_k(t)\cos(\omega_k t)$ with $\omega_k = \sqrt{k^2 + M^2}$, where the amplitude $f_k(t)$ is constant in time. (This phase dependence can be found also in figs. 4.1, 4.4 and 4.6.) In order to remove this phase dependence, we plot a phase independent variable given by

$$N_k = \frac{\omega_k}{2}\left(\frac{|\delta\dot{\phi}_k|^2}{\omega_k^2} + |\delta\phi_k|^2\right). \tag{4.2.8}$$
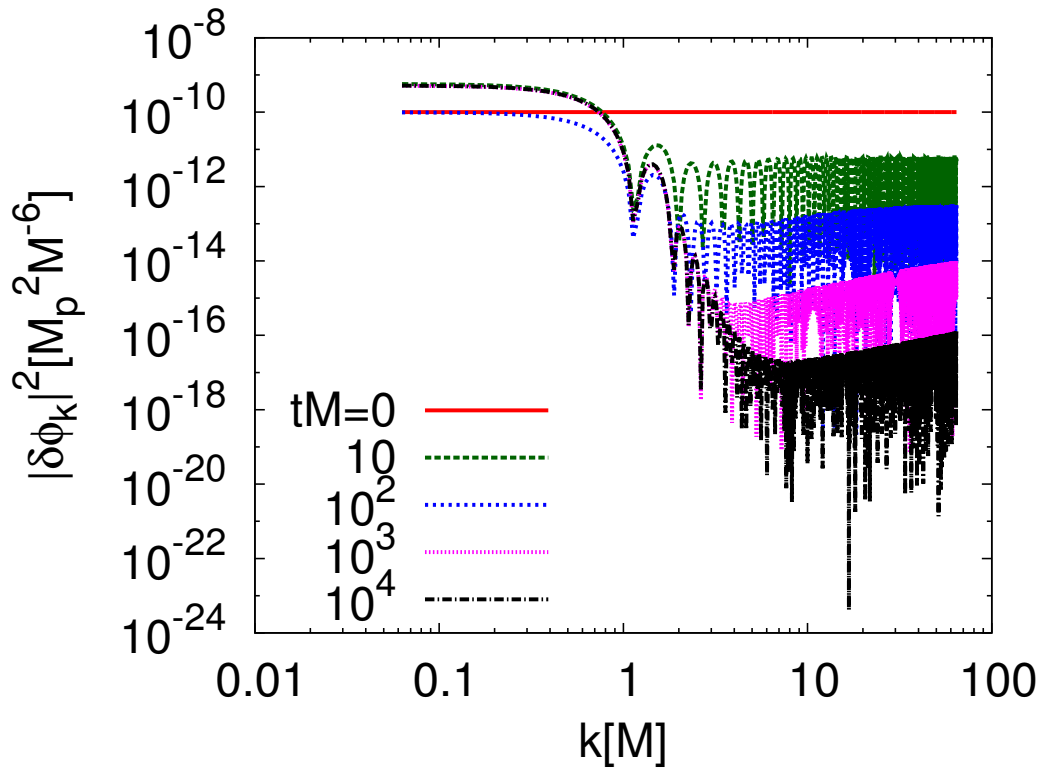
Figure 4.7: Time evolution of fluctuations from $t = 0$ to $t = 10^4/M$ with the Sasaki-Mukhanov equation. Each line is the snapshot of the spectrum of fluctuations at $Mt = 0$, 10, 10^2, 10^3 and 10^4. The vertical axis $\delta\phi_k$ is the Fourier mode of the fluctuation $\delta\phi(x)$, and the horizontal axis k is the corresponding momentum.
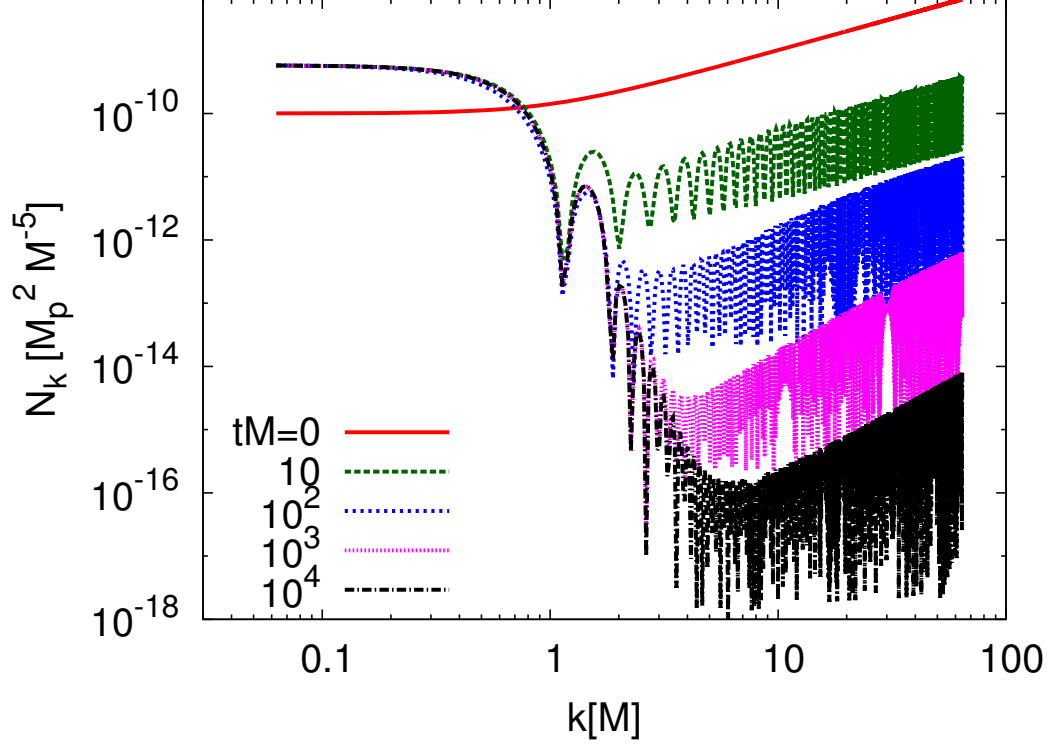
Figure 4.8: Time evolution of N_k from $t = 0$ to $10^4/M$. Each line is the snapshot of the spectrum of N_k at $Mt = 0, 10, 10^2, 10^3$ and 10^4. The horizontal axis k is the comoving momentum corresponding to each N_k.

Time evolution of this variable is shown in fig. 4.8. The phase independent variable jumps to $N_k \simeq 5M^{-5}M_p^2$ at the first half oscillation and stays constant afterward for $k \lesssim M$.

4.2.3 Analytical understanding

We have numerically found that the metric preheating occurs for the R^2 inflation for $k \lesssim M$. The growth rate is balanced with the Hubble expansion rate. This balance and resonance band are understood as following.

We can approximately solve the equation of motion (4.2.3) for the background ϕ_0 as

$$\phi_0(t) \simeq \phi_0(t_{\text{ini}}) \left(\frac{a_{\text{ini}}}{a} \right)^{\frac{3}{2}} \sin (Mt), \qquad (4.2.9)$$

which is consistent with fig. 4.5. Substituting this solution into the frequency of $\delta\phi_k$, we find

$$\omega_k^2 \simeq \frac{k^2}{a^2} + M^2 \left(1 - \sqrt{6} \frac{\phi_0}{M_p} + \frac{2\dot{\phi}_0\phi_0}{HM_p^2} \right). \qquad (4.2.10)$$

Here we have neglected the decaying terms faster than a^{-3}, while the last two terms decay as $a^{-3/2}$. If the origin of the instability is the parametric resonance by the two terms, we can treat each term independently and then can take the linear combination. We first analyze the last term $\omega_k^2 \simeq k^2/a^2 + M^2 + 2\dot{\phi}_0\phi_0 M^2/(HM_p^2)$, which is from the back-reaction of the metric. We rescale the field value and time variable as $\delta\varphi_k \equiv a^{3/2}\delta\phi_k$ and $z \equiv Mt - \pi/4$. By this rescaling, we can remove the Hubble friction term from the equation of motion as

$$\frac{d^2}{dz^2}\varphi_k + [A_{3k} - 2q_3\cos(2z)]\delta\varphi_k = 0, \tag{4.2.11}$$

where we have neglected the term decaying faster than a^{-3}. Here q_3 and A_{3k} are given by

$$q_3 \equiv \frac{a_{\rm ini}^3\phi_0^2(t_{\rm ini})M}{2a^3HM_p^2}, \tag{4.2.12}$$

$$A_{3k} \equiv 1 + \frac{k^2}{a^2M^2}. \tag{4.2.13}$$

Eq. (4.2.11) is the Mathieu equation, and the structure of the resonance is determined by the parameters q_3 and A_{3k}. At the initial time, $q_3 \simeq 1$. Thus, in this case, the narrow resonance occurs for

$$0 \leq \frac{k}{M} \lesssim a_{\rm ini}H_{\rm ini}\sqrt{\frac{3a_{\rm ini}}{aHM}}, \tag{4.2.14}$$

where we have used $3M_p^2H_{\rm ini}^2 \simeq M^2\phi_0^2(t_{\rm ini})/2$. Hence, the first band of the instability starts from $k \lesssim a_{\rm ini}\sqrt{3H_{\rm ini}M}$ at $t = t_{\rm ini}$ and broadens as $a^{1/4}$. Since, in the 1st band of the narrow resonance, the growth rate is given by $\mu = q_3/2$, the fluctuations in the band grow as

$$\delta\varphi_k \propto \exp\left(\int\frac{q_3}{2}dz\right) = \exp\left(\frac{a_{\rm ini}^3\phi_0^2(t_{\rm ini})M^2}{2M_p^2}\int\frac{dt}{a^3H}\right)$$
$$\simeq \exp\left(\frac{3}{2}\int\frac{da}{a}\right). \tag{4.2.15}$$

Therefore, $\delta\phi_k$ in the resonance band stays constant as $\delta\phi_k = a^{-3/2}\delta\varphi_k = $ constant, which accounts for fluctuations at lower momenta in figs. 4.7 and 4.8.

Note that there exists the following second band

$$3a^2 - \frac{3a_{\rm ini}^6H_{\rm ini}^4}{4a^4H^2M^2} \lesssim \frac{k^2}{M^2} \lesssim 3a^2 + \frac{15a_{\rm ini}^6H_{\rm ini}^4}{4a^4H^2M^2}, \tag{4.2.16}$$

the width of which narrows as a^{-1}, and disappears quickly.

Next let us consider the second-to-last term in the frequency (4.2.10), which is from self-interactions of the inflaton. This case corresponds to sub-sec. 4.2.1, and $\omega_k^2 \simeq k^2/a^2 + M^2 - \sqrt{6}\phi_0 M^2/M_p$. For this term, we rescale variables as $\delta\varphi_k \equiv a^{3/2}\delta\phi_k$ and $2z \equiv Mt - \pi/2$,

80

and then reduce the equation of motion (4.2.6) to the Mathieu equation with

$$q_4 \equiv 2\sqrt{6}\frac{\phi_0(t_{\text{ini}})a_{\text{ini}}^{3/2}}{M_p a^{3/2}}, \tag{4.2.17}$$

$$A_{4k} \equiv 4 + \frac{4k^2}{a^2 M^2}. \tag{4.2.18}$$

Although $q_4 = 4\sqrt{6} > 1$ at $t = t_{\text{ini}}$, it becomes smaller than unity within a few e-folds of the expansion as $q_4 \propto a^{-3/2}$. The first band of the narrow resonance is given by

$$\frac{k^2}{M^2} < -\frac{3}{4}a^2 + \frac{\sqrt{6}\phi_0(t_{\text{ini}})a_{\text{ini}}^{3/2}\sqrt{a}}{2M_p}, \tag{4.2.19}$$

which closes rapidly as $\propto a^2$. The second band is given by

$$\frac{k^2}{M^2} < \frac{5\phi_0^2(t_{\text{ini}})a_{\text{ini}}^3}{2M_p^2 a}, \tag{4.2.20}$$

which narrows as $\propto a^{-1}$. In sec. 4.1, we have learned that it takes $t \gtrsim 10^3/M$ for instabilities to grow at the second band; the value of q_4 is too small before this time. In fact, we have confirmed that there is no instability in fig. 4.5 by using a variable $a^{3/2}\delta\phi_k$ that counteracts the effect of the Hubble expansion. Thus, the resonance band closes, and fluctuations stop growing long before the growth overcomes the Hubble damping.

We have confirmed the origin of the resonance, which is the narrow resonance at the first band induced by the last term of the frequency in (4.2.10) with q_3. Using this parameter, we can calculate the ratio of the growth rate to the Hubble expansion rate as

$$\frac{\mu_k M}{H} \simeq \frac{1}{2}\frac{q_3}{H} \simeq \frac{1}{2}\frac{\phi_0(t_{\text{ini}})^2 M^2}{(a/a_i)^3 H^2 M_p^2}$$

$$\simeq \frac{3}{2} = 1.5, \tag{4.2.21}$$

where we have used relation for the initial condition as $3H_i^2 M_p^2 \simeq M^2\phi_0(t_{\text{ini}})^2/2$. This ratio means that the fluctuations do not increase nor decrease. As explained in sec. 3.2, for the formation of I-balls, fluctuations need to grow (Numerical value is given by $\langle\mu_k M/H\rangle \gtrsim 4 - 5$ in (3.2.19) and (3.2.27)). Thus, we can see that the formation of I-balls does not occur for the R^2 inflation even including the back reaction of the metric.

Here we note about the spectrum. In figs. 4.6 and 4.7, there are intermediate regions of blue spectra with $|\delta\phi_k|^2 \propto k$ for $k \gtrsim M$. For sufficiently higher k, the spectra are flat (not shown for $t = 10^3/M$ and $10^4/M$). The appearance of the blue spectra can simply be understood by the time evolution of $\delta\phi_k$ in the absence of interactions. For $k > aM$, eq. (4.2.6) is approximated by $\ddot{\delta\phi}_k + 3H\dot{\delta\phi}_k + (k/a)^2\delta\phi_k \simeq 0$, the solution of which is $\delta\phi_k \propto a^{-1}$; while for $k < aM$, $\ddot{\delta\phi}_k + 3H\dot{\delta\phi}_k + M^2\delta\phi_k \simeq 0$, the solution of which is $\delta\phi_k \propto a^{-3/2}$. Since physical momentum k/a is red-shifted by the Hubble expansion, more fluctuations become "heavy" and decay relatively faster as time passes. Thus, the flat spectrum develops to the blue one for $k < aM$.

4.3 Possibility of the I-ball formation

Heuristically it is known that, for some class of potentials that are flatter than the quadratic one, there may occur the formation of I-balls. The potential of the R^2 inflation is indeed the flatter one, and inflation is achieved where the curvature of the potential is negative. Thus, there is a possibility that the inflaton of the R^2 inflation would form I-balls after inflation, and they dominate the Universe.

The conditions for the production of I-balls were investigated by numerical simulations in the previous studies. Especially, in the expanding Universe, a heuristic condition for the growth rate of fluctuations were studied in [66–68], and then it is shown that for the formation, amplitude of fluctuations need to grow as $\langle \mu_k M/H \rangle > 3/2$ (Numerical value is given by $\langle \mu_k M/H \rangle \gtrsim 4 - 5$ in (3.2.19) and (3.2.27)). We have studied whether the R^2 inflation satisfies this condition.

In sec. 4.1, we have investigated the evolution of fluctuations of the inflaton in the Minkowski space-time. Then, we have numerically shown that the enhancement of the fluctuations occurs, and analytically understood that the resonance is induced by the parametric resonance. The mechanism of the resonance is classified by the amplitude of the background field Φ. In the case $\Phi < 0.2M_p$, the narrow resonance at the second band occurs for the momenta $0 \leq k < 2M\Phi/(\sqrt{3}M_p)$ (4.1.21). In the case $\Phi > 0.2M_p$, the broad resonance occurs for the momenta with eq. (4.1.18) ($\Phi \lesssim 2M_p$) and for the momenta with eq. (4.1.26) ($\Phi \gtrsim 2M_p$).

Then, we have investigated the growth of fluctuations in the expanding Universe, especially during reheating. As we can see from the Einstein equation, the evolution of the fluctuations of the field is correlated with those of the metric. First, we have neglected the effect of the metric. Then, in sec. 4.2, we have shown that the effect of the Hubble expansion makes the parametric resonance ineffective. This is because, before the sufficient growth of the fluctuations, the background of the field damps by the expansion, and its expansion also dilutes the fluctuations. Thus, as the fluctuations do not grow, I-balls are not formed.

Next, we investigated the evolution including the effect of fluctuations of the metric. Then, we have found that the metric preheating happens by the narrow resonance in the first band $0 \leq k \lesssim a_{\text{ini}} H_{\text{ini}} < \sqrt{3a_{\text{ini}} M/(aH)}$. For this metric preheating, the growth rate of the fluctuations is balanced with the Hubble parameter $\mu_k M/H \simeq 1.5$. Thus, we can see that, even included the effect of the fluctuations of the metric, there does not occur the sufficient growth of the fluctuations, and the sufficient production of I-balls for the R^2 inflation does not take place. Therefore, the original predictions of the R^2 inflation for the decay rate of the inflaton is held, and the cosmological scenario is unchanged.

Chapter 5

Formation of I-balls for a logarithmic potential

We move to the investigation of the production of I-balls for a more general case. Including the inflaton, a scalar field may have interactions with other particles, and then the potential would be corrected so that it becomes flatter than the quadratic one. For instances, in supersymmetric (SUSY) theories, when the breaking of SUSY takes place by the gauge mediation [95], the potential becomes a logarithmic one. In this case, if the scalar field has a $U(1)$ charge, its fluctuations are amplified for the phase direction leading to the fragmentation of the field into Q-balls [96, 97]. However, if the phase direction has a large mass for some reasons, and the motion of the scalar field is restricted in the radial direction, I-balls may be produced. Furthermore, another class of logarithmic potentials appears in more general situations, especially during reheating. After inflation, the decay of the inflaton produces a thermal bath. If a scalar field interacts with the thermal plasma, its potential has a thermal log correction $V_{\mathrm{th}} \simeq T^4 \ln(\phi^2/T^2)$ [31].

If there really occurs the formation of I-balls for the logarithmic potentials, the formation would affect the decay process of scalar fields in various scenarios such as the curvaton scenario [10–12] and non-thermal leptogenesis scenario [15, 16, 98]. Thus, in order to determine the cosmological scenario correctly, we study whether there occurs the production of I-balls. In this study, to clarify the nature of the logarithmic potential, we consider the following simple potential $V = M^2 \Lambda^2 \ln\left[1 + \phi^2/\Lambda^2\right]$.

Apart from the cosmological motivation, this logarithmic potential is attractive for the understanding of the formation of I-balls. The potentials which leading to the production of I-balls in the previous studies [23–25, 67, 68, 99], are quasi-quadratic ones where the polynomial terms are added to the quadratic potential, and the formation occurs when the field value damps so that the quadratic term dominates. As shown later in chap. 6, the separable form of the field, which is assumed for the proof of the conservation of the adiabatic charge, is achieved for the potential that is dominated by the quadratic one. Thus, if the adiabatic charge is crucial for the stability of I-balls, the quadratic term is important. For the case of the logarithmic potential, we can not simply write the potential as polynomials for larger field value, which is infinite series of higher order polynomials. Thus, by investigating the formation of I-balls for the logarithmic potential, we may clarify

83

some role of the quadratic term.

First, we confirm the production of I-balls performing lattice simulations. Next, we study the structure of the resonance for the logarithmic potential. Then, we analytically estimate the nature of I-balls based on the adiabatic charge. This chapter is based on the work with Masahiro Kawasaki [100].

5.1 Simulation

First, we investigate the formation of I-balls for a scalar field ϕ with a logarithmic potential given by

$$V = M^2\Lambda^2 \ln\left[1 + \frac{\phi^2}{\Lambda^2}\right], \tag{5.1.1}$$

performing lattice simulations. Here M is the mass of the field, and Λ is a constant of mass dimension $(D-1)/2$. We perform lattice simulations in the space of $D = 1$ in order to follow the dynamics of the scalar field for a sufficiently long time. In the cosmic time, the equation of motion for ϕ is given by [1]

$$\ddot{\phi} + DH\dot{\phi} - \frac{\nabla^2}{a^2}\phi + V'(\phi) = 0. \tag{5.1.2}$$

In the simulations, we solve the equation of motion in the conformal time $d\tau = dt/a$. In the case of $D = 1$, the equation of motion is written as

$$\frac{d^2}{d\tau^2}\phi - \nabla^2\phi + a^2 V'(\phi) = 0. \tag{5.1.3}$$

Note that, in this dimension, ϕ and Λ are dimensionless. Here we suppose that the Universe expands as like the matter dominated one.[2] In this case, the scale factor is given by

$$\frac{a}{a_0} = \left(\frac{\tau}{\tau_0}\right)^2, \tag{5.1.4}$$

where a_0 and τ_0 are the initial values of a and τ. The relation between the cosmic time t and the conformal time τ is given by

$$t = t_0 + \frac{\tau_0}{3}\left[\left(\frac{\tau}{\tau_0}\right)^3 - 1\right] \tag{5.1.5}$$

$$= \frac{\tau_0}{3}\left[\left(\frac{\tau}{\tau_0}\right)^3 + 2\right], \tag{5.1.6}$$

---

[1]Here we note that for $D = 1$ and 2 cases, the Hubble friction term is hypothetical one.

[2]The time dependence of the scale factor we have adopted is for the case that the Universe is dominated by non-relativistic particles for $D = 3$ and it is ad hoc for $D = 1$. We include the Hubble expansion in order to see stable I-balls in the simulation. Without the expansion, I-balls collides each other frequently and are destroyed in the simulation for $D = 1$. The expansion dilutes the I-balls and avoids unwanted collisions. So the precise time dependence of the scale factor is not important. To confirm this, we have performed the simulations for the scale factor to evolve as relativistic particles dominate the Universe and found that the result is not changed.

where we have set the initial value of t equal to that of τ as $t_0 = \tau_0$. The Hubble parameter is given by

$$H = 2\frac{\tau_0^2}{\tau^3}. \tag{5.1.7}$$

We set the initial value of H_0 equal to the mass of the field as $H_0 = M$. Thus, the initial value τ_0 is given by

$$\tau_0 = \frac{2}{M}. \tag{5.1.8}$$

We investigate whether the production of I-balls occurs for the coherently oscillating scalar field. Thus, we set the initial conditions of the filed by nearly homogeneous ϕ_0 with small fluctuations $\delta\phi_0$ as

$$\phi(\tau_0, x) = \phi_0 + \delta\phi_0(x),$$
$$\frac{d\phi}{d\tau}(\tau_0, x) = 0. \tag{5.1.9}$$

We perform simulations for several initial values of the homogeneous mode as $\phi_0/\Lambda = 10^{-1}$, 1, 10 and 10^2. We set the initial fluctuations $\delta\phi_0(x)$ at each lattice grids by random variables which follow the Gaussian probability function $P(\delta\phi(x))$ given by

$$P(\delta\phi(x)) = \frac{1}{\sqrt{2\pi\sigma^2}}\exp\left(-\frac{\delta\phi(x)^2}{2\sigma^2}\right), \tag{5.1.10}$$

where σ is the variance set to $10^{-5}\Lambda$.

Now let us present the result of simulations in fig. 5.1. In the simulation, the initial amplitude of the background field is set to $\phi_0 = \Lambda$. This figure shows the snap shots of the spatial distribution of the energy density

$$\rho = \frac{1}{2}\dot{\phi}^2 + \frac{1}{2a^2}(\nabla\phi)^2 + V \tag{5.1.11}$$

$$= \frac{1}{a^2}\left[\frac{1}{2}\left(\frac{d\phi}{d\tau}\right)^2 + \frac{1}{2}(\nabla\phi)^2\right] + V \tag{5.1.12}$$

at $Mt = 0, 4\times10^3, 4\times10^4$ and 4×10^5. In this simulation, we set the box size L and grid number N to $(L, N) = (5/M, 32768)$, which gives the comoving spatial resolution $\Delta x = 1.5\times10^{-4}/M$, and physical spatial resolution at the end of the simulation $\Delta x_{\mathrm{phy,e}} = 2.0/M$. From the figure, we can see that first ρ decreases by the Hubble expansion. At the same time, the fluctuations are enhanced. Then, after $\Delta t \simeq 10^4/M$, the fluctuations of the field start to fragment into I-balls. By this simulation, the formation of I-balls is confirmed for the logarithmic potential, which occurs after the enhancement of fluctuations. The formation of I-balls also takes place for other initial values $\phi_0/\Lambda = 0.3, 10$ and 100. The results of the simulations are summarized in fig. 5.2. The panels in the figure show the snap shot of the spatial distribution of the energy density after the formation of I-balls for each ϕ_0. The box size, grid number and the spatial resolution are summarized in Table 5.1. The time step is set to be $\Delta\tau/\Delta x < 1/5$. In Appendix B, we have studied the dependence of the results on the spatial resolution for a reference value $\phi_0/\Lambda = 10$. Furthermore, in Appendix C, we have investigated the finite box effect on the formation process.

ϕ_0/Λ	0.3	1	10	100
$M\Delta t_{\text{max}}$	10^7	10^6	10^4	10^5
ML	5	5	1	0.1
N	65032	32768	1024	256
$M\Delta x$	7.7×10^{-5}	1.5×10^{-4}	9.8×10^{-4}	3.9×10^{-4}
$M\Delta x_{\text{phy,e}}$	4.6	2.0	5.5×10^{-1}	1.1

Table 5.1: The numerical values of the parameters and spatial resolutions for the simulations of $\phi_0/\Lambda = 0.3$, 10 and 10^2.

From the distributions shown in fig. 5.2, we have determined the typical amplitude of I-balls for each ϕ_0. As the field is oscillating within I-balls, it has a phase dependence. In order to remove the phase dependence, we used a relation between the energy density $\rho(r=0)$ and amplitude $\Phi(r=0)$ at the center of an I-ball $r=0$:

$$\rho(r=0) = \frac{1}{2}\dot{\phi}^2 + V = V(\Phi). \tag{5.1.13}$$

To confirm the formation time of I-balls, we define a quantity

$$E_{\text{over}} \equiv a \int dx\, \rho\, \theta\left(\rho - 2\langle\rho\rangle\right) \tag{5.1.14}$$

$$\simeq a\frac{L}{N}\sum_i^N \rho\, \theta\left(\rho - 2\langle\rho\rangle\right), \tag{5.1.15}$$

where θ is the heaviside function, and $\langle\rho\rangle$ is the total average of the energy density. Dividing this quantity by L, we obtain the density of E_{over} as

$$\epsilon_{\text{over}} = \frac{E_{\text{over}}}{L} \tag{5.1.16}$$

$$= a\frac{1}{N}\sum_i^N \rho\, \theta\left(\rho - 2\langle\rho\rangle\right). \tag{5.1.17}$$

We are now considering the situation that the initial energy density is homogeneous. Thus, at the initial time, the deviation of the energy density from the average is small, and hence ϵ_{over} is nearly zero. After some oscillations of the field, fluctuations are expected to be enhanced by the parametric resonance. Then, ρ exceeds $\langle\rho\rangle$ at some regions, and hence ϵ_{over} increases. Through the enhancement of the fluctuations, the field would fragment and form I-balls. After the completion of the formation, the evolution of the amplitude in I-balls decouples from the Hubble expansion, and the comoving energy density of them becomes constant. Therefore, after the completion of the formation of I-balls, ϵ_{over} takes a constant value. We show the time evolution of this variable for $\phi_0 = 10\Lambda$ in fig. 5.3. We

can see that ϵ_{over} becomes constant at $t \simeq 10^3/M$, which is the time that the formation of I-balls are completed as explained. We summarize the order of magnitude estimation of the formation time ΔT and the typical amplitude $\Phi(0)$ for each initial value ϕ_0 in Table 5.2.

$\phi_0\,[\Lambda]$	0.3	1	10	100
$\Delta T\,[1/M]$	10^6	10^5	10^3	10^4
$\Phi(0)\,[\Lambda]$	10^{-3}	10^{-1}	1	1

Table 5.2: Typical values of formation time ΔT and I-ball amplitude $\Phi(0)$ for each initial value ϕ_0.

From the simulations, it seems that the quadratic term is important for the formation of I-balls. For the logarithmic potential (5.1.1), the inflection point is $\phi = \Lambda$. The deviation from the quadratic potential becomes significant beyond this point. Table 5.2 shows that, the formation of I-balls occurs even for the larger initial amplitude than the inflection point: $\phi_0 \gg \Lambda$.[3] On the other hand, the table also shows that I-balls are formed with the amplitude $\Phi \lesssim \Lambda$ even for the larger initial amplitude. In the case of $\phi_0 \gg \Lambda$, although the enhancement of fluctuations starts even at the larger value of the background field than the inflection point $\gtrsim \Lambda$, the formation of I-balls is completed when the amplitude drops to $\mathcal{O}(\Lambda)$ due to the Hubble expansion. In previously known cases, I-balls are formed with quasi-quadratic potentials. For the case of the logarithmic potential, I-balls are also formed, and the formation occurs when the scalar field oscillates in the region where the potential is approximately given by a quadratic form, which results in $\Phi(0)/\Lambda \leq 1$ as seen in Table 5.2. This fact that I-balls are formed when the quadratic term is dominant is consistent with the idea that the adiabatic charge is crucial in the formation of I-balls.

In addition, we see that the time scale of the formation of I-balls becomes shorter as ϕ_0 is larger up to $\phi_0 < 10\Lambda$, but becomes longer as $\phi_0 > 10\Lambda$. This amplitude dependence is related to the growth rate of the fluctuations. In the logarithmic potential, the amplification of the fluctuations per one oscillation becomes larger as the amplitude is larger, but the period of a single oscillation becomes longer for larger amplitude than Λ. As a consequence, the growth rate in unit time of $1/M$ becomes larger as the amplitude is larger up to $\phi_0 \lesssim 10\Lambda$, but becomes smaller for $\phi_0 \gtrsim 10\Lambda$, which leads to the amplitude dependence of the time scale of the formation.

5.2 Structure of the resonance

We have shown that the formation of I-balls occurs for the logarithmic potential, and it does after the growth of fluctuations. It is expected that the growth would be induced by the parametric resonance. In this section, we clarify the structure of resonance for the logarithmic potential.

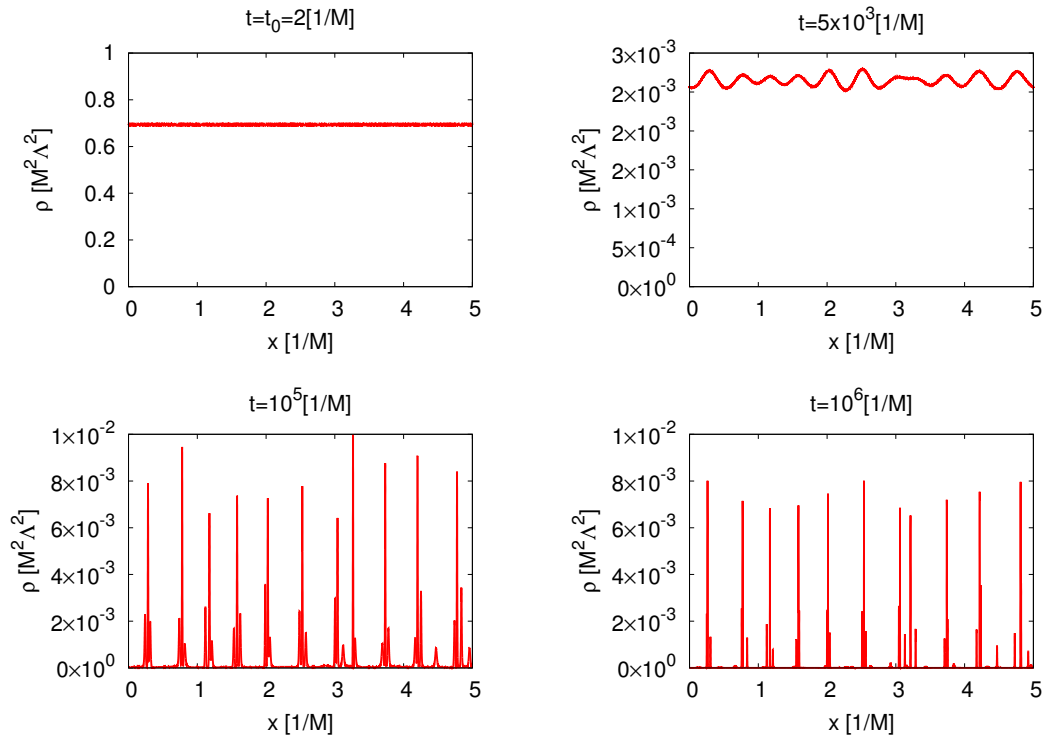[3]Note, in space of $D = 1$, Λ is a dimension less parameter. We set it unity for simplicity.

Figure 5.1: Snap shots of the spatial distribution of the energy density ρ at $Mt = 2(= Mt_0)$, 5×10^3, 10^5 and 10^6, respectively from the top left panel to the bottom right panel. The initial amplitude is set to $\phi_0 = 1\Lambda$. The box size and grid number are set to $L = 5/M$ and $N = 32768$. The horizontal axis is the comoving spatial coordinate.
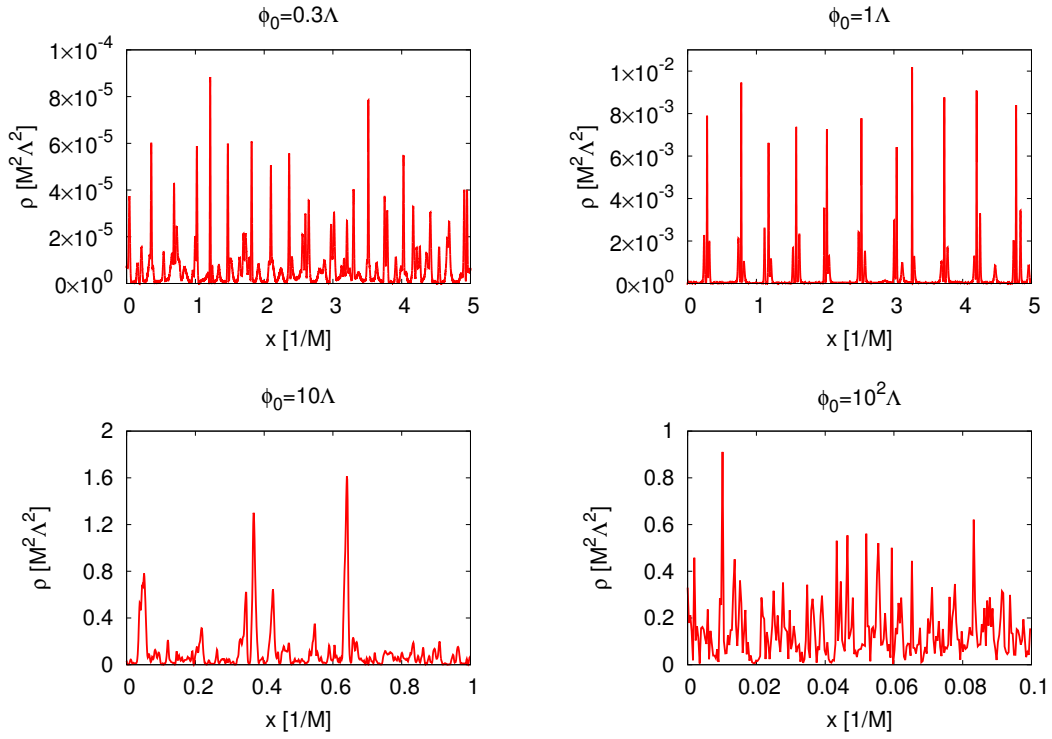
Figure 5.2: Snap shots of the distribution of the energy density after the formation of I-balls for each initial condition $\phi_0/\Lambda = 0.3, 1, 10$ and 100. The times that the snap shots are plotted are $Mt = 5 \times 10^6$, 10^5, 3×10^3 and 5×10^4, respectively from the top to the right bottom panel. The horizontal axis is the comoving spatial coordinate.
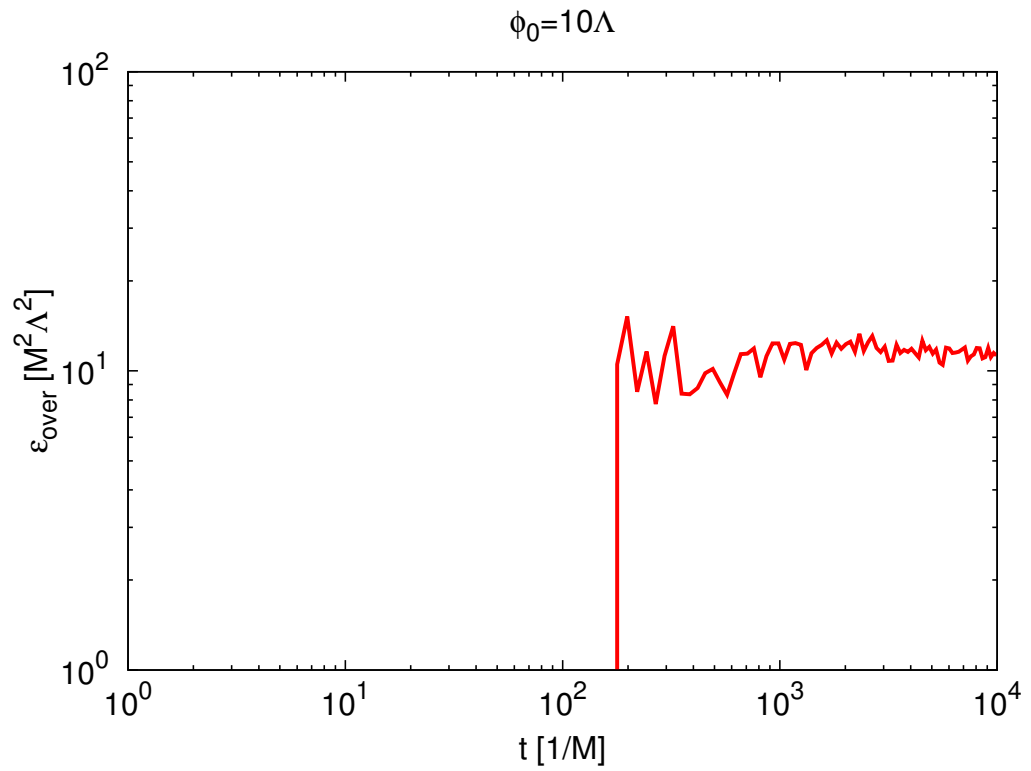
Figure 5.3: Time evolution of ϵ_{over} (5.1.16) for $\phi_0 = 10\Lambda$ from $t = 2/M$ to $10^4/M$.

For simplicity, first, we ignore the cosmic expansion and consider the Minkowski space-time. In order to study the structure of resonance, we treat the fluctuations by linear perturbations dividing the field into the background and fluctuations as $\phi(t, \vec{x}) = \phi_{\rm bg}(t) + \delta\phi(t, \vec{x})$. By this division, the equations of motion for $\phi_{\rm bg}$ and $\delta\phi$ are written as

$$\ddot{\phi}_{\rm bg} + \frac{2M^2}{1 + \phi_{\rm bg}^2/\Lambda^2}\phi_{\rm bg} = 0, \tag{5.2.1}$$

$$\delta\ddot{\phi} + \left[-\nabla^2 + 2M^2\frac{1 - \phi_{\rm bg}^2/\Lambda^2}{\left(1 + \phi_{\rm bg}^2/\Lambda^2\right)^2}\right]\delta\phi = 0. \tag{5.2.2}$$

In the Fourier space, the equation of motion for the fluctuation $\delta\phi_{\mathbf{k}}$ is given by

$$\delta\ddot{\phi}_{\mathbf{k}} + \left[k^2 + 2M^2\frac{1 - \phi_{\rm bg}^2/\Lambda^2}{\left(1 + \phi_{\rm bg}^2/\Lambda^2\right)^2}\right]\delta\phi_{\mathbf{k}} = 0. \tag{5.2.3}$$

From the equations we can see that the frequency of fluctuations becomes a periodic function by the oscillation of the background. As we explained in sec. 3.1, by the modulation of the frequency, the parametric resonance would occur.

Let us first consider the case that the background field is smaller than the inflection point $\phi_{\rm bg} < \Lambda$. In this case, eq. (5.2.3) is approximated as

$$\delta\ddot{\phi}_{\mathbf{k}} + \left[k^2 + 2M^2(1 - \phi_{\rm bg}^2/\Lambda^2)\right]\delta\phi_{\mathbf{k}} = 0. \tag{5.2.4}$$

Since below the inflection point the potential is dominated by the quadratic term, we can approximate the oscillation of the background field by a harmonic one with a constant amplitude $\Phi_{\rm bg}$ as $\phi_{\rm bg}(t) = \Phi_{\rm bg}\cos(\sqrt{2}Mt)$. Substituting this into the above equation, we obtain the Mathieu equation,

$$\frac{d^2}{dz^2}\delta\phi_k + [A_k - 2q\cos(2z)]\delta\phi_k = 0, \tag{5.2.5}$$

with parameters q and A_k given by

$$q = \frac{1}{4}\left(\frac{\Phi_{\rm bg}}{\Lambda}\right)^2, \quad A_k = \frac{1}{2}\left(\frac{k}{M}\right)^2 + 1 - 2q. \tag{5.2.6}$$

Here we have rescaled the time variable as $z \equiv \sqrt{2}Mt$. As we are now considering the case of $\Phi_{\rm bg} < \Lambda$, q is smaller than unity. Thus, the resonance is induced by the narrow resonance, and the most efficient mode is in the first band $A_k \simeq 1$, which is reduced to

$$\frac{k}{M} \simeq \sqrt{4q} = \frac{\Phi_{\rm bg}}{\Lambda}. \tag{5.2.7}$$

Therefore, for the field oscillating with amplitude $\Phi_{\rm bg}$ smaller than the inflection point, the parametric resonance takes place, and the fluctuations with $k \simeq (\Phi_{\rm bg}/\Lambda)M$ grow.

For larger amplitude $\phi_0 > \Lambda$, the deviation from the quadratic term becomes significant, and we cannot simply approximate the oscillation of the field by the harmonic one, but it is represented by a periodic function $g(t)$ as $\phi_{\mathrm{bg}}(t) = \Phi_{\mathrm{bg}}\,g(t)$. In this case, we study the structure of the resonance by solving the equations of motion numerically. As the equation (5.2.4) is a linear one for $\delta\phi_k$, the growth rate of it is independent on initial conditions. Thus, to clarify the structure of the resonance, we set the initial conditions by hand to a flat spectrum: $\delta\phi_k(t_0) = 10^{-5}\Lambda M^{-D}$.[4] We study the structure of the resonance for four different amplitudes of the background field: $\Phi_{\mathrm{bg}}/\Lambda = 1, 5, 10$ and 100. The results of simulations are summarized in fig. 5.4. From the results, we can see that there occurs the enhancement of the fluctuations in more multi-bands of momenta for the larger Φ_{bg}. For the larger amplitude than the inflection point, the higher polynomials contribute to the oscillation of the field, and it would trigger the enhancement in the multi-bands. The most rapidly growing mode is typically located at $k \sim \mathcal{O}(0.01) - \mathcal{O}(0.1)/M$. Here we note that the absolute value of the amplitude is unphysical because for such amplitudes as shown in the figure, the re-scattering with other modes becomes efficient, and then the growth would be suppressed, which is beyond the scope of the linear analysis. The location of the resonance and its growth rate are important.

Next, we study the structure of the resonance including the expansion of the space. The equations of motion for the background and fluctuations are given by

$$\ddot{\phi}_{\mathrm{bg}} + H\dot{\phi}_{\mathrm{bg}} + \frac{2M^2}{1 + \phi_{\mathrm{bg}}^2/\Lambda^2}\phi_{\mathrm{bg}} = 0 \tag{5.2.8}$$

and

$$\ddot{\delta\phi}_k + H\dot{\delta\phi}_k + \left[\frac{k^2}{a^2} + 2M^2\frac{1 - \phi_{\mathrm{bg}}^2/\Lambda^2}{\left(1 + \phi_{\mathrm{bg}}^2/\Lambda^2\right)^2}\right]\delta\phi_k = 0. \tag{5.2.9}$$

Here we consider the space of $D = 1$. We have numerically solved the coupled equations for four different initial amplitudes of the background field, $\phi_{\mathrm{bg}}(t_0)/\Lambda = 1, 5, 10$ and 100. As for the fluctuations, we set the initial spectrum to the flat one as $\delta\phi_k(t_0) = 10^{-5}\Lambda M^{-D}$ in the same way as without the expansion. In fig. 5.5, we show the snapshot of of the spectrum of fluctuations at several times. We can see that the fluctuations are diluted, and their momenta are red-shifted by the cosmic expansion. In the expanding Universe, the multi-instabilities at higher momenta disappear.

We have investigated the structure of the resonance of the logarithmic potential with linear perturbations methods. However, if we take into account the non-linear interactions, the re-scattering of fluctuations becomes efficient, and then the growth of fluctuations stops. As we have verified in the previous section, by the non-linear processes, there occurs the fragmentation of the fluctuations into I-balls.

5.3 Analytical estimation

We have numerically confirmed that I-balls are formed for the logarithmic potential, and furthermore studied the structure of the resonance of the fluctuations. After the formation,

---

[4]Again we note that the mass dimension of Λ depends on the dimension of space as $\dim(\Lambda) = (D-1)/2$.

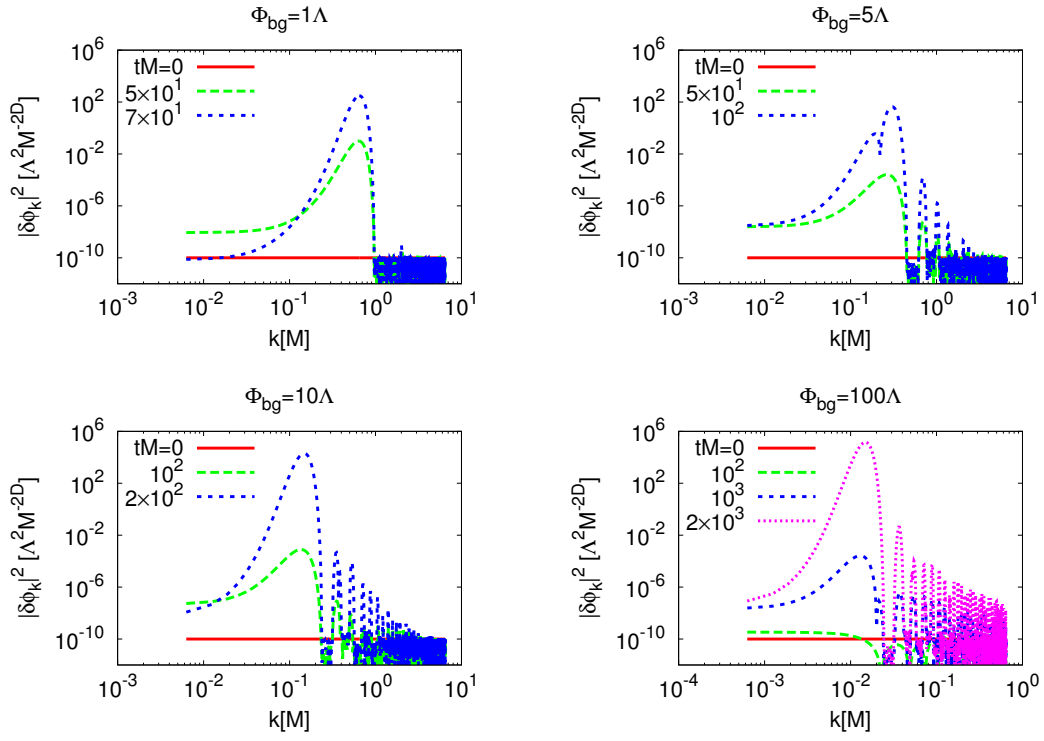Figure 5.4: Evolution of the instabilities in the Minkowski spacetime for $\phi_0/\Lambda = 1, 5, 10$ and 100. The vertical axis is the amplitude of the fluctuation, and the horizontal axis is the corresponding momentum.
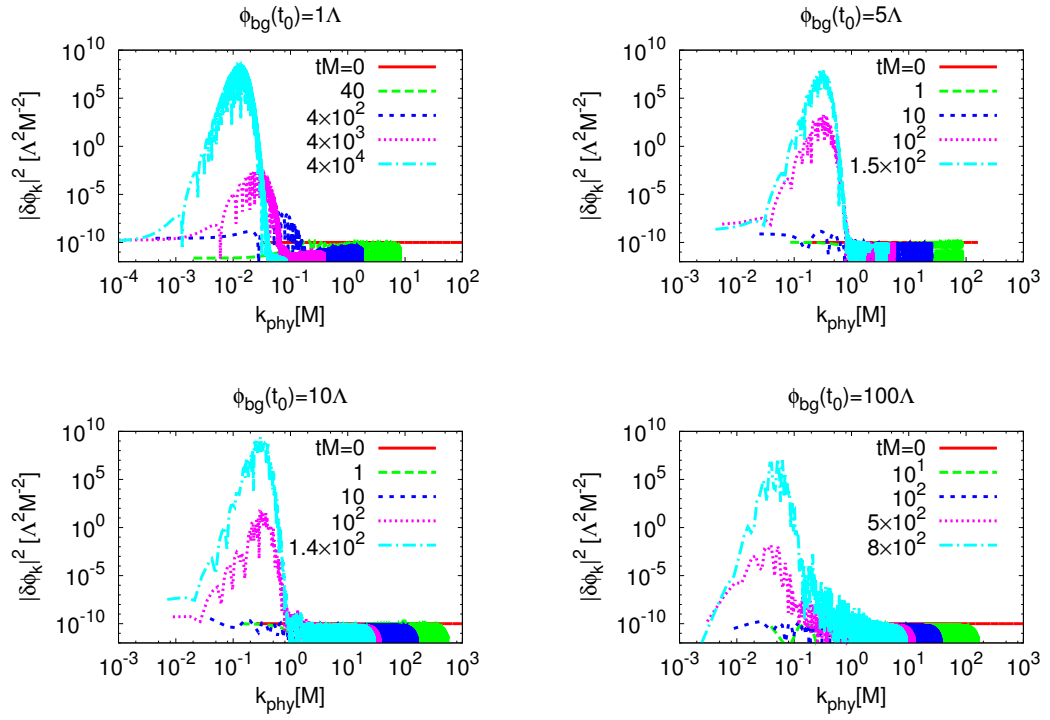
Figure 5.5: Evolution of instabilities in the expanding spacetime for $D = 1$ with $\phi_0/\Lambda = 1, 5, 10$ and 100. The vertical axis is the amplitude of the fluctuation, and the horizontal axis is the corresponding physical momentum.

their profiles oscillate with time around some values. This oscillating behavior is also confirmed in the case of Q-balls in [101], where the state is called Q-axiton. It is found that the energy of the Q-axiton is larger than Q-balls. This state is considered as the excited state of Q-balls. In [101], it is numerically shown that the Q-axiton emits radiations, and then the energy gradually decreases. As for the case of I-balls, the oscillating behavior might also represent the excited state of I-balls, and finally settle down to the lowest energy state. In our simulation time, we could not confirm the sufficient relaxation of I-balls to the lowest energy state, but the typical amplitude of them is resolved as summarized in Table 5.2. It shows that the I-balls are formed when the potential is dominated by the quadratic term. Indeed, the amplitude of I-balls is limited from above $\Phi(0) \leq \Lambda$ as shown in the Table 5.2.

It is suggested that for the stability of I-balls the adiabatic charge is important. If the adiabatic charge is conserved, the configuration of the field at the lowest energy state becomes a spatially localized one. In this section, we derive the configuration assuming the conservation of the adiabatic charge.

As we have explained in chap. 3, the adiabatic charge is defined by

$$I = \int d^D x \frac{\overline{\dot{\phi}^2}}{\omega}, \tag{5.3.1}$$

where the over line means the time average over oscillations, and ω is the frequency of the field. Let us minimize the energy of the field for a fixed value of I using a Lagrange multiplier $\tilde{\omega}$ as

$$\begin{aligned}
\overline{E}_{\tilde{\omega}} &\equiv \overline{E} + \tilde{\omega} \left[I - \int d^D x \frac{\overline{\dot{\phi}^2}}{\omega} \right] \\
&= \int d^D x \left[\left(1 - 2\frac{\tilde{\omega}}{\omega} \right) \frac{1}{2} \overline{\dot{\phi}^2} + \frac{1}{2} \overline{(\nabla\phi)^2} + \overline{V(\phi)} \right].
\end{aligned} \tag{5.3.2}$$

Since we have confirmed that I-balls are formed with amplitude $\lesssim \Lambda$, we consider the case that the potential is dominated by the quadratic one and expand the potential up to the quartic term as

$$V \simeq M^2 \phi^2 - \frac{1}{2} \left(\frac{M}{\Lambda} \right)^2 \phi^4. \tag{5.3.3}$$

As shown in the next chapter, for the potential that is dominated by the quadratic term, the oscillation of ϕ is approximately periodic one, i.e., ϕ is separated into a periodically oscillating part and time independent part as

$$\phi(x) \simeq \Phi(\vec{x}) f(t). \tag{5.3.4}$$

As we have proved in chap. 3, the adiabatic charge is conserved for this separable form. Thus, the assignment of the fixed I might be plausible. In the region where the potential is dominated by the quadratic term, we can approximate f as a harmonic function with a frequency $\omega \simeq \sqrt{2}M$. By this approximation, we can evaluate the time average of functions of f and of its time derivative as

$$\overline{f^2} \simeq \frac{1}{2}, \ \overline{f^4} \simeq \frac{3}{8}, \ \overline{\dot{f}^2} \simeq \frac{1}{2}\omega^2. \tag{5.3.5}$$

Thus, the time averages of functions of ϕ and of its time derivative are given by

$$
\begin{cases}
\overline{\phi^2} \simeq \dfrac{1}{2}\Phi^2, \\[2mm]
\overline{\dot\phi^2} \simeq \dfrac{\omega^2}{2}\Phi^2, \\[2mm]
\overline{\nabla\phi^2} \simeq \dfrac{1}{2}\left(\nabla\Phi\right)^2, \\[2mm]
\overline{V(\phi)} \simeq M^2\Lambda^2 \left[\dfrac{1}{2}\left(\dfrac{\Phi}{\Lambda}\right)^2 - \dfrac{3}{16}\left(\dfrac{\Phi}{\Lambda}\right)^4 \right].
\end{cases}
\tag{5.3.6}
$$

Then, we obtain

$$
\overline{E}_{\tilde\omega} = \frac{1}{4}\int d^D x \left\{ (\nabla\Phi)^2 + \omega^2\left(1 - 2\frac{\tilde\omega}{\omega}\right)\Phi^2 + M^2\Lambda^2\left[2\left(\frac{\Phi}{\Lambda}\right)^2 - \frac{3}{4}\left(\frac{\Phi}{\Lambda}\right)^4\right]\right\}.
\tag{5.3.7}
$$

To find the lowest energy state, let us consider the variation of $\overline{E}_{\tilde\omega}$ with respect to Φ:

$$
\delta\overline{E}_{\tilde\omega} = \frac{1}{2}\int d^D x\,\delta\Phi\left\{ -\nabla^2\Phi + \omega^2\left(1 - 2\frac{\tilde\omega}{\omega}\right)\Phi + M^2\Lambda\left[2\frac{\Phi}{\Lambda} - \frac{3}{2}\left(\frac{\Phi}{\Lambda}\right)^3\right]\right\}.
\tag{5.3.8}
$$

From the lowest energy condition $\delta\overline{E}_{\tilde\omega} = 0$, we obtain a bounce equation for Φ as

$$
\nabla^2\Phi - \left[m^2 + \omega^2\left(1 - 2\frac{\tilde\omega}{\omega}\right)\right]\Phi + \frac{3}{2}\left(\frac{M}{\Lambda}\right)^2\Phi^3 = 0.
\tag{5.3.9}
$$

We assume that the solution of the bounce equation is spherically symmetric, $\Phi = \Phi(r)$, where r is the radial coordinate. Then the Laplacian operator can be written as

$$
\nabla^2 = \frac{d^2}{dr^2} + \frac{D-1}{r}\frac{d}{dr}
\tag{5.3.10}
$$

depending on the dimension of the space. To solve the equation, let us rescale variables as

$$
\tilde\Phi \equiv \frac{\Phi}{\Lambda}, \quad \tilde r \equiv Wr,
\tag{5.3.11}
$$

where

$$
W \equiv \sqrt{2M^2 + \omega^2\left(1 - 2\frac{\tilde\omega}{\omega}\right)}.
\tag{5.3.12}
$$

With these rescalings, the bounce equation is reduced to

$$
\frac{d^2}{d\tilde r^2}\tilde\Phi + \frac{D-1}{\tilde r}\frac{d}{d\tilde r}\tilde\Phi - \tilde\Phi + \frac{3}{2}\left(\frac{M}{W}\right)^2\tilde\Phi^3 = 0.
\tag{5.3.13}
$$

We can solve the equation exactly in the case of $D = 1$, and the solution is given by

$$
\tilde\Phi = \frac{2}{\sqrt{3}}\frac{W}{M}\mathrm{sech}(\tilde r) \text{ for } D = 1.
\tag{5.3.14}
$$

96

With the other dimensions, by the effect of the friction term in the bounce equation $(D - 1)/\tilde{r}(d\tilde{\Phi}/d\tilde{r})$, the solution slightly deviates from the one for $D = 1$, but it is approximately identical to the hyperbolic function. Thus, we obtain the solution of the bounce equation as

$$\Phi \simeq \frac{2}{\sqrt{3}} \Lambda \frac{W}{M} \text{sech}(Wr). \tag{5.3.15}$$

From this result, we can estimate the typical radius and amplitude at the center of the I-ball as

$$\Phi_c \simeq \frac{2}{\sqrt{3}} \frac{W}{M} \Lambda \simeq \Lambda,$$
$$R \simeq 1/W \simeq 1/M. \tag{5.3.16}$$

Let us here compare the analytical profile derived based on the adiabatic charge to the results of simulations. For the analytical profile (5.3.15), the energy density is given by

$$\rho_{\text{ana}} = M^2 \Phi^2 \left[1 + \frac{3}{16} \left(\frac{\Phi_c}{\Lambda} \right)^2 \tanh^2 \left(\frac{\sqrt{3}}{2} \frac{\Phi_c}{\Lambda} Mr \right) \right], \tag{5.3.17}$$

where we have approximated the potential energy by the quadratic term as $V \simeq M^2 \phi^2$, and have used the time average of the oscillation as $\overline{f^2} \simeq 1/2$. In fig. 5.6, we show the comparison of this analytical profile (5.3.17) to the result of the simulation, where we set the initial amplitude of ϕ to $\phi_0 = 10\Lambda$. The left (right) panel shows the snapshot of ρ at $t = 10^3/m$ $(10^6/m)$. Since I-balls are in the excited state just after the formation $(t = 10^3/m)$, the energy density is larger than the analytical profile as shown in the left panel. At later time $t = 10^6/m$, the difference between the analytical profile and the numerical results becomes small, which would suggest the relaxation of I-balls toward the lowest energy state.
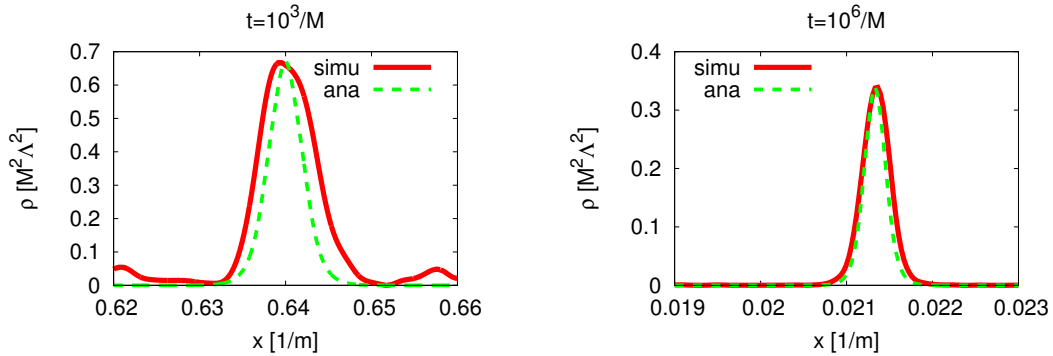

Figure 5.6: The comparison of the analytical form of the energy density (5.3.17) to the numerical result. The set of parameters is $(ML, N) = (1, 32768)$. The left (right) panel is the snapshot of ρ at $t = 10^3/m$ $(10^6/m)$.

As we have obtained the profile of I-balls, we can evaluate the adiabatic charge explicitly for each I-ball,

$$I = \int d^D x \frac{\overline{\dot{\phi}^2}}{\omega} \simeq \int d^D x \frac{\overline{\dot{f}^2}}{\omega} \Phi^2$$

$$\simeq \int d^D x \frac{\overline{\dot{f}^2}}{\omega} \Phi_c^2 \operatorname{sech}^2 (W|\vec{x}|)$$

$$\simeq b(D) \frac{2}{3} \frac{\omega W^{2-D}}{M^2} \Lambda^2, \tag{5.3.18}$$

where we have used the time average of $\dot{f}$: $\overline{\dot{f}^2} \simeq \omega^2/2$. Here $b(D)$ is the integration of the hyperbolic secant function over the space of the dimension of D as

$$b(D) \equiv \int_{-\infty}^{\infty} d^D x \operatorname{sech}^2(|\vec{x}|), \tag{5.3.19}$$

and its value is typically order one: $\{b(1), b(2), b(3)\} = \{2, 2\pi \ln(2), \pi^2/3\}$. Substituting the definition of W into the above expression, we can obtain a relation between ω and I as

$$M^2 \Lambda^{-2} I \simeq \omega \left(2M^2 + \omega^2\right)^{1-D/2}, \tag{5.3.20}$$

where we have neglected the order one coefficient.

We have derived the localized configuration assuming the conservation of the adiabatic charge. Then, the typical amplitude is estimated as $\Phi \simeq \Lambda$. This typical value agrees with the numerical results summarized in Table 5.2. As for the initial amplitude smaller than the inflection point $\phi_0 < \Lambda$, the amplitude of I-balls are smaller than the typical one $\Phi(0) < \Lambda$. For the smaller initial value, the adiabatic charge is small from the beginning as seen from the definition $I = \int d^D x \dot{\phi}^2/\omega \lesssim \Lambda^2 M \int d^D x$. On the other hand, the adiabatic charge for the analytical estimation (5.3.18) is proportional to the square of the amplitude as $I \simeq \Phi_c^2 M \int_V d^D x \operatorname{sech}(Wx)$. Here V is the volume of the localized configuration, determined by the radius as $V \simeq (1/R)^D \simeq (1/W)^D$. For this smaller value of the adiabatic charge, the derived amplitude Φ is smaller than Λ.

As we have explained in sec. 3.2, I-balls for the double well and axion-like potentials decay gradually by the emission of radiations from the tail as shown in fig. 3.5 and 3.6. As explained later, stable I-balls are achieved for a specific potential, which is a quadratic potential with a correction of a logarithmic term as $(m^2/2)\phi^2 \left[1 - K \ln \left(\phi^2/M^2\right)\right]$ where K is a dimensionless parameter smaller than unity. Deviated from this form, the I-balls would decay gradually. As for the logarithmic potential, the I-balls would also decay. By the decay of I-balls, the amplitude decrease. We assume that by the decay of I-balls, the adiabatic charge would gradually decrease.

Here let us suggest the evolution of the localized configuration (5.3.15) assuming that the adiabatic charge gradually decreases. We pay attention to the relation (5.3.20) between ω and I. The explicit forms of the relation for each dimension $D = 1, 2$ and $D = 3$ are written as

$$M^4 \Lambda^{-4} I^2 \simeq \begin{cases} \omega^2 \left(2M^2 + \omega^2\right) & (D = 1) \\ \omega^2 & (D = 2) \\ \omega^2/\left(2M^2 + \omega^2\right) & (D = 3). \end{cases} \tag{5.3.21}$$

In the relations, the right hand sides are all monotonically increasing functions of ω. Thus, as I decreases, ω would become smaller in each dimension. From the profile given by (5.3.15), it can be seen that the profile is determined by W; the amplitude is proportional to W ($\Phi(0) \propto W$), and the radius is proportional to inverse of W ($R \propto 1/W$). By the decrease of ω, W would also become smaller because it is a monotonically increasing function of ω, which can be seen from (5.3.12). Therefore, we expect that by the decrease of I, I-balls would deform so that the amplitude (radius) decreases (increases). In the relations (5.3.21), ω dependence of I becomes weaker for the higher dimensions. Thus, we expect that the deformation of I-balls would be milder in the higher dimensions when we consider the same amount of decrease of the adiabatic charge I.

We have discussed the evolution of I-balls assuming a decrease of the adiabatic charge and that the localized configuration (5.3.15) really represents the profile of I-balls. Then, we have suggested that the amplitude of I-balls decreases with a increase of the radius for each dimension. Furthermore, we have suggested that the deformation would be milder in the case of the higher dimensions of the space if we assume the same amount of the decrease of the adiabatic charge. However, to estimate the evolution of I-balls completely, we have to clarify the dynamics of the decrease of the adiabatic charge.

Chapter 6

Understanding of I-balls based on the adiabatic charge

I-balls are spatially localized objects of a real scalar field. As we have explained, they are formed from a nearly coherent oscillation of the field. The formation of I-balls is confirmed by numerical simulations, and the properties of I-balls are known heuristically. Interestingly, the lifetime of I-balls is significantly long or even exactly stable at classical level. However, analytical understandings of the stability is yet to be completely clarified. In the case of other solitons such as Q-balls or topological solitons, their natures are extensively investigated. Then, it is clarified that some conserved quantities are crucial to guarantee the stability; $U(1)$ charge accounts for the stability of Q-balls, and the topological number does for topological defects. We expect that, as for I-balls, there would also exist some conserved quantity. In chap. 3, we have conjectured that the adiabatic charge is a candidate to guarantee the stability of I-balls.

As we have explained, the adiabatic charge is a quantity conserved for the quasi-periodical oscillation of a field like the adiabatic invariant in a classical mechanical system. In the case of a scalar field, it has the gradient energy. Thus, through the gradient term, there exists a flow of the current. This is different from the mechanical system. As a result the energy density of the field at each point of the space is not a constant of the motion even without the external force on the system. In the proof of the adiabatic invariant in the classical mechanical system, we have used the fact that the momentum is a function of the coordinate and energy because in that case the energy is a constant of motion, which is the crucial point of the proof. In contrast, in the case of the field theory, we can not obtain the canonical momentum by solving the energy density with respect to the momentum because the energy density is not the constant of motion. However even in this case, we can prove the conservation of the adiabatic charge with an additional assumption. In the proof, we have assumed that there exists a potential that allows the periodic motion of the field, i.e., the field is separated to a temporal and spatial dependent part: $\phi(t, \vec{x}) = \Phi(\vec{x}) f(t)$. If the separation of the field is really allowed, we can find a constant of motion in the system $\tilde{\mathcal{H}} = \mathcal{H} - (1/2)\partial_i(\phi\partial\phi_i)$ at each point of the space. Owing to this constant of motion instead of the energy density, we can write down the canonical momentum by the canonical variable. Then, we have proved the conservation of the adiabatic charge.

Therefore, the existence of the potential that allows the periodic motion of the field is crucial for the proof.

In this chapter, we investigate the potential that allows the periodic motion. We then show that the potential to allow the periodic motion is uniquely determined to the quadratic potential with a logarithmic correction like $V = (m^2/2)\phi^2 \left[1 - K \ln\left(\phi^2/2M^2\right)\right]$, where K is the coefficient of the logarithmic correction. For the formation of I-balls, K must be positive. Such logarithmic correction determines the strength of non-linear effects. In particular, the I-ball radius is determined by K (and m). We also perform numerical simulations to confirm that the adiabatic charge of I-balls is indeed conserved. Specifically we vary the value of K sufficiently slowly with time and follow the evolution of the I-ball configuration to see if their behavior agrees with the analytical solution based on the conservation of the adiabatic charge.

This chapter is based on the paper collaborated with Masahiro Kawasaki and Fuminobu Takahashi [87].

6.1 Potential to allow the separable form

For the proof of the conservation of the adiabatic charge, we have assumed the existence of a potential $V(\phi)$ that allows periodic motion of the field for which the solution is given in a separable form,

$$\phi(t, \vec{c}) = \Phi(\vec{x})f(t), \tag{6.1.1}$$

where the periodic function $f(t)$ is normalized so that its maximum value is equal to unity. Now we determine the form of such potential. Substituting the separable form of the solution into the equation of motion, we obtain

$$\frac{\ddot{f}}{f} - \frac{\nabla^2 \Phi}{\Phi} = -\frac{V'(\Phi f)}{\Phi f}. \tag{6.1.2}$$

This equation implies that the derivative of the potential in the right-hand side should take a form of

$$\frac{V'(\Phi f)}{\Phi f} = A(\Phi) + B(f), \tag{6.1.3}$$

where $A(\Phi)$ are $B(f)$ are functions of Φ and f respectively. On the other hand, as the potential is a function of ϕ, the derivative of the potential is given by

$$\frac{V'(\Phi f)}{\Phi f} = C(\Phi f), \tag{6.1.4}$$

where $C(\phi)$ is a function of ϕ. Combining the relations (6.1.3) and (6.1.4), we obtain an algebraic equation for C:

$$\begin{aligned} C(\Phi f) &= A(\Phi) + B(f) = C(\Phi) + C(f) - A(a) - B(1) \\ &= C(\Phi) + C(f) - C(1). \end{aligned} \tag{6.1.5}$$

This equation is satisfied if and only if $C(\phi) = a \ln (\phi/b)$, where a and b are constants.[1] Then, we obtain

$$V = \frac{1}{2}m^2\phi^2 \left[1 - K \ln \frac{\phi^2}{2M^2}\right], \qquad (6.1.7)$$

where m is a constant with mass dimension $(D-1)/2$ and K is a dimensionless constant. Therefore, the scalar potential must be the quadratic potential with the logarithmic correction, and we call it the logarithmically running (LR) mass term potential in the following. Note that there are in fact only two independent parameters, as M can be absorbed by rescaling m and K. The above argument does not fix the magnitude and sign of the parameters. As we shall see in the next section, the I-ball solution exists if $m^2 > 0$ and $0 < K \ll 1$.

6.2 I-ball solution

In this section, we derive the profile of I-balls for the LR mass term potential. For the derivation, we again assume that the I-ball is formed as the lowest energy state for a given value of the adiabatic charge. Then, we derive that the configuration of I-balls is given by a Gaussian distribution. Furthermore, we numerically confirm that the scalar field dynamics is periodic and $\tilde{\mathcal{H}} = \tilde{\rho}$ is really a constant of motion for the I-ball solution. Note that the proof of the conservation of the adiabatic charge and the form of the potential are valid for any number of spatial dimensions D, and we consider the case of $D = 1, 2, 3$ in numerical simulations.

6.2.1 Gaussian field Configuration

Profile

We would like to find a configuration of the field that minimizes the energy for a given value of the adiabatic charge I. To solve this problem, we use the method of the Lagrange multipliers. Thus, let us minimize the following energy with a multiplier $\tilde{\omega}$:

$$\begin{aligned}
E_{\tilde{\omega}} &= \int d^D x \, \tilde{\rho}(x) + \tilde{\omega} \left(I - \int d^D x \, \frac{\overline{\dot{\phi}^2}}{\omega}\right) \\
&= \tilde{\omega}I + \int d^D x \left[\left(\frac{1}{2} - \frac{\tilde{\omega}}{\omega}\right)\overline{\dot{\phi}^2} - \frac{1}{2}\overline{\phi\nabla^2\phi} + \overline{V(\phi)}\right], \qquad (6.2.1)
\end{aligned}$$

where $\tilde{\rho}$ is a constant of motion given by

$$\tilde{\rho} \equiv \tilde{\mathcal{H}} = \frac{1}{2}\dot{\phi}^2 - \frac{1}{2}\phi\nabla^2\phi + V. \qquad (6.2.2)$$

---

[1]This can be seen by noting that one can derive the following differential equation for $C(\phi)$,

$$\frac{dC(\phi)}{d\phi} = \lim_{\Delta\phi\to 0} \frac{C(\phi + \Delta\phi) - C(\phi)}{\Delta\phi} = \lim_{\Delta\phi\to 0} \frac{C(1 + \Delta\phi/\phi)}{\Delta\phi/\phi}\frac{1}{\phi} = C'(1)\frac{1}{\phi}. \qquad (6.1.6)$$

Integrating the above equation, we obtain a logarithmic function.

Here we have used $\tilde{\rho} = \bar{\tilde{\rho}}$ in the second equality of (6.2.2).

To evaluate the configuration, we have to perform the time average. For the separable form (6.1.1), we can perform the time average of $f(t)$. If there was not the logarithmic correction, the periodic motion is simply given by a homogeneous scalar field oscillating in a quadratic potential. In this case, the periodic function is given by a harmonic function $f(t) = \cos(mt)$. For this oscillation, the time averages of the oscillating functions are trivial: $\overline{f(t)^2} = 1/2$, $\overline{\dot{f}(t)^2} = m^2/2$ and $\overline{f(t)^2 \ln f(t)^2} = 1/2 - \ln 2$. With the logarithmic potential, those results are modified by a factor of $1 + \mathcal{O}(K)$, and we write them as

$$\overline{f(t)^2} = c, \tag{6.2.3}$$

$$\overline{\dot{f}^2} = d\,\omega^2, \tag{6.2.4}$$

$$\overline{f(t)^2 \ln f(t)^2} = l, \tag{6.2.5}$$

where c, d and l are constants of order unity. Then $E_{\tilde{\omega}}$ is given by

$$E_{\tilde{\omega}} = \tilde{\omega} I + \int d^D x \left[\frac{d}{2} \left(1 - 2\frac{\tilde{\omega}}{\omega} \right) \omega^2 \Phi^2 - \frac{c}{2} \Phi \nabla^2 \Phi \right.$$
$$\left. + \frac{c}{2} m^2 \Phi^2 \left\{ \left(1 - \frac{l}{c} K \right) - K \ln \left(\frac{\Phi^2}{2M^2} \right) \right\} \right]. \tag{6.2.6}$$

The variation of $E_{\tilde{\omega}}$ with respect to Φ is

$$\delta E_{\tilde{\omega}} = \int d^D x\, \delta\Phi \left[d \left(1 - 2\frac{\tilde{\omega}}{\omega} \right) \omega^2 \Phi - c\nabla^2 \Phi \right.$$
$$\left. + cm^2 \Phi \left\{ \left(1 - \frac{l}{c} K \right) - K - K \ln \left(\frac{\Phi^2}{2M^2} \right) \right\} \right]. \tag{6.2.7}$$

Thus, by the lowest energy condition $\delta E_{\tilde{\omega}} = 0$, we obtain a bounce equation,

$$\nabla^2 \Phi - W^2 \Phi + K m^2 \Phi \ln \frac{\Phi^2}{2M^2} = 0, \tag{6.2.8}$$

where we have defined W^2 as

$$W^2 \equiv m^2 \left(1 - K - \frac{l}{c} K \right) + \omega^2 \frac{d}{c} \left(1 - 2\frac{\tilde{\omega}}{\omega} \right). \tag{6.2.9}$$

We assume that the solution of the bounce equation is spherically symmetric, $\Phi = \Phi(r)$, where r is the radial coordinate. Then the Laplacian operator can be written as

$$\nabla^2 = \frac{d^2}{dr^2} + \frac{D-1}{r} \frac{d}{dr}. \tag{6.2.10}$$

The solution is obtained by the Gaussian ansatz [26],

$$\Phi(r) = \Phi_c \exp\left(-r^2/R^2 \right), \tag{6.2.11}$$

where Φ_c is the amplitude of the I-ball at the center, and R is the radius. Substituting the ansatz into the bounce equation (6.2.8), we obtain

$$r^2 \frac{4}{R^2} \left[\frac{1}{R^2} - \frac{K}{2} m^2 \right] - \left[\frac{2D}{R^2} + W^2 - K m^2 \ln \frac{\Phi_c^2}{2M^2} \right] = 0. \tag{6.2.12}$$

This relation should be satisfied for an arbitrary value of r, thus the radius R and the Lagrange multiplier $\tilde{\omega}$ are determined as

$$R = \sqrt{\frac{2}{K}} \frac{1}{m}, \tag{6.2.13}$$

and

$$\tilde{\omega} = \frac{\omega}{2} \left[1 + \frac{c}{d} \frac{m^2}{\omega^2} \left\{ 1 + (D-1) K - \frac{l}{c} K - K \ln \left(\frac{\Phi_c^2}{2M^2} \right) \right\} \right]. \tag{6.2.14}$$

From (6.2.13), we can see that the radius of I-balls is determined by the coefficient K and mass m. As mentioned before, the choice of M is arbitrary as it can be absorbed by rescaling m and K. If we set $M = \Phi_c / \sqrt{2}$, the Lagrange multiplier is given by

$$\tilde{\omega} = \frac{\omega}{2} \left[1 + \frac{c}{d} \frac{m^2}{\omega^2} \left\{ 1 + (D-1) K - \frac{l}{c} K \right\} \right] = \omega \left(1 + \mathcal{O}(K) \right), \tag{6.2.15}$$

where we have used $\omega \simeq m$ and $c \simeq d$ in the second equality.

Analytical form of I, $\tilde{\rho}$ and other variables

We have evaluated the profile of I-balls for the LR potential. Next, using the profile, we evaluate the adiabatic charge I and modified energy density $\tilde{\rho}$. By the construction of the profile, it is evident that $\tilde{\rho}$ is time independent, i.e., a constant of motion. Furthermore, for the later use, we define several variables using $\tilde{\rho}$.

Let us evaluate the adiabatic charge for the profile derived above,

$$I = \int d^D x \frac{1}{\omega} \overline{\dot{\phi}^2} = \frac{1}{\omega} \overline{\dot{f}^2} \int d^D x \, \Phi_c^2 \exp\left(-2r^2/R^2 \right)$$

$$= \left(\frac{1}{m} \sqrt{\frac{\pi}{K}} \right)^D \frac{\Phi_c^2 \overline{\dot{f}^2}}{\omega}. \tag{6.2.16}$$

When the parameters are varied adiabatically, the adiabatic charge I is expected to be conserved. We shall see that this is the case in numerical simulations.

Next we evaluate $\tilde{\rho}$ by substituting the profile (6.2.11) with (6.2.13) into (6.2.2):

$$\tilde{\rho} = \Phi^2 \left[\frac{1}{2} \dot{f}^2 + \frac{1}{2} m^2 f^2 \left\{ 1 + KD - K \ln \left(\frac{\Phi_c^2}{2M^2} f^2 \right) \right\} \right]. \tag{6.2.17}$$

At a first glance, $\tilde{\rho}$ is dependent on time because of f. However, by solving the equation of motion, we can see that it is independent on time. The equation of motion for f is given by substituting the profile (6.2.11) with (6.2.13) into the equation of motion for ϕ (6.1.2),

$$\ddot{f}(t) + m^2 \left[1 + K(D-1) - K \ln \left(\frac{\Phi_c^2}{2M^2} f^2(t) \right) \right] f(t) = 0. \tag{6.2.18}$$

104

We can integrate this equation of motion and obtain

$$\dot{f}^2 = m^2 \left(1 - f^2\right) \left[1 + KD - K \ln\left(\frac{\Phi_c^2}{2M^2}\right)\right] + Km^2 f^2 \ln f^2, \qquad (6.2.19)$$

where we have used the normalization, $f(0) = 1$ when $\dot{f}(0) = 0$. Using (6.2.19), we can rewrite $\tilde{\rho}$ as

$$\tilde{\rho}(r) = \tilde{\rho}_c \exp\left(-2r^2/R^2\right) \qquad (6.2.20)$$

with

$$\tilde{\rho}_c \equiv \frac{m^2 \Phi_c^2}{2} \left[1 + DK - K \ln\left(\frac{\Phi_c^2}{2M^2}\right)\right]. \qquad (6.2.21)$$

From this equation, it is obvious that $\tilde{\rho}$ is the constant of motion as expected.

For comparison with numerical simulations, we define the I-ball radius $R_{1/2}$ where $\tilde{\rho}$ is equal to $\tilde{\rho}_c/2$:

$$R_{1/2} \equiv \sqrt{\frac{\ln 2}{K}} \frac{1}{m}. \qquad (6.2.22)$$

We also define the effective amplitude of the scalar field $\tilde{\Phi}_c$ in terms of $\tilde{\rho}$ as

$$\begin{aligned} \tilde{\Phi}_c &\equiv \sqrt{2\tilde{\rho}_c/m^2} \\ &= \Phi_c \left[1 + DK - K \ln\left(\frac{\Phi_c^2}{2M^2}\right)\right]^{1/2}. \end{aligned} \qquad (6.2.23)$$

Note that $\tilde{\Phi}_c$ is roughly equal to the actual oscillation amplitude Φ_c up to a correction of $\mathcal{O}(K)$.

6.2.2 Numerical simulations

Here we numerically confirm that the profile of I-balls obtained above is indeed a solution of the equation of motion. In particular we will see that $\tilde{\rho}$ is a constant of motion.

The LR mass term potential (6.1.7) contains a logarithmic function of ϕ, and so we have inserted a small parameter ϵ into the potential and its derivative as

$$\begin{cases} V = \dfrac{m^2}{2}\phi^2 \left[1 - K \ln\left(\epsilon + \dfrac{\phi^2}{2M^2}\right)\right], \\[3mm] \dfrac{\partial V}{\partial \phi} = m^2 \phi \left[1 - K \dfrac{1}{\epsilon + \phi^2/(2M^2)} \dfrac{\phi^2}{2M^2} - K \ln\left(\epsilon + \dfrac{\phi^2}{2M^2}\right)\right] \end{cases} \qquad (6.2.24)$$

for numerical stability. We have set $\epsilon = 10^{-30}$ in our numerical simulations, and we have checked that our results are insensitive to the value of ϵ as long as it is much smaller than unity. This regularization is adopted in the numerical simulations here and in sec. 6.3

We have performed lattice simulations for the cases of $D = 1, 2$ and 3. As the initial condition, we adopt the Gaussian profile (6.2.11) with $\Phi_c = 2M$ and $K = 10^{-1}$ and follow

its evolution from $t = 0$ to $10^3/m$. The box size L and number grid N for $D = 1, 2$ and 3 are

$$\begin{cases} D = 1,\ L = 100/m,\ N = 2048, \\ D = 2,\ L = 100/m,\ N = 256^2, \\ D = 3,\ L = 50/m,\ N = 128^3, \end{cases} \tag{6.2.25}$$

for which the spatial resolution is $\Delta mx = 4.8 \times 10^{-2}, 0.39$ and 0.39, respectively. We set the time step to $\Delta t = 10^{-2}/m$.

We show the results for the case of $D = 1$ in fig. 6.1. In the top left panel, the spatial distributions of $\tilde{\rho}_c$ at different times are shown. All the lines are overlapped, implying that the Gaussian ansatz is valid and $\tilde{\rho}_c$ stays a constant in time. From the other panels, we can see that all of $\tilde{\rho}_c$, $R_{1/2}$ and $\tilde{\Phi}_c$ remain constant in time, and their values are in perfect agreements with the analytical results (6.2.21), (6.2.22) and (6.2.22), respectively. We have also confirmed that the time evolution and the properties of the configuration of I-balls in numerical simulations are in very good agreements with the analytic results for the cases of $D = 2$ and 3. Therefore, we conclude that the adiabatic charge I is indeed conserved in the numerical simulations.

6.3   Adiabatic deformation of I-balls

In the previous section, we have derived the configuration of I-balls so that it minimizes the energy for a given adiabatic charge I. We have also numerically confirmed that the obtained configuration indeed satisfies the equation of motion and $\tilde{\rho}$ remains a constant of motion, which plays a crucial role in the proof of the conservation of the adiabatic charge. In this section, in order to further support the conjecture that the stability of I-balls is due to the conservation of the adiabatic charge, we follow the evolution of I-balls while the coefficient of the logarithmic potential K is varied adiabatically. If the adiabatic invariance indeed guarantees the stability of I-balls, the configuration would be gradually deformed into another Gaussian profile with a different value of K, while the adiabatic charge I is conserved.

We introduce the time variation of K as

$$K(t) = \frac{K_0}{(1 + \alpha mt)}, \tag{6.3.1}$$

where K_0 is the initial value of K at $t = 0$, and α is the coefficient of the time variation. For $\alpha \ll 1$, K varies much more slowly than the oscillation period, and therefore, it is expected that an I-ball evolves into another Gaussian profile with a different value of K. Thus, we expect that the I-ball radius R and $R_{1/2}$ evolve as

$$R(t) = \sqrt{\frac{2}{K_0}} (1 + \alpha mt)^{1/2} \frac{1}{m}, \tag{6.3.2}$$

$$R_{1/2}(t) = \sqrt{\frac{\ln 2}{K_0}} (1 + \alpha mt)^{1/2} \frac{1}{m}. \tag{6.3.3}$$
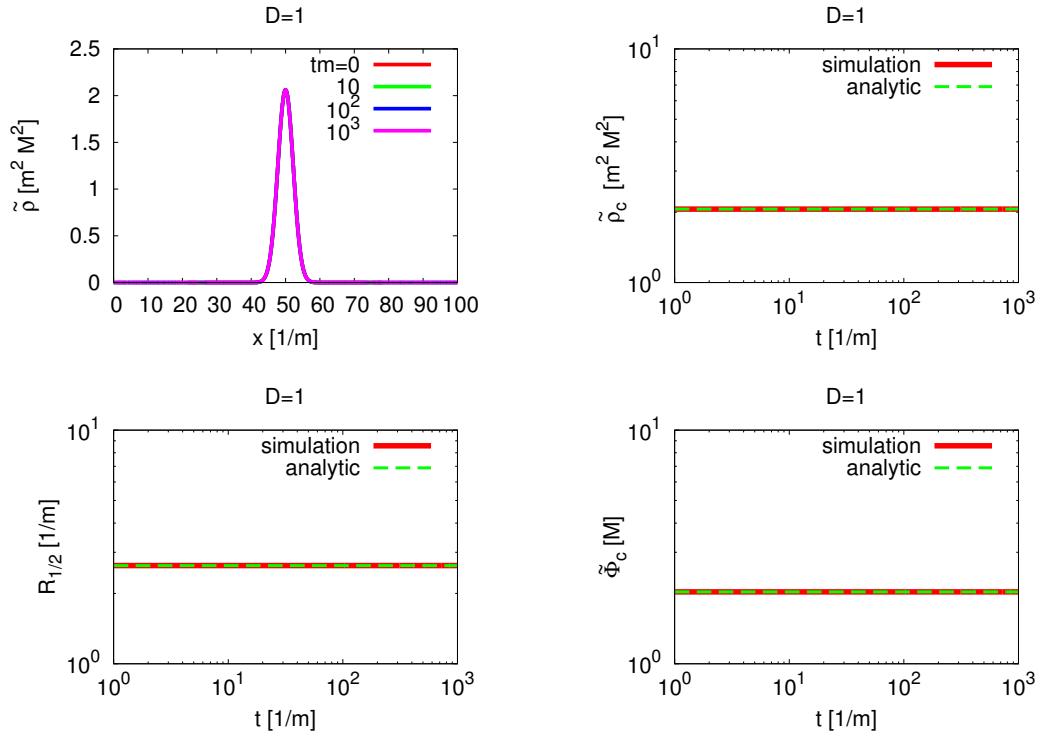
Figure 6.1: Numerical results of the I-ball for the case of $D = 1$. We have set $K = 10^{-1}$ and $\Phi_c = 2M$. The top left panel shows snapshots of the spatial distribution of $\tilde{\rho}$ at $mt = 0$, 10, 10^2 and 10^3, and all the lines are overlapped, implying that $\tilde{\rho}$ is a constant of motion. The top right, bottom left and bottom right panels show the time evolution of $\tilde{\rho}_c$, $\tilde{R}_{1/2}$ and $\tilde{\Phi}_c$ in a very good agreement with the analytical results (6.2.21), (6.2.22) and (6.2.22), respectively. The box size is $L = 100/m$, and the grid number is $N = 2048$.

The typical time scale Δt_R over which the radius R changes significantly is

$$\Delta t_R \simeq \left(\frac{\dot{R}}{R}\right)^{-1} = \left(\frac{\alpha m}{2}\frac{1}{1+\alpha m t}\right)^{-1} \simeq \frac{2}{\alpha m}. \qquad (6.3.4)$$

Therefore, we need to follow the evolution of I-balls for a sufficient long period ($\gg \Delta t_R$) in order to see the adiabatic deformation.

Here we estimate the magnitude of α which allows the I-ball to deform adiabatically. To do this, let us consider the deformation induced by excitations of wave packets inside the I-ball. The typical time scale for the wave packets to transverse the entire region of the I-ball can be estimated as

$$\Delta t_{\delta\phi} \simeq \frac{R}{v_g} \simeq \frac{2}{K_0 m}, \qquad (6.3.5)$$

where v_g is the group velocity, $v_g = \partial\omega/\partial k(k \simeq 1/R) \simeq \sqrt{K_0/2}$. For the adiabatic deformation of the I-ball, this propagation scale $\Delta t_{\delta\phi}$ should be much smaller than Δt_R, i.e., $\Delta t_{\delta\phi} \ll \Delta t_R$, which constrains α and K_0 as

$$\alpha \ll K_0. \qquad (6.3.6)$$

If this condition (6.3.6) is met, the I-ball would deform adiabatically.

The adiabatic charge I of the I-ball is expected to be conserved during the adiabatic deformation,

$$R_0^D \Phi_{c,0}^2 \left(\overline{\frac{\dot{f}^2}{\omega}}\right)_{t=0} = R(t)^D \Phi_c(t)^2 \left(\overline{\frac{\dot{f}^2}{\omega}}\right)_{t=t}, \qquad (6.3.7)$$

where the subscript 0 means that the variable is evaluated at $t = 0$ (6.2.16). As long as $K \ll 1$, the frequency of the oscillation is given by m up to a correction of order K, and so,

$$\left(\overline{\frac{\dot{f}^2}{\omega}}\right)_{t=0} = \left(\overline{\frac{\dot{f}^2}{\omega}}\right)_{t=t} + \mathcal{O}(K). \qquad (6.3.8)$$

Therefore, the amplitude of the oscillation at the center Φ_c should evolve with time as

$$\Phi_c(t) \simeq \Phi_{c,0} \left(\frac{R(t)}{R_0}\right)^{-D/2} = \Phi_{c,0} \left(1 + \alpha m t\right)^{-D/4}, \qquad (6.3.9)$$

up to a small correction of order K. With this approximation, the effective amplitude $\tilde{\Phi}_c$ evolves similarly, $\tilde{\Phi}_c(t) \simeq \Phi_c(t)$ (6.2.23).

First let us perform simulations for the case of $D = 1$, where we set the box size L, grid number N and time step Δt to

$$L = 100\, R_I(t=0), \ N = 2048, \ \Delta t = 10^{-2}\frac{1}{m}. \qquad (6.3.10)$$

We have followed the evolution of an I-ball from $t = 0$ to $10^4/m$ for $K_0 = 10^{-1}$ and $\alpha = 10^{-2}$. As a result, the coefficient $K(t)$ evolves from K_0 to approximately $K_0/100$, and the I-ball radius is expected to become larger by a factor of 10. In fig. 6.2, we show the

results of the simulation. The top two panels show snapshots of the spatial distribution of $\tilde{\rho}$ at $mt = 0$, 10^2, 10^3 and 10^4 with linear and logarithmic scales. One can see that the I-ball radius becomes larger and its amplitude at the center becomes smaller as expected. The two bottom panels show the time evolution of $R_{1/2}$ and $\tilde{\Phi}_c$ in very good agreements with the analytical estimation. This result clearly shows that the adiabatic charge I of the I-ball is indeed conserved and that the configuration of the I-ball follows the analytical solution obtained at the minimal energy state for a given adiabatic charge.

We have similarly studied the deformation of an I-ball in the cases of $D = 2$ and 3 for $K_0 = 10^{-1}$ and $\alpha = 10^{-2}$. We set the box size and grid number as:

$$L = 100/m, \quad N = 256^2, \quad \text{for} \quad D = 2 \tag{6.3.11}$$

$$L = 50/m, \quad N = 128^3, \quad \text{for} \quad D = 3 \tag{6.3.12}$$

and $\Delta t = 10^2/m$ for both cases, and followed the evolution from $t = 0$ to $10^3/m$. The results of the simulations are summarized in fig. 6.3. From the top panels, we can see that as the coefficient K becomes smaller, the I-ball radius becomes larger. This deformation follows the analytic solutions obtained under the assumption of the conservation of the adiabatic charge, as can be seen from the middle and bottom panels in the figure.

We have confirmed the adiabatic deformation of the I-ball for $\alpha = 10^{-2}$. For a larger α, however, the deformation of an I-ball is no longer adiabatic (see (6.3.6)), and it does not follow the analytic profile as the adiabatic charge is not conserved. In fig 6.4, we show results for the case of $D = 1$ with $(K_0, \alpha) = (10^{-1}, 10^{-1})$, for which the condition (6.3.6) is (marginally) broken. The I-ball does not have much time to deform itself in response to the change of K. As one can see from the figure, the configuration of the I-ball does not follow the Gaussian profile any more, and the evolution of the radius and amplitude do not math the analytic one.

6.4   Short Summary

It was conjectured that the stability of I-balls is guaranteed by the adiabatic charge [26]. For the conservation of the adiabatic charge, the periodic motion of the field is important. In this chapter, we have shown that the periodic motion is realised for the specific form of the potential; the quadratic potential with the logarithmic correction $V = (m^2/2)\phi^2 \left[1 - K \ln\left(\phi^2/2M^2\right)\right]$. For this potential, $\tilde{\rho}$ defined as (6.2.2) becomes a constant of motion, which plays a crucial role for the proof of the conservation of the adiabatic charge.

For the LR mass term potential, we have derived the I-ball solution using the Gaussian ansatz, under the condition of the conservation of the adiabatic charge. We have verified that the profile is indeed the solution of the equation of motion, and $\tilde{\rho}$ is the constant of motion, analytically and numerically. Furthermore we have followed the adiabatic deformation of an I-ball while the coefficient of the logarithmic potential K varies sufficiently slowly with time, and confirmed that the numerical results perfectly agree with the analytical estimations based on the conservation of the adiabatic charge. Thus, our results show that the stability of I-balls is due to the conservation of the adiabatic charge.
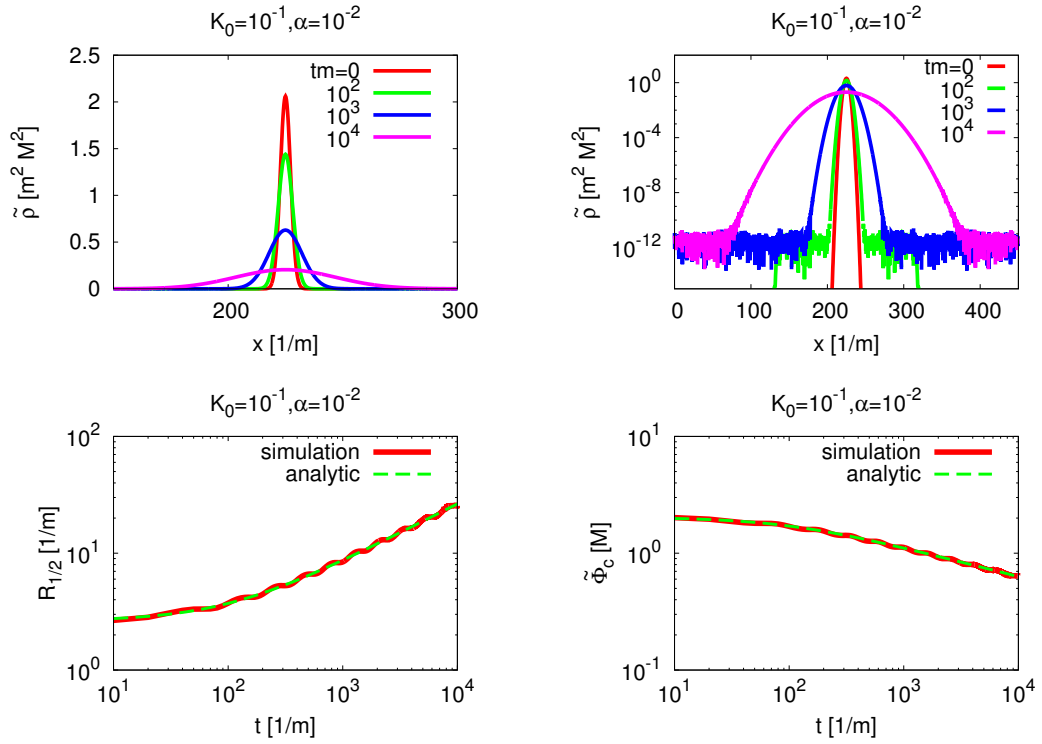
Figure 6.2: The results of the numerical simulation for the parameters of $(K_0, \alpha) = (10^{-1}, 10^{-2})$ for the case of $D = 1$. The top panels show the snapshots of the spatial distribution of $\tilde{\rho}$ at $mt = 0$, 10^2, 10^3 and 10^4 with linear and logarithmic scales. The bottom panels show the evolution of $R_{1/2}$ and $\tilde{\Phi}_c$ from $t = 10/m$ to $10^4/m$. The red (green) line shows the numerical (analytical) result (See (6.3.3) and (6.3.9)).
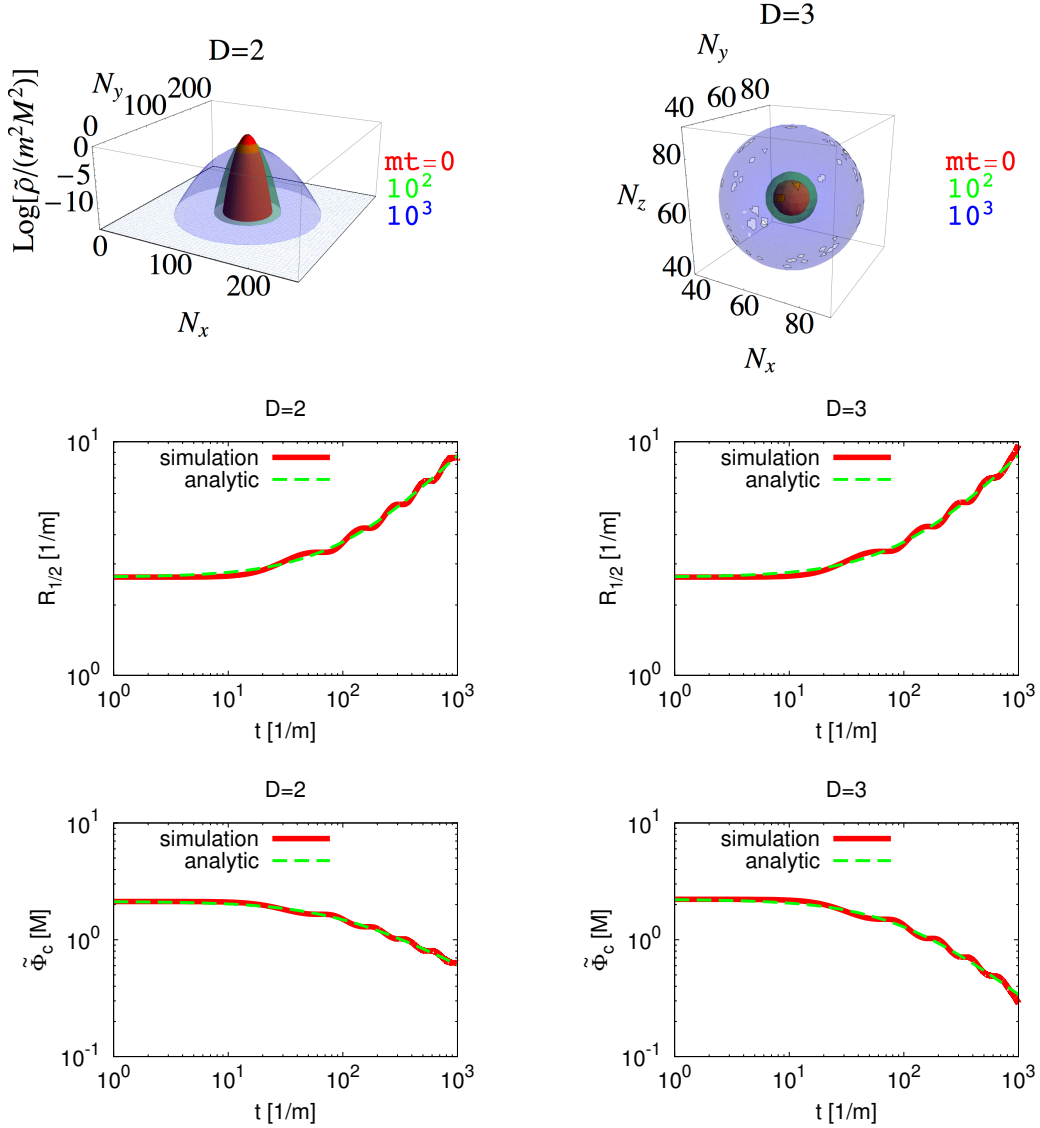
Figure 6.3: The results of the numerical simulations for the parameters of $(K_0, \alpha) = (10^{-1}, 10^{-2})$ for the cases of $D = 2$ and 3. The left (right) panels show the results for the case of $D = 2$ (3). The top two panels show snapshots of the spatial distribution of $\tilde{\rho}$ at $mt = 10, 10^2$ and 10^3, where N_x, N_y and N_z represent the grid point number of the lattice. The middle (bottom) panels show the evolution of $R_{1/2}$ ($\tilde{\Phi}_c$) from $t = 1/m$ to $10^3/m$ in very good agreements with the analytical ones (See (6.3.3) and (6.3.9)).
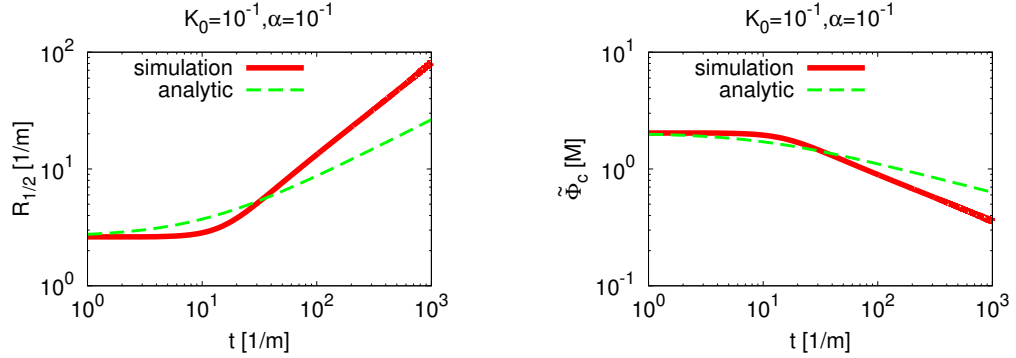
Figure 6.4: Sam as fig. 6.2 but for $\alpha = 10^{-1}$. The deformation of the I-ball is no longer adiabatic, and it does not follow the analytic one.

Here let us comment about the other types of potentials dominated by a quadratic potential. I-balls for such potentials are considered to be long-lived due to the approximate conservation of the adiabatic charge. Let us denote the deviation from the LR mass term potential by a small parameter ϵ. For those potentials, the dynamics of the scalar field is no longer given by the separable form (6.1.1) because of the deviation. In particular, the trajectory over one period is not closed by an amount of ϵ. Noting that the adiabatic invariant in the classical mechanics is a well conserved quantity and its variation is exponentially suppressed for a small breaking of the adiabaticity [37], it is plausible that the approximate conservation of the adiabatic charge accounts for the longevity of I-balls observed in various numerical simulations [64, 65, 79, 102]. As we have explained, I-balls in those simulations emit scalar waves and then gradually decay. The violation of the adiabatic charge may enable us to understand the lifetime of I-balls analytically.

Chapter 7

Conclusions

Scalar fields are expected to play various roles in the early Universe. As reviewed in chap. 2, if the potential energy of an inflaton dominates the Universe, it drives inflation, which is required to solve cosmological problems and is tested by many observations such as CMB and large scale structures. In the high energy state during inflation, other scalar fields might also have large field values, and they would dynamically evolve, especially during reheating.

During reheating, such scalar fields oscillate coherently with small fluctuations. By various numerical simulations, it is confirmed that some of the coherently oscillating scalar fields could fragment and form I-balls if the potential is flatter than the quadratic one as reviewed in chap. 3. The flatter shape of the potential attracts attentions recently; the precise measurement of CMB suggests that the inflaton potential would be a flatter one. Furthermore in the thermal environment during reheating, the logarithmic correction would make the potential flat. In this thesis, we have studied the formation of I-balls for the R^2 inflation and for the logarithmic potential motivated by the thermal correction.

The R^2 inflation is distinctive because only one mass parameter determines the inflaton potential and its interaction with the standard model particles. Thus, by the parameter, we can determine the dynamics of the inflaton uniquely such as the decay rate as reviewed in sec. 2.5. In this thesis, we have studied whether the estimation of the decay rate is valid even including the non-perturbative evolution of the fluctuations of the inflaton, i.e., whether the formation of I-balls takes place in chap. 4. In that chapter, we have investigated the resonance structure of the inflaton. We have verified that, in the Minkowski space-time, the fluctuations are enhanced for momenta below the mass scale of the inflaton, by the parametric resonance. However, we have revealed that the enhancement is suppressed in the expanding Universe, especially during reheating. As the inflaton of the R^2 inflation is an additional scalar degree of freedom of the gravity, the self interaction of the inflaton is so weak that its fluctuations are suppressed by the dilution of the Hubble expansion. Thus, there does not occur the formation of I-balls. Therefore, it is confirmed that the decay rate of the inflaton is accurately estimated by the perturbative way, and we can predict the observables in CMB precisely.

In the early Universe other scalar fields are also expected to oscillate along the logarithmic potential which comes from the correction by the quantum effect or the thermal effect due to the decay products of the inflaton, and they might form I-balls. Thus, we

have considered the logarithmic potential $V = M^2\Lambda^2 \ln(1 + \phi^2/\Lambda^2)$ (See (5.1.1)). Then, in chap. 5, we have confirmed the formation of I-balls for this potential, the results of which are summarized in Table 5.2. By our results, it is expected that the formation of I-balls might occur in the thermal bath, where the potential is the thermal logarithmic one with the temperature dependent coefficient: $\Lambda \simeq T$. By the formation, the energy density of the field would localize in finite regions, and the distribution of it would become highly inhomogeneous. If the decay into fermion particles is restricted by the Pauli blocking as in the case of Q-balls, the decay would be suppressed. If there occurs the bose enhancement inside I-balls, the decay would be enhanced. Therefore, to verify the decay process of scalar fields in the thermal bath during reheating, we have to pay attention to the formation of I-balls.

For many potentials, the formation and longevity of I-balls are confirmed by numerical simulations, but the stability of them is yet to be revealed analytically. It was conjectured that the stability is guaranteed by the adiabatic charge in [26], which explained I-balls as the lowest energy state of the field for a given adiabatic charge. In sec. 3.3, we have gave the rigorous proof of the conservation of the adiabatic charge even in the presence of non-negligible gradient energy, on which the proof is more general compared to the one of [26]. The crucial point of the proof is that we have assumed the potential that allows the periodic motion of the field.

In chap. 6, we have found that the potential to allow the periodic motion is uniquely determined to the quadratic potential with the logarithmic correction $V = (m^2/2)\phi^2\big[1 - K\ln\big(\phi^2/2M^2\big)\big]$ (See (6.1.7)) and derived the I-ball solution using the Gaussian ansatz under the condition of the conservation of the adiabatic charge. By performing lattice simulations, we have confirmed that the profile is indeed the solution of the equation of motion and that the oscillation of the field is periodic. Furthermore, we have followed the adiabatic deformation of an I-ball while the coefficient of the logarithmic potential K varies sufficiently slowly with time, and confirmed that the numerical results perfectly agree with the analytic estimations based on the conservation of the adiabatic charge. Our results show that the stability of I-balls is due to the conservation of the adiabatic charge.

For the LR mass term potential, the adiabatic charge is conserved, and I-balls are absolutely stable at the classical level because the quadratic potential and the logarithmic correction of $\propto \phi^2 \ln \phi^2$ allows the periodic motion. Thus, it is expected that for other types of potentials dominated by the quadratic term, the adiabatic charge is approximately conserved, and it guarantees the stability of I-balls. Indeed, it is numerically confirmed that, for the logarithmic potential $V = M^2\Lambda^2 \ln\big(1 + \phi^2/\Lambda^2\big)$, the formation of I-balls occurs for $\Phi(0) \lesssim \Lambda$ where the potential is dominated by the quadratic term as summarized in Table 5.2.

Observationally and theoretically, the flatter potentials attract attentions in the various situations in the early universe. In order to give general predictions for the formation of I-balls not by the case study, we have to theoretically understand the physical processes of the formation and decay, which are yet clarified. Our study suggests that the adiabatic charge would be important for the stability of I-balls. Using or interpreting the role of the adiabatic charge during the evolution of the scalar field would give us the deep understanding of I-balls.

Acknowledgments

I wish to express my most sincere gratitude and appreciation to my advisor Masahiro Kawasaki, for this guidance, hearty encouragements and stimulating discussions. Without his assistance, the present work would not have been successful.

I am deeply indebted to Yuki Watanabe, who is a collaborator to investigate the I-ball formation in the R^2 inflation. I also greatly thank Fuminobu Takahasi, who is a collaborator to investigate the role of adiabatic charge, and for the proof of the charge. I would like to thank Kazunori Nakayama and Kyohei Mukaida, for useful discussions and comments through my doctor course. I thank all the members at Institute for Cosmic Ray Research for their hospitality, of the cosmology group at IPMU, and at Research Center for the Early Universe. Especially, Tomohiro Takesako, Naoya Kitajima, Etsuko Kawakami, Kunio Kaneta, Ryo Namba, Motohiko Kusakabe, Marcus Christian Werner, Kenjiro Makiura, Mieko Minamisawa, Ken'ichi Saikawa and Noboru Matsuzawa. I thank all of my friends for encouragement. Especially, Takanori Shimazu, Kunihiko Shimazu, Naoki Iguchi, Eisaku Nitta, Atsushi Hirokawa and Daisuke Shogomori. I thank all my ancestors and my brothers. Especially, Noboru Takeda, Kazuko Takeda, Kazuaki Ito, Teruko Ito, Kazuhiko Nitta. I also thank my parents. I thank Kimitoshi Takeda. Together wit Kimitoshi, we have encouraged each other to get over difficulties and then to study natural science in our doctor course. He is most important to me in the Universe.

Finally, I would like to express the will of the greatest thanks to Michihisa Ito. Without his support for me and my family, I could not continue my doctor course, and furthermore, I could not get over the disastrous situation of my family during my doctor course. Again, I express my gratitude to him.

Appendix A

Note on calculation

In this section, we summarize the basic equations.

A.1 Gauge transformation

We summarize the gauge transformation of the metric. We consider the perturbed FRM Universe:

$$
\begin{aligned}
ds^2 = (1 + 2A_g)dt^2 &- 2a(\partial_i B_g - S_{gi})dx^i dt \\
&+ a^2\left[(1 - 2\psi_g)\delta_{ij} + 2\partial_{ij}E_g + \partial_i F_{gj} + \partial_j F_{gi} + h_{ij}\right].
\end{aligned}
\tag{1.1.1}
$$

We summarize the gauge dependence of the metric perturbation for the gauge transformation

$$
x^\mu \to x^\mu + \xi^\mu = x^\mu + (\delta t, \delta^{ij}\partial_i \delta x + \delta x^i).
\tag{1.1.2}
$$

For this transformation, gauge dependence of the metric is given by

$$
\begin{aligned}
\tilde{A}_g &= A_g - \dot{\delta t}, & (1.1.3) \\
\tilde{B}_g &= B_g - a\dot{\delta x} + a^{-a}\delta t, & (1.1.4) \\
\tilde{\psi}_g &= \psi_g + H\delta t, & (1.1.5) \\
\tilde{E}_g &= E - \delta x, & (1.1.6) \\
\tilde{S}_{gi} &= S_i + a\delta_{ij}\dot{\delta x}^j, & (1.1.7) \\
\tilde{F}_{gi} &= F_i - \delta x^j, & (1.1.8) \\
\tilde{h}_{ij} &= h_{ij}. & (1.1.9)
\end{aligned}
$$

Appendix B

Resolution dependence of the simulation

In chap. 5, we have performed simulations for several initial values of the field amplitude, and the formation of I-balls is confirmed. In this appendix, we perform simulations with finer resolutions, and then validate the results.

As a reference value, we perform simulations for $\phi_0 = 10\Lambda$ from $\tau = 2/M(= \tau_0)$ to $49/M$ in conformal time, which corresponds to $t = 2/M(= t_0)$ to $10^4/M$ in the cosmic time. We set the box size $L = 1/M$ and $5/M$, and set the grid number $N = 1024$, 4096 and 8192. In addition to that, we further perform with a much large grid number $N = 131072$ for $L = 1/M$. The comoving spatial resolution Δx for each set of the parameters is summarized in Table B.1, and the physical resolution in the end of simulation $\Delta x_{\mathrm{phy,e}}$ is summarized in Table B.2. We set the time step equal to $\Delta x/5$ as

$$\Delta \tau = \frac{1}{5}\Delta x. \tag{2.0.1}$$

We show the results of the simulations for a set of parameters $(ML, N) = (1, 8192)$, which corresponds to the comoving spatial resolution $\Delta x = 1.2 \times 10^{-4}/M$ and final physical one $\Delta x_{\mathrm{phy,e}} = 7.4 \times 10^{-2}/M$. The time step is set to be $\Delta \tau = 2.44 \times 10^{-5}/M$. We show the snap shots of the spatial distribution of the energy density at $Mt = 2(= Mt_0)$, 10, 10^2, 10^3 and 10^4 in fig. B.1. The localization of the energy density can be seen on the panels of $t = 10^3/M$ and of $10^4/M$. In fig. B.2 we show the last panel of the fig. B.1 by changing the range of the horizontal axis to $x \in [0, 0.4/M]$ and the scaling of the vertical axis, where the vertical axis of the left (right) panels are on semi (log) scale. We can see more clearly the localization of the energy density with typically $\rho \simeq M^2\Lambda^2$. In fig. B.2, we have also plotted the snapshots of the distribution with much high resolution, whose parameters are set to $(ML, N) = (1, 131072)$. We can not observe significant differences between the simulations of the high and low resolutions.

To confirm the formation time, we show the evolution of ϵ_{over} for the sets of the parameters in fig. B.3. We can see that ϵ_{over} stars to increases between $t = 10^2/M$ and $10^3/M$. Among the sets of the parameters, we can not observe the significant differences for the evolution of ϵ_{over}.
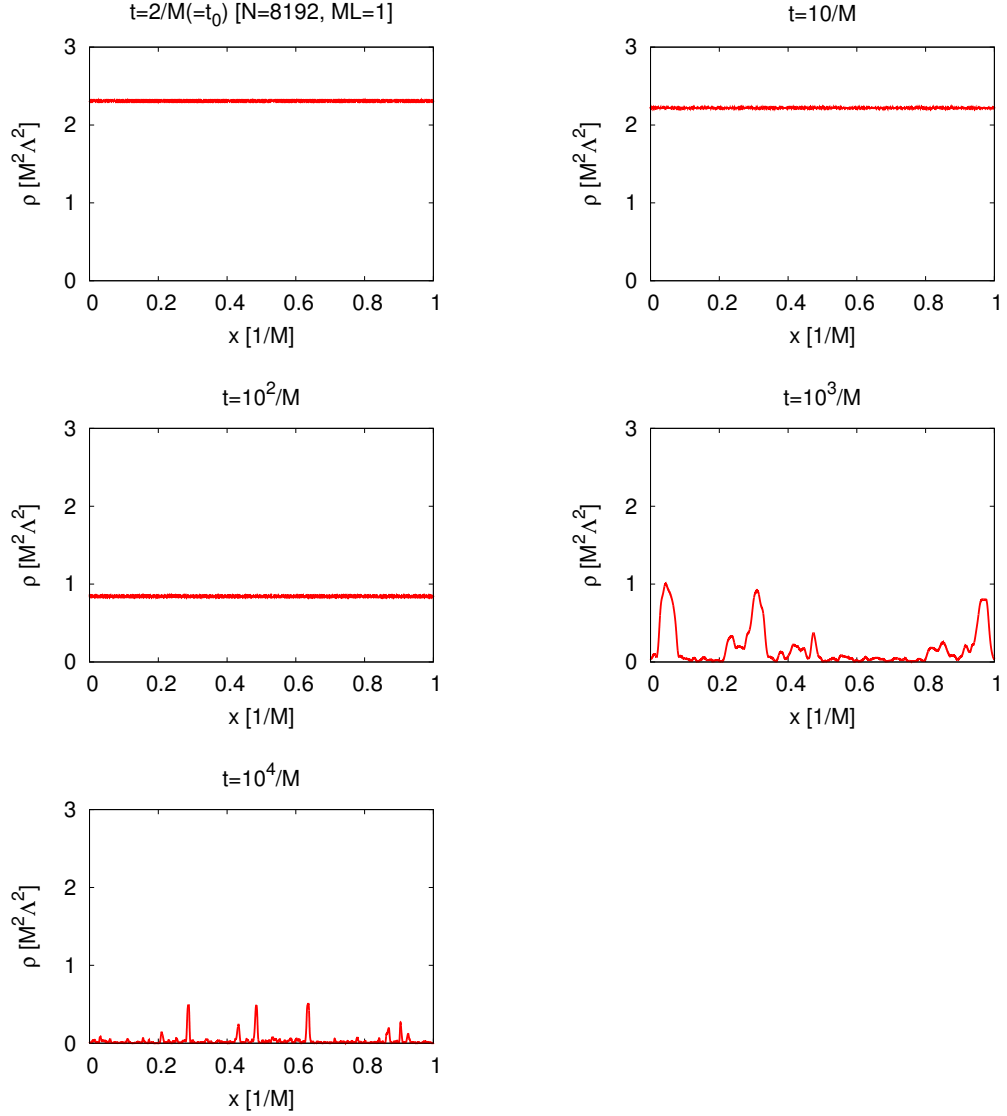
Figure B.1: The snap shots of the spatial distribution of the energy density ρ at $Mt = 2(= Mt_0)$, 10, 10^2, 10^3 and 10^4 from the top left panel to the bottom panel. The initial value of the field is $\phi_0 = 10\Lambda$. Box size and grid number are $L = 1/M$ and $N = 8192$ respectively, which correspond to the comoving spatial resolution $\Delta x = 1.2 \times 10^{-4}/M$ and final physical resolution $\Delta x_{\mathrm{phy,e}} = 7.4 \times 10^{-2}/M$. The horizontal axis is the comoving spatial coordinate.

$M\Delta x$	$N = 1024$	4096	8192	131072
$LM = 1$	9.8×10^{-4}	4.9×10^{-4}	1.2×10^{-4}	7.6×10^{-2}
5	4.9×10^{-3}	1.2×10^{-3}	6.1×10^{-4}	

Table B.1: The comoving spatial resolution Δx for each set of the parameters.

$M\Delta x_{\mathrm{phy,e}}$	$N = 1024$	4096	8192	131072
$ML = 1$	5.9×10^{-1}	1.48×10^{-1}	7.4×10^{-2}	4.6×10^{-3}
5	2.96	7.4×10^{-1}	3.7×10^{-1}	

Table B.2: Spatial resolution at the end of the simulation $\Delta x_{\mathrm{phy,e}}$ for each set of the parameters.
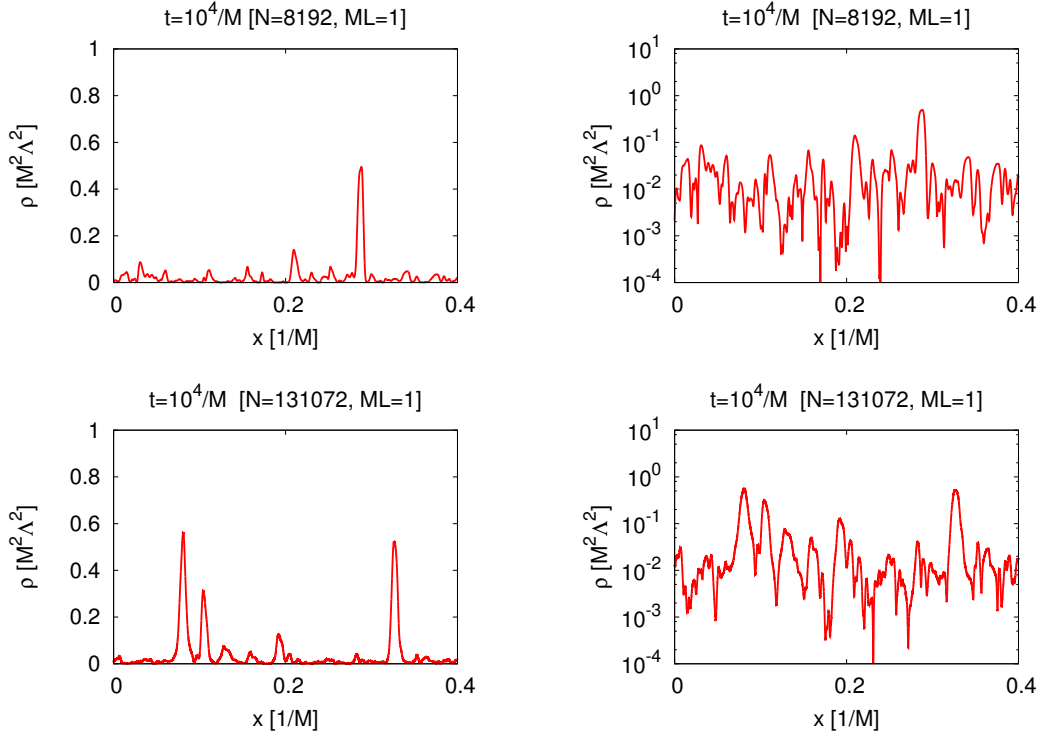

Figure B.2: The snap shots of the distribution of ρ at $t = 10^4/M$, where the initial value of the field is $\phi_0 = 10\Lambda$. On the top panels, the parameters are set to $(ML, N) = (1, 8192)$, and on the bottom panels, the parameters are $(ML, N) = (1, 131072)$. The vertical axis of the left (right) panels is semi scale (log scale). The horizontal axis is the comoving spatial coordinate.
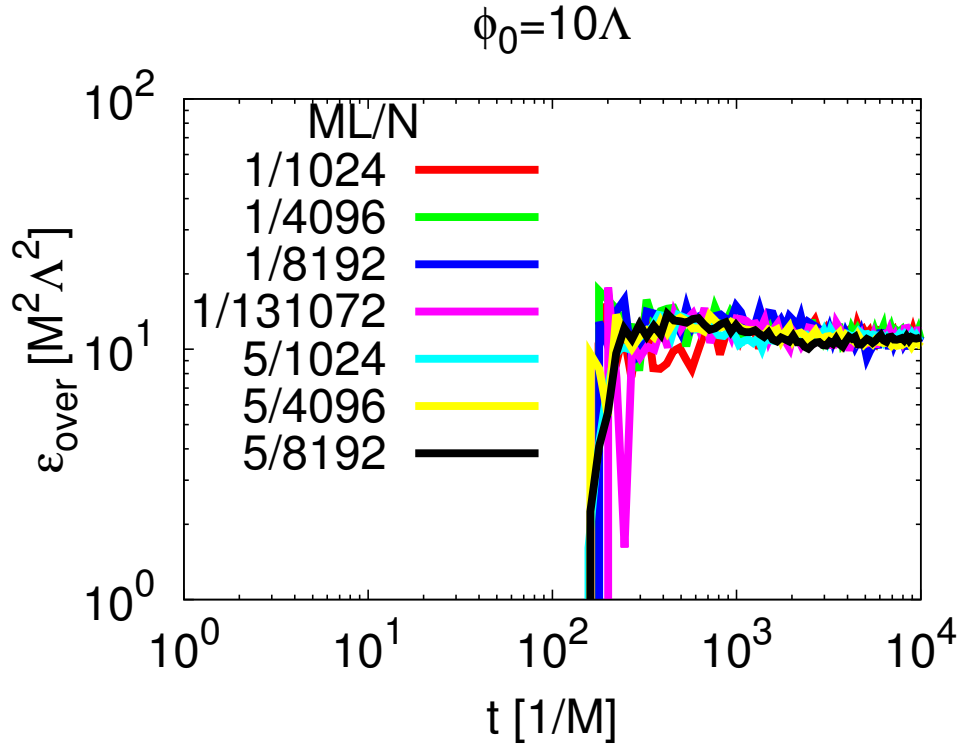
Figure B.3: The evolution of ϵ_{over} in the case of $\phi_0 = 10\Lambda$ from $t = 2/M$ to $10^4/M$. The values of parameters L and N are shown in the figure.

Appendix C

Finite box effect

In chap. 5, we have confirmed the formation of I-balls. However, due to the limitation of the size of the simulation box, scalar waves could propagate through the simulation box many times if the simulation time is significantly large. This propagation is unphysical, and it might affect the formation of I-balls. Thus, to study the effect of the unphysical propagation, we perform simulations with a sufficiently large size of the simulation box.

The distance that the scalar waves can propagate is limited by the speed of light $c = 1$, and hence the maximal distance is estimated by c times simulation time. Thus, to remove the propagation effects, we set the size of the box to be larger than $c \times \Delta T_{\max}$, where $\Delta T_{\max}$ is the simulation time.

As a reference value, we study the formation for $\phi_0 = 10\,\Lambda$ from $t = 2/M$ to $10^3/M$. To remove the effect of the box size, we set the box size to be larger than the distance that the light can propagate during the simulation to

$$L > c \times \Delta T_{\max} \simeq 10^3 \, \frac{1}{M}. \tag{3.0.1}$$

We perform a simulation for the set of parameters $(ML, N) = (1024, 1024 \times 1024 = 1.048576 \times 10^6)$, which gives the comoving spatial resolution $\Delta x \simeq 10^{-3}/M$ and physical one at the end of the simulation $\Delta x_{\mathrm{phy,e}} \simeq 6.2 \times 10^{-2}/M$. We show the snap shots of the spatial distribution of the energy density at $Mt = 2(= Mt_0)$, 10, 10^2 or 10^3 in fig. C.1. We can see the fragmentation and localization of ϕ into I-balls on the panel of $t = 10^3/M$ as the same way in the smaller box size $L = 1/M$. We show the last panel of fig. C.1 by changing the range of the horizontal axis to $x \in [0, 1/M]$ in fig. C.2, where vertical axis on the left (right) panel is semi (log) scale.

We have seen that the localization occurs even for this large box size. To confirm the formation time, we show the evolution of ϵ_{over} in fig. C.3, where we also plot the result in the case of smaller box size $L = 1/M$. From the figure, we can see that ϵ_{over} stars to increase and saturate on the same time scale for both sizes $L = 1/M$ and $1024/M$.
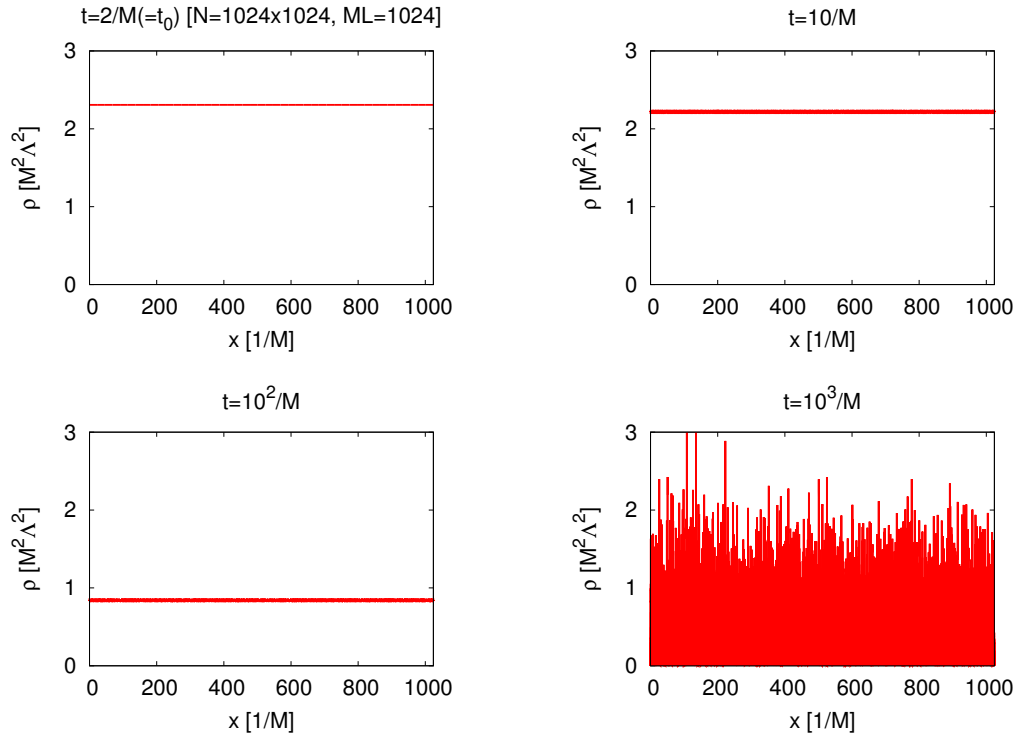
Figure C.1: The snap shots of the distribution of the energy density ρ at $Mt = 2(= Mt_0)$, 10, 10^2 and 10^3 from the top left panel to the bottom right panel. The initial value of the field is $\phi_0 = 10\Lambda$. Box size and grid number are $L = 1024/M$ and $N = 1024 \times 1024$ respectively, which corresponds to the comoving spatial resolution $\Delta x = 10^{-3}/M$ and final physical spatial resolution $\Delta x_{\mathrm{phy,e}} = 6.2 \times 10^{-2}/M$. The horizontal axis is the comoving spatial coordinate.
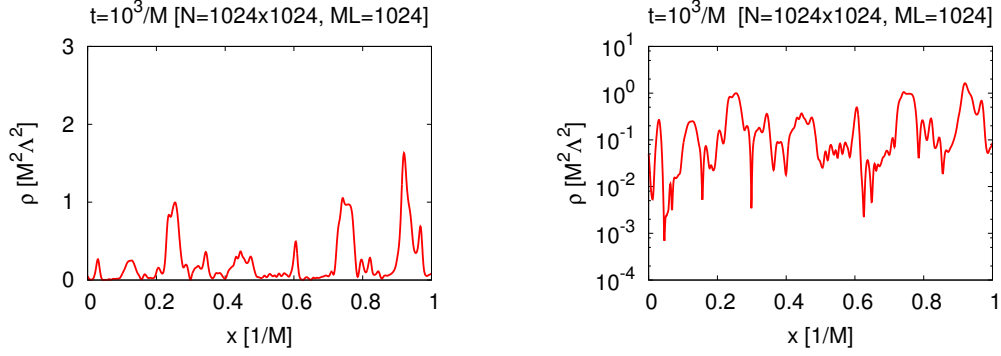
Figure C.2: The snap shot of the distribution of ρ at $t = 10^3/M$, where the initial value of the field is $\phi_0 = 10\Lambda$. The set of parameters is $(ML, N) = (1024, 1024 \times 1024)$. The left (right) panel shows the distribution in semi scale (log scale). The horizontal axis is the comoving spatial coordinate.
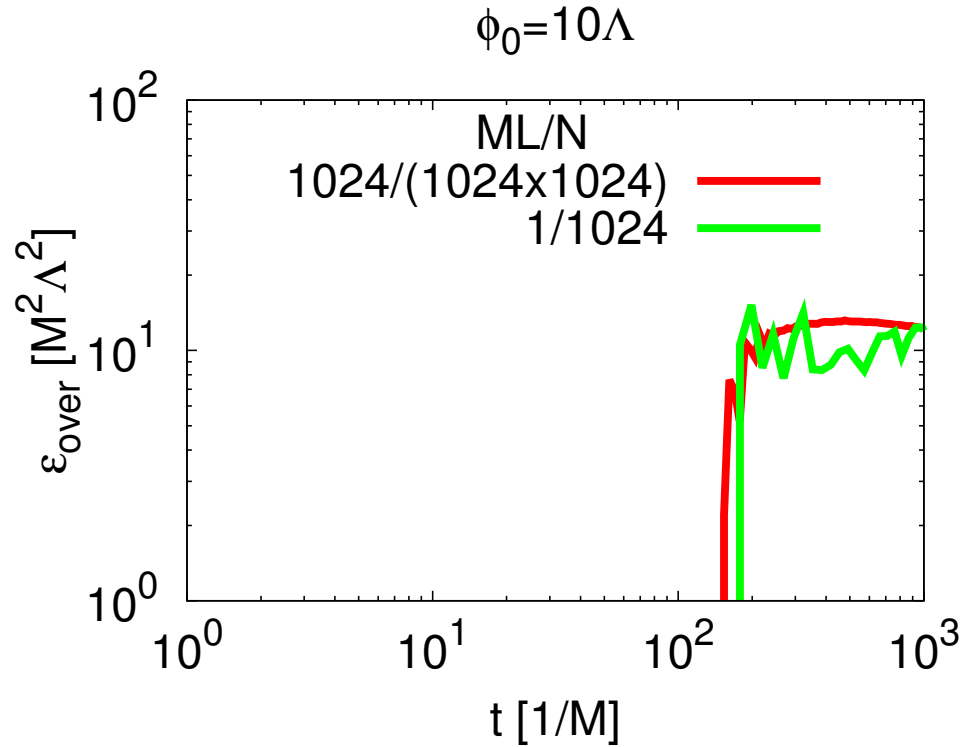

Figure C.3: The evolution of ϵ_{over} in the case of $\phi_0 = 10\Lambda$ from $t = 2/M$ to $10^3/M$. The values of parameters L and N are shown in the figure.

123

Bibliography

[1] **ATLAS** Collaboration, Aad, Georges and others, "Observation of a new particle in the search for the Standard Model Higgs boson with the ATLAS detector at the LHC," *Phys.Lett.* **B716** (2012) 1–29, `1207.7214`.

[2] **CMS** Collaboration, Chatrchyan, Serguei and others, "Observation of a new boson at a mass of 125 GeV with the CMS experiment at the LHC," *Phys.Lett.* **B716** (2012) 30–61, `1207.7235`.

[3] Sato, K., "First Order Phase Transition of a Vacuum and Expansion of the Universe," *Mon.Not.Roy.Astron.Soc.* **195** (1981) 467–479.

[4] Guth, Alan H., "The Inflationary Universe: A Possible Solution to the Horizon and Flatness Problems," *Phys.Rev.* **D23** (1981) 347–356.

[5] Starobinsky, Alexei A., "A New Type of Isotropic Cosmological Models Without Singularity," *Phys.Lett.* **B91** (1980) 99–102.

[6] Linde, Andrei D., "A New Inflationary Universe Scenario: A Possible Solution of the Horizon, Flatness, Homogeneity, Isotropy and Primordial Monopole Problems," *Phys.Lett.* **B108** (1982) 389–393.

[7] Albrecht, Andreas and Steinhardt, Paul J., "Cosmology for Grand Unified Theories with Radiatively Induced Symmetry Breaking," *Phys.Rev.Lett.* **48** (1982) 1220–1223.

[8] Weinberg, Steven, "A New Light Boson?," *Phys.Rev.Lett.* **40** (1978) 223–226.

[9] Wilczek, Frank, "Problem of Strong p and t Invariance in the Presence of Instantons," *Phys.Rev.Lett.* **40** (1978) 279–282.

[10] Enqvist, Kari and Sloth, Martin S., "Adiabatic CMB perturbations in pre - big bang string cosmology," *Nucl.Phys.* **B626** (2002) 395–409, `hep-ph/0109214`.

[11] Lyth, David H. and Wands, David, "Generating the curvature perturbation without an inflaton," *Phys.Lett.* **B524** (2002) 5–14, `hep-ph/0110002`.

[12] Moroi, Takeo and Takahashi, Tomo, "Effects of cosmological moduli fields on cosmic microwave background," *Phys.Lett.* **B522** (2001) 215–221, `hep-ph/0110096`.

[13] Affleck, Ian and Dine, Michael, "A New Mechanism for Baryogenesis," *Nucl.Phys.* **B249** (1985) 361.

[14] Dine, Michael and Randall, Lisa and Thomas, Scott D., "Baryogenesis from flat directions of the supersymmetric standard model," *Nucl.Phys.* **B458** (1996) 291–326, `hep-ph/9507453`.

[15] Murayama, H. and Suzuki, Hiroshi and Yanagida, T. and Yokoyama, Jun'ichi, "Chaotic inflation and baryogenesis by right-handed sneutrinos," *Phys.Rev.Lett.* **70** (1993) 1912–1915.

[16] Hamaguchi, Koichi and Murayama, Hitoshi and Yanagida, T., "Leptogenesis from N dominated early universe," *Phys.Rev.* **D65** (2002) 043512, `hep-ph/0109030`.

[17] Coughlan, G.D. and Fischler, W. and Kolb, Edward W. and Raby, S. and Ross, Graham G., "Cosmological Problems for the Polonyi Potential," *Phys.Lett.* **B131** (1983) 59.

[18] Banks, Tom and Kaplan, David B. and Nelson, Ann E., "Cosmological implications of dynamical supersymmetry breaking," *Phys.Rev.* **D49** (1994) 779–787, `hep-ph/9308292`.

[19] Endo, Motoi and Hamaguchi, Koichi and Takahashi, Fuminobu, "Moduli-induced gravitino problem," *Phys.Rev.Lett.* **96** (2006) 211301, `hep-ph/0602061`.

[20] Zeldovich, Ya. B. and Kobzarev, I. Yu. and Okun, L. B., "Cosmological Consequences of the Spontaneous Breakdown of Discrete Symmetry," *Zh. Eksp. Teor. Fiz.* **67** (1974) 3–11. [Sov. Phys. JETP40,1(1974)].

[21] Kibble, T. W. B., "Topology of Cosmic Domains and Strings," *J. Phys.* **A9** (1976) 1387–1398.

[22] Cohen, Andrew G. and Coleman, Sidney R. and Georgi, Howard and Manohar, Aneesh, "The Evaporation of Q Balls," *Nucl.Phys.* **B272** (1986) 301.

[23] Bogolyubsky, I.L. and Makhankov, V.G., "Lifetime of Pulsating Solitons in Some Classical Models," *Pisma Zh.Eksp.Teor.Fiz.* **24** (1976) 15–18.

[24] Bogolyubsky, I.L. and Makhankov, V.G., "Dynamics of Heavy Spherically-Symmetric Pulsons," *Pisma Zh.Eksp.Teor.Fiz.* **25** (1977) 120–123.

[25] Gleiser, Marcelo, "Pseudostable bubbles," *Phys.Rev.* **D49** (1994) 2978–2981, `hep-ph/9308279`.

[26] Kasuya, S. and Kawasaki, M. and Takahashi, Fuminobu, "I-balls," *Phys.Lett.* **B559** (2003) 99–106, `hep-ph/0209358`.

[27] Kawasaki, Masahiro and Yamada, Masaki, "Decay rates of Gaussian-type I-balls and Bose-enhancement effects in 3+1 dimensions," *JCAP* **1402** (2014) 001, `1311.0985`.

[28] Shtanov, Y. and Traschen, Jennie H. and Brandenberger, Robert H., "Universe reheating after inflation," *Phys.Rev.* **D51** (1995) 5438–5455, `hep-ph/9407247`.

[29] Kofman, Lev and Linde, Andrei D. and Starobinsky, Alexei A., "Reheating after inflation," *Phys.Rev.Lett.* **73** (1994) 3195–3198, `hep-th/9405187`.

[30] **Planck** Collaboration, Ade, P.A.R. and others, "Planck 2015 results. XX. Constraints on inflation," `1502.02114`.

[31] Anisimov, Alexey and Dine, Michael, "Some issues in flat direction baryogenesis," *Nucl.Phys.* **B619** (2001) 729–740, `hep-ph/0008058`.

[32] A. A. Starobinsky, "in: *Quantum Gravity, Proc. of the Second Seminar "Quantum Theory of Gravity" (Moscow, 13-15 Oct. 1981)*, eds. M. A. Markov and P. C. West (Plenum Publ. Co., New York, 1984) pp. 103-128.,".

[33] Watanabe, Yuki and Komatsu, Eiichiro, "Reheating of the universe after inflation with f(phi)R gravity," *Phys.Rev.* **D75** (2007) 061301, `gr-qc/0612120`.

[34] Watanabe, Yuki, "Rate of gravitational inflaton decay via gauge trace anomaly," *Phys.Rev.* **D83** (2011) 043511, `1011.3348`.

[35] Gorbunov, D.S. and Panin, A.G., "Scalaron the mighty: producing dark matter and baryon asymmetry at reheating," *Phys.Lett.* **B700** (2011) 157–162, `1009.2448`.

[36] Gamow, G., "Expanding universe and the origin of elements," *Phys.Rev.* **70** (1946) 572–573.

[37] L. D. Landau and E. M. Lifshitz, "*Mechanics*, 2nd ed. (Misuzu, Tokyo). ,".

[38] Sin-Itiro Tomonaga, "*Quantum Mechanics 1*, 2nd ed. (Pergamon Press Ltd., Oxford). ,".

[39] Penzias, Arno A. and Wilson, Robert Woodrow, "A Measurement of excess antenna temperature at 4080-Mc/s," *Astrophys.J.* **142** (1965) 419–421.

[40] Smoot, George F. and Bennett, C.L. and Kogut, A. and Wright, E.L. and Aymon, J. and others, "Structure in the COBE differential microwave radiometer first year maps," *Astrophys.J.* **396** (1992) L1–L5.

[41] **WMAP** Collaboration, Hinshaw, G. and others, "Nine-Year Wilkinson Microwave Anisotropy Probe (WMAP) Observations: Cosmological Parameter Results," *Astrophys.J.Suppl.* **208** (2013) 19, `1212.5226`.

[42] Dolgov, A.D. and Linde, Andrei D., "Baryon Asymmetry in Inflationary Universe," *Phys.Lett.* **B116** (1982) 329.

[43] Abbott, L.F. and Farhi, Edward and Wise, Mark B., "Particle Production in the New Inflationary Cosmology," *Phys.Lett.* **B117** (1982) 29.

[44] Bassett, Bruce A. and Tsujikawa, Shinji and Wands, David, "Inflation dynamics and reheating," *Rev.Mod.Phys.* **78** (2006) 537–589, `astro-ph/0507632`.

[45] Allahverdi, Rouzbeh and Brandenberger, Robert and Cyr-Racine, Francis-Yan and Mazumdar, Anupam, "Reheating in Inflationary Cosmology: Theory and Applications," *Ann.Rev.Nucl.Part.Sci.* **60** (2010) 27–51, 1001.2600.

[46] Amin, Mustafa A. and Hertzberg, Mark P. and Kaiser, David I. and Karouby, Johanna, "Nonperturbative Dynamics Of Reheating After Inflation: A Review," *Int.J.Mod.Phys.* **D24** (2014), no. 01, 1530003, 1410.3808.

[47] Liddle, Andrew R. and Lyth, D.H., "Cosmological inflation and large scale structure,".

[48] Mukhanov, Viatcheslav F. and Chibisov, G. V., "Quantum Fluctuation and Nonsingular Universe. (In Russian)," *JETP Lett.* **33** (1981) 532–535.

[49] Mukhanov, Viatcheslav F. and Chibisov, G.V., "The Vacuum energy and large scale structure of the universe," *Sov.Phys.JETP* **56** (1982) 258–265.

[50] Mukhanov, Viatcheslav F., "Gravitational Instability of the Universe Filled with a Scalar Field," *JETP Lett.* **41** (1985) 493–496.

[51] Mukhanov, Viatcheslav F., "Quantum Theory of Gauge Invariant Cosmological Perturbations," *Sov.Phys.JETP* **67** (1988) 1297–1302.

[52] Sasaki, Misao, "Large Scale Quantum Fluctuations in the Inflationary Universe," *Prog.Theor.Phys.* **76** (1986) 1036.

[53] Stewart, Ewan D. and Lyth, David H., "A More accurate analytic calculation of the spectrum of cosmological perturbations produced during inflation," *Phys.Lett.* **B302** (1993) 171–175, gr-qc/9302019.

[54] Lidsey, James E. and Liddle, Andrew R. and Kolb, Edward W. and Copeland, Edmund J. and Barreiro, Tiago and others, "Reconstructing the inflation potential : An overview," *Rev.Mod.Phys.* **69** (1997) 373–410, astro-ph/9508078.

[55] Greene, Patrick B. and Kofman, Lev, "On the theory of fermionic preheating," *Phys. Rev.* **D62** (2000) 123516, hep-ph/0003018.

[56] Hertzberg, Mark P., "Quantum Radiation of Oscillons," *Phys.Rev.* **D82** (2010) 045022, 1003.3459.

[57] Khlebnikov, S. Yu. and Tkachev, I.I., "Resonant decay of Bose condensates," *Phys.Rev.Lett.* **79** (1997) 1607–1610, hep-ph/9610477.

[58] Vilenkin, Alexander, "Classical and Quantum Cosmology of the Starobinsky Inflationary Model," *Phys.Rev.* **D32** (1985) 2511.

[59] Mijic, Milan B. and Morris, Michael S. and Suen, Wai-Mo, "The R**2 Cosmology: Inflation Without a Phase Transition," *Phys.Rev.* **D34** (1986) 2934.

[60] Whitt, Brian, "Fourth Order Gravity as General Relativity Plus Matter," *Phys.Lett.* **B145** (1984) 176.

[61] Jakubiec, A. and Kijowski, J., "On Theories of Gravitation With Nonlinear Lagrangians," *Phys.Rev.* **D37** (1988) 1406–1409.

[62] Mukhanov, Viatcheslav F., "Quantum Theory of Cosmological Perturbations in R(2) Gravity," *Phys.Lett.* **B218** (1989) 17–20.

[63] Segur, H. and Kruskal, M. D., "Nonexistence of Small Amplitude Breather Solutions in ϕ^4 Theory," *Phys. Rev. Lett.* **58** (1987) 747–750.

[64] Salmi, Petja and Hindmarsh, Mark, "Radiation and Relaxation of Oscillons," *Phys.Rev.* **D85** (2012) 085033, 1201.1934.

[65] Graham, N. and Stamatopoulos, N., "Unnatural Oscillon Lifetimes in an Expanding Background," *Phys. Lett.* **B639** (2006) 541–545, hep-th/0604134.

[66] Amin, Mustafa A. and Easther, Richard and Finkel, Hal and Flauger, Raphael and Hertzberg, Mark P., "Oscillons After Inflation," *Phys.Rev.Lett.* **108** (2012) 241302, 1106.3335.

[67] Amin, Mustafa A., "Inflaton fragmentation: Emergence of pseudo-stable inflaton lumps (oscillons) after inflation," 1006.3075.

[68] Amin, Mustafa A. and Easther, Richard and Finkel, Hal, "Inflaton Fragmentation and Oscillon Formation in Three Dimensions," *JCAP* **1012** (2010) 001, 1009.2505.

[69] M. Abramowitz and I. A. Stegun, "*Handbook of Mathematical Functions: with Formulas, Graphs, and Mathematical Tables* (Dover, New York, 1965). ,".

[70] Kofman, Lev and Linde, Andrei D. and Starobinsky, Alexei A., "Towards the theory of reheating after inflation," *Phys.Rev.* **D56** (1997) 3258–3295, hep-ph/9704452.

[71] Greene, Patrick B. and Kofman, Lev and Linde, Andrei D. and Starobinsky, Alexei A., "Structure of resonance in preheating after inflation," *Phys.Rev.* **D56** (1997) 6175–6192, hep-ph/9705347.

[72] Greene, Brian R. and Prokopec, Tomislav and Roos, Thomas G., "Inflaton decay and heavy particle production with negative coupling," *Phys.Rev.* **D56** (1997) 6484–6507, hep-ph/9705357.

[73] Shuhmaher, Natalia and Brandenberger, Robert, "Non-perturbative instabilities as a solution of the cosmological moduli problem," *Phys.Rev.* **D73** (2006) 043519, hep-th/0507103.

[74] Dufaux, Jean Francois and Felder, Gary N. and Kofman, L. and Peloso, M. and Podolsky, D., "Preheating with trilinear interactions: Tachyonic resonance," *JCAP* **0607** (2006) 006, hep-ph/0602144.

[75] Abolhasani, Ali Akbar and Firouzjahi, Hassan and Sheikh-Jabbari, M.M., "Tachyonic Resonance Preheating in Expanding Universe," *Phys.Rev.* **D81** (2010) 043524, 0912.1021.

[76] Felder, Gary N. and Garcia-Bellido, Juan and Greene, Patrick B. and Kofman, Lev and Linde, Andrei D. and others, "Dynamics of symmetry breaking and tachyonic preheating," *Phys.Rev.Lett.* **87** (2001) 011601, `hep-ph/0012142`.

[77] Felder, Gary N. and Kofman, Lev and Linde, Andrei D., "Tachyonic instability and dynamics of spontaneous symmetry breaking," *Phys.Rev.* **D64** (2001) 123517, `hep-th/0106179`.

[78] Khlebnikov, S. Yu. and Tkachev, I.I., "The Universe after inflation: The Wide resonance case," *Phys.Lett.* **B390** (1997) 80–86, `hep-ph/9608458`.

[79] Hindmarsh, Mark and Salmi, Petja, "Numerical investigations of oscillons in 2 dimensions," *Phys.Rev.* **D74** (2006) 105005, `hep-th/0606016`.

[80] Gleiser, Marcelo and Sicilia, David, "Analytical Characterization of Oscillon Energy and Lifetime," *Phys.Rev.Lett.* **101** (2008) 011602, `0804.0791`.

[81] Gleiser, Marcelo and Sicilia, David, "A General Theory of Oscillon Dynamics," *Phys.Rev.* **D80** (2009) 125037, `0910.5922`.

[82] Farhi, E. and Graham, N. and Guth, Alan H. and Iqbal, N. and Rosales, R.R. and others, "Emergence of Oscillons in an Expanding Background," *Phys.Rev.* **D77** (2008) 085019, `0712.3034`.

[83] Gleiser, Marcelo and Graham, Noah and Stamatopoulos, Nikitas, "Generation of Coherent Structures After Cosmic Inflation," *Phys.Rev.* **D83** (2011) 096010, `1103.1911`.

[84] Gleiser, Marcelo and Howell, Rafael C., "Resonant nucleation of spatio temporal order via parametric modal amplification," *Phys.Rev.* **E68** (2003) 065203, `cond-mat/0310157`.

[85] Gleiser, Marcelo and Howell, Rafael C., "Resonant nucleation," *Phys.Rev.Lett.* **94** (2005) 151601, `hep-ph/0409179`.

[86] Gleiser, Marcelo and Howell, Rafael C., "Emergence of complex spatio-temporal behavior in nonlinear field theories," *AIP Conf.Proc.* **861** (2006) 501–508, `hep-ph/0604067`.

[87] Kawasaki, Masahiro and Takahashi, Fuminobu and Takeda, Naoyuki, "Adiabatic Invariance of Oscillons/I-balls," `1508.01028`.

[88] Takeda, Naoyuki and Watanabe, Yuki, "No quasistable scalaron lump forms after R^2 inflation," *Phys.Rev.* **D90** (2014), no. 2, 023519, `1405.3830`.

[89] Nambu, Yasusada and Sasaki, Misao, "Quantum Treatment of Cosmological Axion Perturbations," *Phys.Rev.* **D42** (1990) 3918–3924.

[90] Kodama, Hideo and Hamazaki, Takashi, "Evolution of cosmological perturbations in a stage dominated by an oscillatory scalar field," *Prog.Theor.Phys.* **96** (1996) 949–970, `gr-qc/9608022`.

[91] Nambu, Yasusada and Taruya, Atsushi, "Evolution of cosmological perturbation in reheating phase of the universe," *Prog.Theor.Phys.* **97** (1997) 83–89, `gr-qc/9609029`.

[92] Finelli, F. and Brandenberger, Robert H., "Parametric amplification of gravitational fluctuations during reheating," *Phys.Rev.Lett.* **82** (1999) 1362–1365, `hep-ph/9809490`.

[93] Jedamzik, Karsten and Lemoine, Martin and Martin, Jerome, "Collapse of Small-Scale Density Perturbations during Preheating in Single Field Inflation," *JCAP* **1009** (2010) 034, `1002.3039`.

[94] Easther, Richard and Flauger, Raphael and Gilmore, James B., "Delayed Reheating and the Breakdown of Coherent Oscillations," *JCAP* **1104** (2011) 027, `1003.3011`.

[95] de Gouvea, Andre and Moroi, Takeo and Murayama, Hitoshi, "Cosmology of supersymmetric models with low-energy gauge mediation," *Phys.Rev.* **D56** (1997) 1281–1299, `hep-ph/9701244`.

[96] Coleman, Sidney R., "Q Balls," *Nucl.Phys.* **B262** (1985) 263.

[97] Enqvist, Kari and McDonald, John, "Q balls and baryogenesis in the MSSM," *Phys.Lett.* **B425** (1998) 309–321, `hep-ph/9711514`.

[98] Murayama, Hitoshi and Yanagida, T., "Leptogenesis in supersymmetric standard model with right-handed neutrino," *Phys.Lett.* **B322** (1994) 349–354, `hep-ph/9310297`.

[99] Adib, Artur B. and Gleiser, Marcelo and Almeida, Carlos A.S., "Long lived oscillons from asymmetric bubbles: Existence and stability," *Phys.Rev.* **D66** (2002) 085011, `hep-th/0203072`.

[100] Kawasaki, Masahiro and Takeda, Naoyuki, "I-ball formation with logarithmic potential," *JCAP* **1407** (2014) 038, `1310.4615`.

[101] Enqvist, Kari and McDonald, John, "The Dynamics of Affleck-Dine condensate collapse," *Nucl. Phys.* **B570** (2000) 407–422, `hep-ph/9908316`.

[102] Saffin, Paul M. and Tranberg, Anders, "Oscillons and quasi-breathers in D+1 dimensions," *JHEP* **01** (2007) 030, `hep-th/0610191`.